Particulate emissions from cooking ~~activities~~: emission factors, emission dynamics, and mass spectrometric analysis for different ~~preparation~~ cooking methods

Julia Pikmann[1], Frank Drewnick[1], Friederike Fachinger[1], Stephan Borrmann[1,2]

[1]Particle Chemistry Department, Max Planck Institute for Chemistry, Mainz, 55128, Germany
[2]Institute for Atmospheric Physics, Johannes Gutenberg University Mainz, Mainz, 55128, Germany

Correspondence to: Frank Drewnick (frank.drewnick@mpic.de)

Abstract.

Since~~As~~ most people, especially in developed countries, spend most of their time indoors, they are ~~strongly~~ heavily exposed to indoor aerosols, which can potentially ~~can~~ lead to adverse health effects. A major source of indoor aerosols are cooking activities, which releas~~e~~ing large amounts of particulate emissions~~,~~ (in terms of both number and mass~~) wise~~, ~~with~~ often with complex compositions. To investigate the characteristics of cooking emissions and what ~~the external parameters, which~~ influences these ~~characteristics~~ emissions, we conducted a comprehensive study~~,~~ ~~in form of a measurement series~~ by cooking 19 dishes with different ingredients and ~~preparation~~ cooking methods. The emissions were monitored in real time with ~~multiple~~ several on-line instruments that measur~~ed~~ing both physical and chemical particle properties as well as trace gas concentrations. ~~With t~~The same instrumentation~~,~~ was used to study the influence of cooking emissions on the ambient aerosol load ~~was studied~~ at two German Christmas markets. In contrast to previous studies, which often focus on individual aspects or emission variables, this broad and coherent approach allows a comparison between the influence of different parameters (e.g., ingredients, cooking method, cooking temperature, cooking activities) on the emissions.

For six variables~~,~~ we ~~observed~~ found evidence of emissions from ~~changes during the~~ cooking: particle number concentration of smaller (particle diameter d_p > 5 nm) and larger particles (d_p > 250 nm), PM (PM_1, $PM_{2.5}$, PM_{10}), BC, PAH and organic~~s~~ aerosol mass concentration~~s~~. In ~~G~~general~~ly~~, similar emission characteristics were observed for dishes with the same cooking ~~preparation~~ method, mainly due to similar cooking temperature and use of oil. The ~~emission~~ temporal dynamics in the emissions of the ~~above~~ aforementioned variables, as well as the sizes of the emitted particles, were ~~mostly~~ mainly influenced by the cooking temperature and the activities during cooking. ~~The e~~Emissions were quantified ~~via~~ using emission factors, with the highest values for grilled dishes, one to two orders of magnitude ~~smaller ones~~lower for oil-based cooking (baking, stir-frying, deep-frying), and the ~~smallest~~ lowest for boiled dishes.

For the identification of cooking emissions with the Aerodyne A~~a~~erosol M~~m~~ass S~~s~~pectrometer (AMS), and more generally for the identification of new AMS markers for individual organic aerosol types, we propose a new ~~diagram~~ plot type ~~where~~ that takes into account the mass spectral variability ~~of the mass spectra of different~~ for individual aerosol~~s is considered~~ types. Combining our results and those ~~from~~ of previous studies for the quantification of cooking-related organic aerosols with the AMS, we recommend ~~using values for~~the use of ~~the~~ relative ionization efficiency values higher ~~which are larger~~ than the default value for organics (RIE_{Org} = 1.4): ~~for rapeseed oil based cooking~~ 2.17 ± 0.48 for rapeseed oil-based cooking and ~~for soy oil based cooking~~ 5.16 ± 0.77 for soybean oil-based cooking.

1 Introduction

Aerosols ~~influence~~ affect the ~~e~~Earth's climate~~, as well as~~ air quality, and human health (IPCC, 2021; WHO, 2021). ~~According to calculations of t~~The ~~WHO (~~World Health Organization (WHO) estimates that air pollution ~~leads to~~causes 6.7 million premature deaths ~~every~~ each year~~, and~~ almost half of ~~them were~~which are attributable~~d~~ to indoor air pollution (WHO, 2023). People tend to spend an increasing ~~fraction~~ proportion of their time indoors, ~~especially~~ particularly in developed countries with about 90%~~,; they~~ and are therefore exposed ~~over long periods~~ to ~~the~~ indoor aerosol and ~~the therein contained~~its pollutants for long periods of time (Diffey, 2011; Goldstein et al., 2021; Liu et al., 2022). When ~~I~~inhaled, these pollutants can cause the formation of radicals that lead~~ing~~ to oxidative stress and the formation of oxygenated species ~~which~~ that can induce inflammatory~~ion~~ processes (Kreyling et al., 2006). The resulting ~~impacts on~~ health effects are ~~versatile~~ diverse and include respiratory diseases, cardiovascular diseases, allergies, infectious diseases, and cancer (Pope et al., 2004; Pope and Dockery, 2006; Shiraiwa et al., 2017; Xu et al., 2022).

~~The composition of the i~~Indoor aerosol composition is influenced by ~~the~~ atmospheric aerosol infiltrating through ventilation and leaks, as well as ~~by~~ multiple indoor emission sources ~~indoors~~ (Abbatt and Wang, 2020; Marval and Tronville, 2022). Aerosols can be generated ~~through~~ by the evaporation of substances from furnishings, building materials, and consumer products. The human body itself is a direct and indirect source of aerosols ~~due to~~through perspiration, breathing, talking, etc. ~~Furthermore~~In addition, ~~different~~ various activities ~~at~~ in the home (~~like~~ such as cleaning and moving around) lead to the resuspension and emission of aerosol particles. Combustion processes ~~like~~ such as cigarette smoking, candle or wood burning also cause strong indoor emissions (Abbatt and Wang, 2020).

Cooking is considered to be one of the most important indoor emission sources, an activity ~~which~~ that often occurs on a daily basis ~~at~~ in homes as well as on a larger scale~~s, in~~ e.g., in restaurants. In a study evaluating ~~the~~ personal exposure to indoor aerosol, cooking was identified as the largest contributor to indoor PM (particulate matter) (Zhao et al., 2006). ~~The i~~Indoor PM concentrations can increase tremendously depending on ~~the~~ cooking activity, with $PM_{2.5}$ peak concentrations (PM of aerodynamic diameter with d_p < 2.5 µm) of up to 1400 µg m^{-3} (Abdullahi et al., 2013). In developing countries, where solid fuels are often used for cooking, the health burden through the stronger emissions is even higher (Chafe et al., 2014; Martin et al; Nasir and Colbeck, 2013).

Cooking activities also have an impact on ~~the~~ ambient aerosol. In urban areas, cooking contributes 5-30% of the organic aerosol in fine particles during ~~the~~ typical meal times, as shown by various measurements, including ~~measurements~~ such ones with the AMS (A~~a~~erosol M~~m~~ass spectrometer; Crippa et al., 2013; Mohr et al., 2012; Struckmeier et al., 2016), TAG (thermal desorption aerosol gas chromatography−mass spectrometry; Wang et al., 2020), and filter measurements (Rogge et al., 1991). ~~During~~ In mapping measurements ~~in the proximity of~~near restaurants, performed by Robinson et al. (2018) with an AMS, most of the measured organic aerosol plumes were attributed to cooking emissions with concentrations ~~of~~ up to 100 µg m^{-3}, ~~showing~~ demonstrating the potential of cooking emissions to affect local air quality.

During cooking, a large fraction of the emitted particle mass is in the form of fine particles ($PM_{2.5}$), while the particle number concentrations of the emissions are dominated by ultrafine particles (d_p < 100 nm). Accordingly, the number and mass size distributions are dominated by Aitken and accumulation mode particles, respectively (Buonanno et al., 2009; Marval and Tronville, 2022; Wallace et al., 2004; Wallace and Ott, 2011; Yeung and To, 2008). When inhaled, these particles can ~~enter~~ penetrate deep into the lung~~s~~ to the alveoli. ~~Especially~~ In particular, ~~the~~ ultrafine particles~~, due to their larger specific surface area,~~ can cause stronger reactions or inflammatory~~ion~~ processes in the body~~, compared to~~than larger particles ~~with~~ of the same total mass due to their larger specific surface area (Baron et al., 2011; Marval and Tronville, 2022; Thomas, 2013).

~~A large~~Cooking releases a variety of substances~~, is emitted during cooking~~ including volatile organic compounds (VOCs) and particulate matter. The major constituents are saturated and unsaturated fatty acids, glycerides, ~~as well as~~and sugars and their

decomposition products, ~~like~~ such as levoglucosan. ~~Furthermore~~In addition, aromatics, PAHs (polycyclic aromatic hydrocarbons), and aldehydes ~~might~~ may be emitted, many of which are hazardous to health (Abdullahi et al., 2013; Cheng et al., 2016; Klein et al., 2016; Liu et al., 2018; Zhao et al., 2007; Zhao et al., 2019).

Studies on~~f~~ individual aspects of emissions from cooking activities have shown that the composition and quantity of ~~the~~ emissions are affected by various parameters, ~~like~~ such as the ~~preparation~~ cooking method, ingredients, cooking temperature, and ~~used~~ the type of fuel ~~type~~ used (e.g., Zhang et al., 2010). The particle sizes as well as number and mass concentrations increase with increasing temperature during cooking (Amouei Torkmahalleh et al., 2012; Buonanno et al., 2009; Klein et al., 2016; Zhang et al., 2010). The comparison of different ~~preparation~~ cooking methods ~~like~~ such as steaming, boiling, baking, deep~~-~~ frying, stir~~-~~ frying, and grilling showed that the lowest emissions were observed from steaming and boiling, while the ~~strongest~~ highest were observed from grilling, followed by deep~~-~~ frying and stir~~-~~ frying (Alves et al., 2015; Lee et al., 2001; Olson and Burke, 2006). The differences are mainly due to the different cooking temperatures and the use of oil. For example, See and Balasubramanian (2006) measured the particle size distribution of emissions from cooking tofu ~~with~~ using five different ~~preparation~~ cooking methods and observed a 24-fold increase in particle number concentration compared to ~~the~~ background during ~~deep~~ frying, compared to a 1.5-fold increase during steaming. Another aspect ~~which is~~ relevant ~~for~~ to the ~~amount~~ level of particulate emissions is the smoke point of the oil used ~~oil~~. Studies measuring the emissions from heating different oils showed that for oils with high smoke points, such as sunflower and soybean oil, the emissions were 4-9 times lower compared to olive oil with a lower smoke point~~, the emissions were 4 – 9 times lower~~ (Amouei Torkmahalleh et al., 2012; Gao et al., 2013).

In addition to primary aerosol particles, cooking emissions contain substantial amounts of VOCs (e.g., Katragadda et al., 2010; Klein et al., 2016), S/IVOCs (Semi/Intermediate VOCs; ~~(~~Yu et al., 2022), and aldehydes (Takhar et al., 2021), which are potential precursors for secondary organic aerosol (SOA) formation. SOA production rates from cooking-related gaseous emissions have been determined using oxidation flow reactors that simulate defined intervals of atmospheric aging. These experiments have shown that the amount of SOA from cooking processes compared to the primary aerosol emissions ranges from similar values to more than an order of magnitude higher amounts (Liu et al., 2018; Yu et al., 2022; Zhou et al., 2021) and is strongly dependent on the cooking method (Zhu et al., 2021).

The analysis of cooking emissions is challenging due to the high complexity of the emitted substance mixture, as well as the high emission dynamics with strong concentration variability ~~in concentrations~~ during ~~the~~ cooking. ~~Especially~~ In particular, the ingredients and the ~~preparation~~ cooking method have a strong influence on the emissions (Abdullahi et al., 2013; Marć et al., 2018; Zhang et al., 2010). In addition, the sampling approach itself (e.g., sampling location or dilution of samples) and the analysis procedure (e.g., focusing on peak levels or integrating over the entire cooking process) can have a strong influence on the resulting emission data.

As shown above, there are several studies in the literature that focus on individual aspects of particulate or gas phase emissions from cooking. Few of these studies focus on the emission dynamics during cooking and their dependence on, for example, cooking related activities. Others focus on the physical particle characteristics of the emitted aerosol or on the chemical composition of the emissions. Even within those studies that provide emission factors for different aerosol properties (e.g., particle number or mass), substantial differences in the experimental setup often prevent direct comparability of emission factors obtained in different studies. ~~So far~~To date, there are very few systematic studies that have both ~~covering~~ investigated the influence of different cooking parameters on the emissions ~~while~~ and measur~~ed~~ing a ~~large~~ wide variety of chemical and physical aerosol properties in parallel.

Therefore, we conducted a comprehensive study of cooking emissions by performing a series of measurement~~s series,~~ cooking 19 dishes with different ingredients and ~~preparation~~ cooking methods. During the cooking, ~~various~~ several chemical and physical properties of the emitted primary aerosol were monitored in real time with our mobile laboratory (MoLa, used in stationary

measurement mode in the laboratory), including PM, organics and non-refractory inorganics, BC and PAH mass concentrations, ~~as well as the~~and particle number concentration and size distribution. These on-line measurements allowed ~~for~~ the analysis of the emission dynamics during ~~the~~ cooking and of the influence of different cooking activities during ~~the~~ preparation on the emissions. The emissions were quantified and emission factors related to the amount of food were determined for all relevant variables. Based on the laboratory measurements, we investigated how the identification of cooking emissions with the AMS and ~~generally~~ the identification of new AMS markers in general can be further improved by using a new ~~diagram~~ plot type. Furthermore, the influence of cooking emissions on ambient aerosol was ~~studied~~ investigated at two German Christmas markets ~~with~~ using MoLa. Based on these measurements, ~~we examined~~ the applicability of the laboratory-derived emission factors to ambient data was investigated.

2 Methods and instrumentation

2.1 Laboratory study design and experimental procedures

For a systematic study, 19 different dishes were cooked in the laboratory (Table 1~~Table 1~~). The concept was to prepare dishes that are commonly ~~often~~ cooked in Central Europe (Germany), ~~while~~ including different classes of ingredients and ~~preparation~~ cooking methods, i.e., boiling, stir-frying, deep-frying, baking, and grilling with gas and charcoal. Each dish was ~~cooked with an amount for~~prepared to serve approximately four ~~persons~~ people, and all ingredients were weighed before preparation (Table S1). Rapeseed oil was used ~~for~~ in the ~~preparation~~ cooking of all dishes except ~~for~~ the boiled dishes, frozen pizza, and brownies. Only salt and pepper were used as ~~seasoning~~ condiments unless~~if not stated~~ otherwise noted in Table S1.

Table 1: List of dishes prepared ~~dishes~~ for the laboratory study (~~for details~~ see Table S1 for details).

~~Preparation~~ Cooking method	Dishes
Boiling	Boiled potatoes, rice, noodles
Stir-frying	Fried potatoes, bratwurst, schnitzel, fish, spaghetti Bolognese, stir-fried vegetables, Indian curry
Deep-frying	French fries (in pot), French fries (deep fryer), Bavarian doughnut (in pot)
Baking	Baked potatoes, frozen pizza, brownies
Grilling on gas grill	Steaks, vegetable skewers
Grilling on charcoal grill	Steaks

Each dish was cooked three times on the same day to assess the variability of ~~the~~ emissions due to variations in ingredients and ~~performance of the~~ cooking process performance between ~~the repetitions~~replicates. Background measurements were ~~performed~~ taken for~~over~~ 20 minutes ~~right before~~immediately prior to the start of ~~the~~ cooking. Between ~~repetitions~~replicates, we waited for the aerosol concentration to return to a stable background level; if necessary, the room was ventilated. The cooking process was recorded using a webcam (HD Pro Webcam C920, Logitech, Switzerland) to ~~apportion~~ assign individual concentration changes to activities during ~~the~~ cooking. ~~Furthermore~~In addition, the surface temperature of the cooked food and ~~of the~~ cookware was measured repeatedly at selected locations (typically every few min) with an IR thermometer (Fluke 568, Fluke Corporation, USA). During the baking experiments, the temperature of the air inside the oven was ~~monitored~~ continuously monitored using the same thermometer with a thermocouple ~~as~~ sensor. The ambient temperature around the kitchen setup was not measured. We estimate that it ranged ~~between~~from about 18 °C ~~and~~to 25 °C, depending on the ~~outdoor ambient~~ outside temperature~~s~~.

The measurements were performed in an experimental hall with a custom-built~~made~~ kitchen setup consisting of a ~~regular~~ standard household electric stove with oven (30540 P, Privileg, Germany) and a ~~fume~~ hood ~~above~~ (CH 44060-60 GA, Respekta®, Germany) above it, ~~which was~~ connected to an exhaust ~~ventilation~~ (Fig. 1). The exhaust flow rate Q_E was 7.5 m^3 min^{-1}. ~~To~~ In order to quantitatively capture the cooking emissions, the space between the stove and the ~~fume~~ hood was enclosed ~~encased~~ by four ~~p~~Plexiglass walls and only the front glass was left partially open, leaving a gap of ~~ca.~~about 50 cm to ~~be able to~~allow access to the cookware. For the oven and barbecue experiments, additional screens were used ~~for a~~to completely capture ~~of~~ the emissions. The cooking emissions were sub-sampled from~~From the pipe of~~ the exhaust pipe ~~ventilation~~ above the ~~fume~~ hood ~~the cooking emissions were sub-sampled~~, diluted (1:13) with a dilution system (VKL 10 E, Palas, Germany) using dry, particle-free compressed air (1 bar), and transferred to the instruments inside our mobile laboratory MoLa. ~~As~~ Since the dilution with dry air ~~led to~~resulted in low relative humidity (< 7 %) we measured dry particles, which ~~might~~ may differ in particle size (and~~, therefore,~~ thus mass) from particles measured without dilution ~~close to~~near the source. The particle loss within the setup was calculated using the particle loss calculator (von der Weiden et al., 2009) and was found to be negligible for the particle size range relevant ~~in~~ to this study.

The stir-fried dishes were prepared in a Teflon-coated frying pan, the boiled dishes in a stainless ~~-~~steel pot, and the deep-fried dishes in a stainless ~~-~~steel pot or a deep fryer (FT 2400.9, 2300 W, 2.5 L oil, Tevion, Germany). ~~For the barbecue experiments, a~~ A gas and a charcoal grill were used for the barbecue experiments.

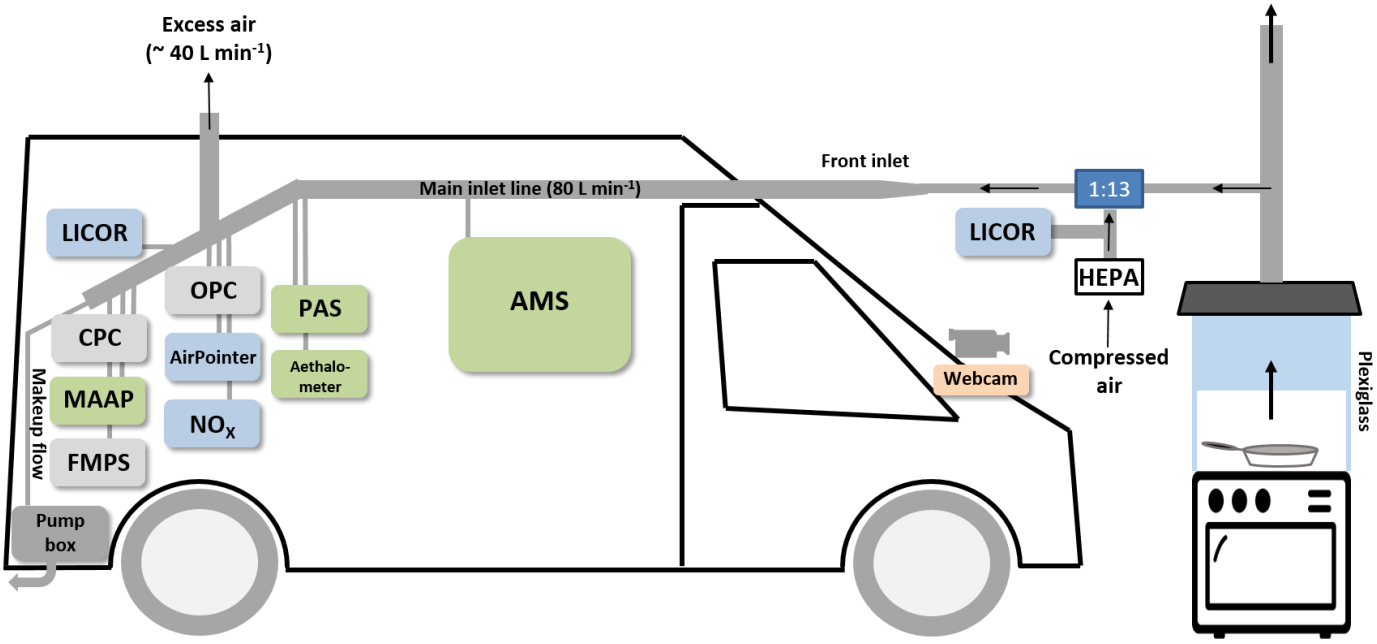

Figure 1: Scheme of the laboratory setup for the cooking experiments (MoLa scheme adapted from Drewnick et al., 2012). HEPA: high-efficiency particulate air filter. For details ~~regarding~~ on the instrumentation, see Table S2.

2.2 Ambient measurements at two German Christmas markets

Measurements to assess the ~~influence~~ impact of cooking emissions on ~~the~~ local air quality under ambient conditions were performed at two Christmas markets in Germany:

- Ingelheim (~~05.12.~~5 ~~until~~ to 8 December 2019~~08.12.2019~~)

  The Christmas market in Ingelheim (~~ca.~~approx. 35000 inhabitants) was located around the Burgkirche; the mobile laboratory MoLa was ~~situated~~ placed directly behind a circle of seven food stands, offering burgers, French fries, flame-grilled salmon, waffles, vegan food, and mulled wine~~,~~ at the eastern edge of the market. A wood fire barrel ~~for wood fire~~ was placed 25 meters from MoLa on 7 and 8 December 2019~~, at a distance of 25 m from MoLa~~ and another barrel was

placed in the middle of the food stand~~s~~ circle next to MoLa (~~distance approximately~~about 10 meters away) during all evenings. ~~More~~ Other food stands and wood~~-~~-fired barrels were distributed over the market, which covered an area of ~~ca.~~about 100 m by 50 m. The opening hours were 6 December~~.~~ 5 pm~~PM until~~ to 10 pm~~PM~~, 7 December 3 pm~~PM~~ ~~until~~ to 10 pm~~PM~~, and 8 December 3 ~~PM~~pm ~~until~~ to 9 pm~~PM~~.

- Bingen (13 ~~until~~ to 15 December 2019)

  The Christmas market in Bingen (~~ca.~~approx. 25000 inhabitants) was spread over the city center. MoLa was located at the eastern edge of the Bürgermeister-Neff ~~Square~~ Platz, an open area of ~~ca.~~about 50 m by 25 m, with the ~~closest~~ nearest food stand at a distance of 25 m. The six food stands on the square were arranged in a semicircle, offering Langos, French fries, bratwurst, barbecue, crepes, raclette, tarte flambée, sweets, and mulled wine, ~~were arranged in a half circle~~. On ~~the~~ 14 December, a suckling pig was grilled over an open wood fire ~~next to~~on the western edge of the square. ~~Furthermore, o~~On 14 and 15 December, a wood fire barrel ~~for wood fire~~ was placed in the middle of the square and another barrel was placed on a cross~~ing~~ road at the western edge of the square. The opening hours were 13 December 4 pm~~PM~~ ~~until~~ to 9 pm~~PM~~, 14 December 11 am~~AM~~ ~~until~~ to 9 pm~~PM~~, and 15 December 11 am~~AM~~ ~~until~~ to 7 pm~~PM~~.

The inlet height for the MoLa instrumentation was ~~at~~ 5 m above ground level. We measured mostly dry particles as the elevated temperature ~~within~~ inside MoLa led to low relative humidity (< 32 %) in the inlet lines. During the Ingelheim measurements ~~in Ingelheim~~, we additionally measured black carbon mass concentrations with a portable aethalometer (microAeth® MA200, AethLabs, USA) ~~the black carbon mass concentrations~~ during random walks ~~across~~ through the market.

The temperatures during the measurements at both ~~locations~~ sites were in the range of 4 – 11 °C and there were~~light~~ occasional light rain showers ~~occurred~~. The wind direction in Ingelheim was mainly from south-southwest with wind speeds of 1 – 4 m s^{-1} and in Bingen from west with wind speeds of 0.5 – 2 m s^{-1}, which resulted in the mobile laboratory being downwind of the Christmas markets most of the time.

2.3 Instrumentation

Within the mobile laboratory (MoLa) various instruments were used to measure different aerosol properties ~~like~~ such as~~the~~ particle number concentration (measured with a condensation particle counter CPC for particles with d_p > 5 nm and with an optical particle counter OPC for particles with d_p > 250 nm) and particle size distribution (d_p = 5.6 nm – 32 µm, measured with two different instruments: the F~~f~~ast M~~m~~obility P~~p~~article S~~s~~izer FMPS and the OPC), the mass concentration for the ~~fractions~~ PM_1, $PM_{2.5}$, PM_{10} fractions, and the chemical components black carbon (BC) and PAHs in the PM_1 fraction as well as the trace gas concentrations of NO_x, O_3, SO_2, CO, and CO_2. The HR-ToF-AMS (high-resolution time-of-flight aerosol mass spectrometer) was ~~applied~~ used to measure the non-refractory chemical composition of PM_1 and was operated in V-mode for maximum sensitivity, with a time resolution of 15 s for the laboratory measurements and 30 s for the Christmas market measurements. An overview of the MoLa instruments, ~~the~~ measured variables, time resolutions, and measurement uncertainties is provided in Table S2; for further details ~~regarding~~ on MoLa, see Drewnick et al. (2012).

2.4 Data processing

All data processing was performed ~~with~~ using Igor Pro (versions 6 – 8, WaveMetrics, Inc., USA). ~~The d~~Data from the laboratory (Christmas market) measurements were averaged on a common 15 s (30 s) time base. All data were corrected for sampling time delays, checked for invalid data~~,~~ (e.g., due to ~~e.g.~~ internal calibrations), and normalized to standard conditions (T = 20 °C, p = 1013.25 hPa). ~~In the further analysis of the cooking experiments, t~~The sampling dilution (1:13) was ~~considered~~taken into account in the further analysis of the cooking experiments. ~~From the combined FMPS and OPC size distribution data t~~The PM_1, $PM_{2.5}$, and

PM_{10} mass concentrations were calculated from the combined FMPS and OPC size distribution data (SI Sect. S1). The time-averaged data from theof individual experiments were averaged over the three repetitions replicates (if notunless otherwise stated otherwise), such so that the corresponding standard deviation reflects the variability between the repetitionsreplicates. For the Christmas market measurements, the periods with opened and closed market periods, respectively, were averaged separately over all days.

To calculate the cooking emissions from the laboratory data, the averaged background concentrations (c_{Back}) measured before each experiment were subtracted from the concentrations measured during the cooking (c_{Cook}). Identified trends in the background concentrations were corrected accordingly. Emission factors (EF) were calculated to estimate the total emissions from cooking per kilogram of food according to Eq. (1) from the average concentration of the respective variable ($c_{Avg} = c_{Cook} - c_{Back}$), the exhaust volume flow rate of the exhaust Q_E (7.5 m^3 min^{-1}), the preparation time t, the dilution factor D (13), and the mass of the ingredients m.

$$EF = \frac{c_{Avg} \cdot Q_E \cdot t \cdot D}{m} \quad (1)$$

The analysis of the high -resolution AMS data was performed with the software tools SQUIRREL 1.63I and PIKA 1.23I within Igor Pro following the standard procedures (Canagaratna et al., 2007). The ionization efficiency of the AMS as well as the relative ionization efficiencyies for ammonium (4.21) and sulfate (1.31) were determined in calibrations before and after the measurements. For the laboratory data, a collection efficiency (CE) of 1 was applied as because we assumed that the emitted particles were mostly composed of liquid components., This assumption is valid only for the laboratory measurements and is based on the observation that BC and other co-emitted (non-organic) components contribute only about 1% toof the total submicron aerosol mass (see Table S6). Using this approach, we can determine and for each dish the relative ionization efficiency for organics (RIE_{COA}) was determined for each dish separately (see Sect. 3.1.4). For the Christmas market data, the standard values for the CE (0.5) and RIE_{Org} (1.4) were applied (Canagaratna et al., 2007), except for the cooking organic aerosol fraction, as described in Sect. 3.5.1.

For comparison of the measured mass spectra with the onesthose of different organic aerosol types from previous studies (Table 2Table 2), all available high-resolution mass spectra of the respective aerosol types were taken from the AMS spectra database (Ulbrich et al., 2009; Ulbrich et al., 2023), as listed in Table S3.

Positive matrix factorization (PMF, Paatero and Tapper, 1994) was performed on the AMS organic high resolution mass spectra up to *m/z* 116 using the PMF Evaluation Tool (PET) v3.07C (Ulbrich et al., 2009, see SI Sect. S2 for details).

Table 2: List of organic aerosol types and their acronyms.

Acronym	Aerosol type
COA	Cooking organic aerosol
BBOA	Biomass burning organic aerosol
HOA	Hydrocarbon-like organic aerosol
OOA	Oxygenated organic aerosol
LVOOA	Low-volatile oxygenated organic aerosol
SVOOA	Semi-volatile oxygenated organic aerosol
LOOOA	Less oxidized oxygenated organic aerosol
MOOOA	More oxidized oxygenated organic aerosol
NOA	Nitrogen-enriched organic aerosol
CCOA	Coal combustion organic aerosol
CSOA	Cigarette smoke-related organic aerosol
IEPOX-SOA	Isoprene-epoxydiol-derived secondary organic aerosol

3 Results and discussion

3.1 Chemical analysis of cooking emissions with HR-ToF-AMS

3.1.1 Average chemical composition and correlation of mass spectra

The mass spectra of ~~the~~ non-refractory PM_1 cooking emissions from different dishes show a high similarity ~~between each other~~. On average, the measured aerosol consisted mainly of organics (96.7 – 99.9 %) with minor contributions ~~of~~ from nitrate (< LOD – 2.8 %), ammonium (< LOD – 0.5 %), sulfate (< LOD – 1.8 %), and chloride (< LOD – 0.4 %). Most of the ions ~~of~~ in the organic fraction were attributed to the C_xH_y family (77.8 – 91.8 %), indicating a weakly oxidized aerosol. The remaining ions were mostly oxygen containing ions ($C_xH_yO_1$: 6.5 – 17.4 %; $C_xH_yO_{>1}$: < LOD – 6.2 %) with a small fraction attributed to the C_xH_yN family (< LOD – 2.3 %) and the C_x family (0.1 – 0.8 %). For two dishes, Indian curry and spaghetti Bolognese, small fractions of the ions were attributed to the C_xS family (0.1 %) and ~~also~~ the sulfate fraction was also slightly elevated (0.3 – 0.7 %), presumably due to the emission of sulfur-containing substances from onions in the food (Boelens et al., 1971).

To obtain quantitative information on ~~how~~ the similarity of ~~the~~ emissions from different experiments ~~are~~, linear correlations were calculated between all ~~the~~ averaged normalized organic mass spectra (unit mass resolution) of ~~the~~ emissions from all dishes ~~were calculated~~ (Fig. 2). ~~Additionally~~In addition, the mass spectrum of emissions from heated rapeseed oil (Fig. S1) was included in this ~~analysis~~ comparison. ~~as~~This ~~selection~~choice of ~~for~~ a comparison spectrum is based on the fact that rapeseed oil was used ~~for~~ in all dishes where oil was required. Most of the spectra show a high degree of similarity ~~between~~ to each other and ~~with~~ to the spectrum of rapeseed oil (Pearson's r > 0.94), ~~and we conclude~~suggesting that the emissions are associated with oil, which might~~consisted mostly of~~ have vaporized and re-condensed ~~oil~~. Consistently, the mass spectra of the emissions from boiled dishes and steaks grilled ~~with~~ on charcoal are less similar to those of the ~~rest~~others: For the boiled dishes, no oil was used, and for the steaks, the mass spectrum is strongly influenced by the emissions from the charcoal itself. ~~Additionally~~In addition, the correlations of the cooking mass spectra with those ~~ones~~ of ~~various~~ different fatty acids (palmitic, stearic, oleic, and linoleic acid), all measured ~~with the~~by AMS (Ulbrich et al., 2023, not shown in Fig. 2), show the highest similarity with ~~the one~~that of oleic acid (r = 0.85 – 0.94), the main component of rapeseed oil and many other cooking oils. These observations suggest that a substantial fraction of cooking-related emissions are fatty acids, either from the used cooking oils or from components of the prepared food. This is

consistent with the fact that oil components may vaporize and recondense, and fats contained in the food may produce condensable fatty acids after decomposition. In contrast, peptides and carbohydrates are more likely to decompose into products that either remain in the gas phase or do not vaporize under the cooking conditions.

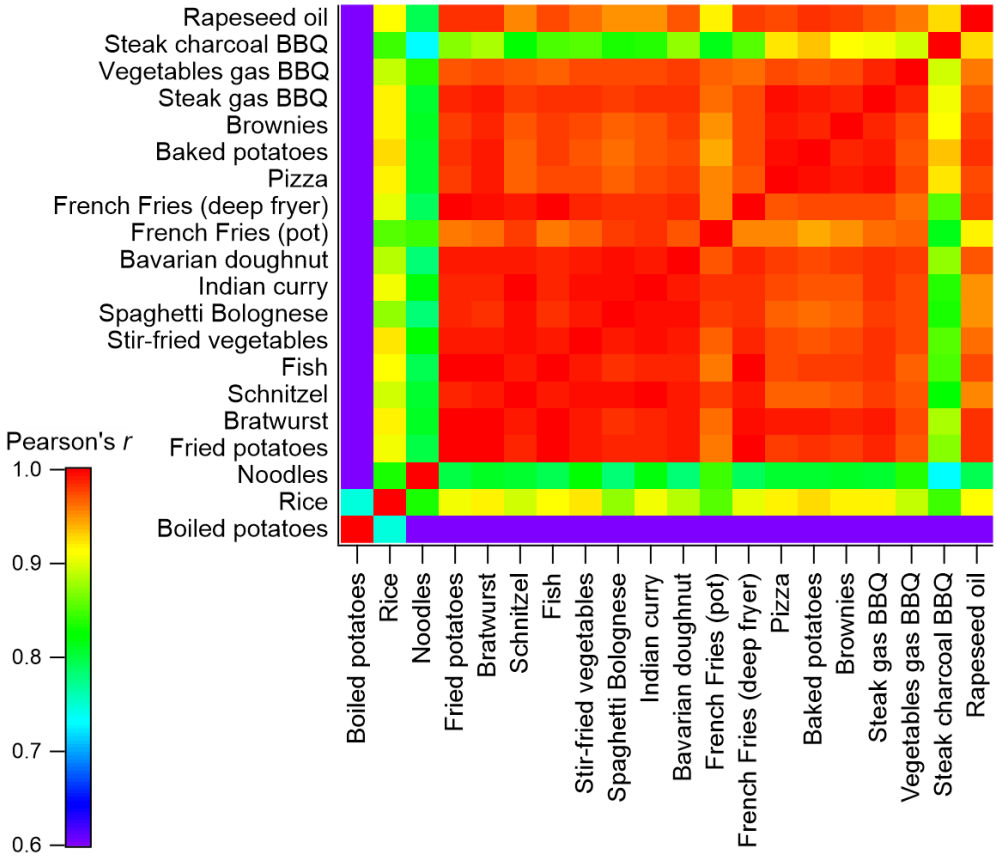

Figure 2: Linear correlation of the averaged mass spectra of cooking emissions for all laboratory experiments and pure rapeseed oil, color-coded based on the respective correlation coefficient (Pearson's *r*).

Furthermore, correlations of the cooking mass spectra from this study with mass spectra of different organic aerosol types from previous studies were calculated (Fig. S2). The latter, obtained ~~through~~ by PMF analysis of field measurement data, were taken from the AMS spectra database (Ulbrich et al., 2023) and averaged over all available spectra for the respective aerosol type (see Table S3 for the list of ~~used~~ mass spectra used). The highest similarity of mass spectra related to oil- or fat-containing dishes was observed with the average COA mass spectrum (r = 0.92 – 0.98); therefore, we ~~assume~~ conclude that also during field measurements, the mass spectra of ~~detected~~ cooking-related emissions are significantly influenced by the mass spectral patterns~~mostly consisted~~ of vaporized and re-condensed oil or fatty acids. Furthermore, a strong correlation was observed between the mass spectra ~~from~~ of the steak over charcoal grilling experiment ~~with the one~~and that of HOA, presumably due to the contribution of charcoal combustion to the ~~overall~~ total emissions in this case.

3.1.2 Characteristics of mass spectra from cooking emissions

The main characteristics of the mass spectra from the cooking experiments are ~~agree with those of previous studies , exemplarily~~ shown in Fig. ~~S~~3 for the "frying bratwurst" experiment as an example. The highest signal intensities were found at *m/z* 41 and 55, except for the boiled dish experiments. These signals are due to emissions of unsaturated hydrocarbons, presumably unsaturated fatty acids (He et al., 2010; Mohr et al., 2009). The most prominent ion series in the mass spectra are $C_nH_{2n+1}^+$ and $C_mH_{2m+1}CO^+$

(m/z 29, 43, 57, 71, …), and $C_nH_{2n-1}^+$ and $C_mH_{2m-1}CO^+$ (m/z 41, 55, 69, 83, …) from alkanes, alkenes, and oxygenated substances ~~like~~ such as acids, especially fatty acids. In addition, the ion series $C_nH_{2n-3}^+$ (m/z 67, 81, 95, 107, …) and $C_6H_5C_nH_{2n}^+$ (m/z 77, 91, 105) indicate the presence of cycloalkanes and aromatic hydrocarbons (Alfarra et al., 2004; He et al., 2010; McLafferty and Turecek, 1993; Mohr et al., 2009).

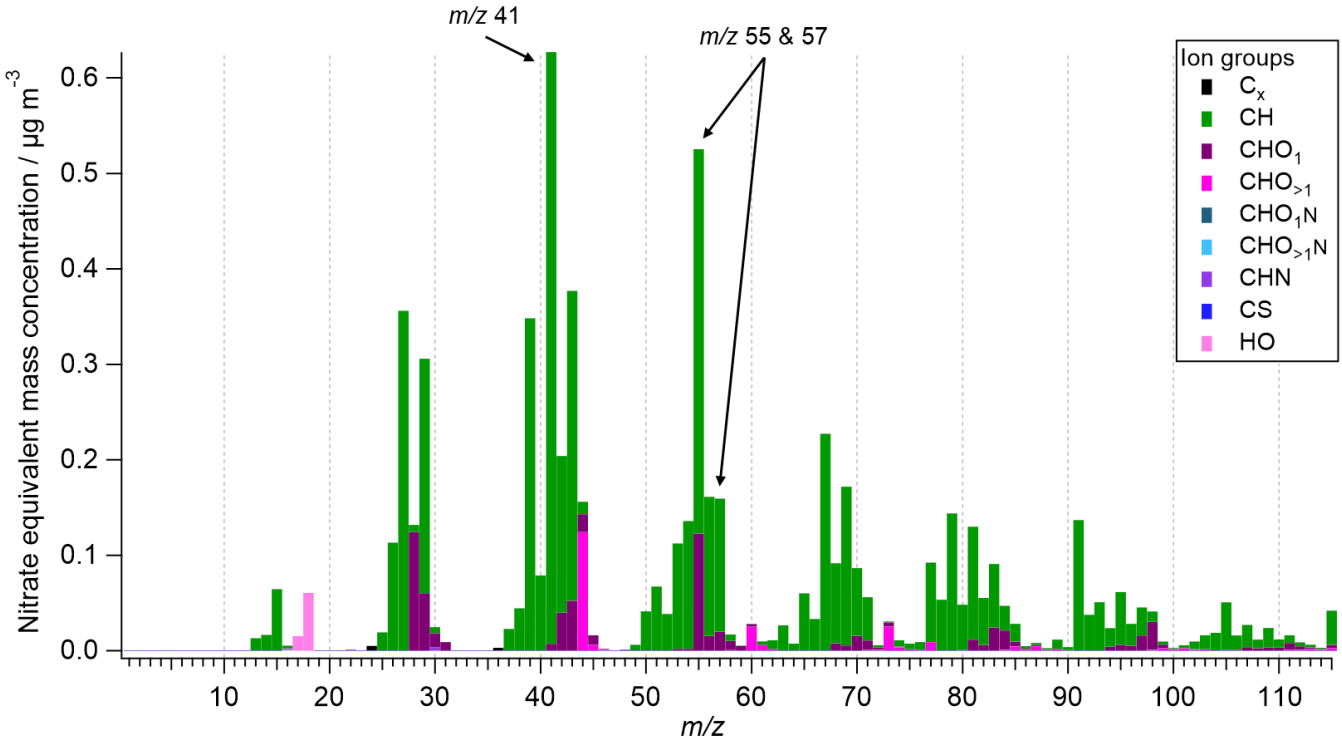

Figure 3: Unit-resolution mass spectrum of ~~emitted~~ organic aerosol emitted from frying bratwurst with important m/z marked.

A~~n well known~~ indicator~~ion~~ for COA is a high ratio of m/z 55 to m/z 57 in the mass spectra.~~, typically above two (Mohr et al., 2012; Sun et al., 2011; Xu et al., 2020).~~ ~~For the presented~~In our experiments, the observed ratio was 2.3 ─ 4.5, except for the boiled potatoes and the charcoal grilled steaks ~~grilled with charcoal~~ with 1.3 and 1.7, presumably due to the fact that the respective emissions are not dominated by vaporized oil and decomposed fats. This is in good agreement with the observation of ratios of typically above two for COA-related mass spectra (Mohr et al., 2012; Sun et al., 2011; Xu et al., 2020).

As another meaningful marker for cooking-related organic aerosol ~~is~~we identified the ~~comparison of the mass spectra with those of other typical aerosol types from the AMS spectra data base (Ulbrich et al.) indicates that a~~ ratio of m/z 67 to m/z 69 in the spectra~~above 1 might be another potential COA marker~~. ~~This ratio for HOA, BBOA, LVOOA, and SVOOA is ranging from 0.63 to 0.88 (Table S4).~~ For ~~the~~ our cooking experiments, thi~~s~~e ratio was in the range of 1.1 – 1.6, again excluding the boiled potatoes and the charcoal grilled steaks ~~over charcoal grilling~~ experiments with 0.81 and 0.7, respectively. The ratio for COA obtained from previous PMF analyses of ambient measurements is 1.2 ± 0.1 (Ulbrich et al., 2023) ~~(Ulbrich et al.)~~, while different results have been obtained from direct measurements of cooking aerosols ~~differing results were obtained~~. For emissions from Chinese cooking, heating sunflower, soybean, corn, and rapeseed oil, and frying sausages and French fries with rapeseed and sunflower oil, the ratio was above 1 (Faber et al., 2013; He et al., 2010; Liu et al., 2017a; Liu et al., 2017b; Xu et al., 2020), while Allan et al. (2010) and Zhang et al. (2021) measured ratios below 1 ~~from~~ for heating or cooking with rapeseed, sunflower, peanut, and corn oils; ~~further~~ it was also below or close to 1 for barbecue emissions, frying meat, heating olive and palm oils, and lard (Kaltsonoudis et al., 2017;

Liu et al., 2018; Xu et al., 2020). ~~This ratio f~~For HOA, BBOA, LVOOA, and SVOOA, ~~is~~ratios ranging from 0.63 to 0.88 were observed (Table S4).

Considering these studies, we conclude that the ratio of *m/z* 67 to *m/z* 69 in the mass spectra ~~is~~ depend~~s~~ent on the fatty acid composition and the fraction of polyunsaturated fatty acids in the measured aerosol. For saturated and monounsaturated fatty acids the ion series $C_nH_{2n-1}^+$ and $C_mH_{2m-1}CO^+$ (*m/z* 41, 55, **69**, 83, …) are more prominent, while for polyunsaturated fatty acids the ion series $C_nH_{2n-3}^+$ (*m/z* **67**, 81, 95, 107, …) is dominant (Christie 2023; Hallgren et al., 1959). For ~~oils from~~ rapeseed, sunflower, and corn oils the ~~fraction of~~ polyunsaturated fatty acid~~s~~ fraction is above 25% and the ratio of *m/z* 67 to *m/z* 69 is ~~mainly~~ mostly above 1. For oils with lower fractions of polyunsaturated fatty acids, ~~like~~ such as palm or olive oil, and animal fats, ~~like~~ such as lard, the ratio is below 1. Thus, the ratio of *m/z* 67 to *m/z* 69 ~~might~~ could be an indicator ~~for~~ of the composition of the oil used for cooking. ~~Emissions from biomass burning are mostly identified by the high signal intensity at *m/z* 60 and 73 which is due to the fragments $C_2H_4O_2^+$ and $C_3H_5O_2^+$ of levoglucosan generated by pyrolysis of cellulose .~~

During the laboratory cooking experiments, ~~also elevated~~ increased signal intensities were observed for *m/z* 60 and 73~~these ions were observed, however less intense than for biomass burning aerosols~~. We also found t~~T~~hese ~~elevated~~ enhanced signal intensities ~~were also measured~~ for emissions from pure heated rapeseed oil and they were also observed in reference mass spectra of the fatty acids oleic, stearic, and palmitic acid (AMS spectra database, Ulbrich et al.2023). ~~Typically~~Frequently, ~~in AMS mass spectra,~~ high signal intensities at *m/z* 60 and 73 in AMS mass spectra are ~~an~~ indicative~~on~~ of biomass burning aerosol~~,~~ due to the fragments $C_2H_4O_2^+$ and $C_3H_5O_2^+$ of levoglucosan generated by pyrolysis of cellulose (Schneider et al., 2006).~~,~~ However, ~~E~~elevated signal intensities at these *m/z* in cooking-related aerosols ~~therefore~~ are likely to originate~~and therefore in these cases likely originate~~ from fatty acids rather than from levoglucosan, i.e. the ion structure contains a carboxyl group rather than a diol (Fachinger et al., 2017), leading to a different fragmentation pattern. Thus, ~~A~~aone possibility to differentiate between biomass burning and cooking emissions ~~therefore might~~ could be the ratio of *m/z* 60 to 73. The ratios for pure levoglucosan and BBOA are 3.7 and 1.5, respectively, while the ratios from the cooking experiments, excluding the boiled dishes due to low organic concentrations and high uncertainty, ambient COA, and fatty acids are at most 1.1 (Table 3~~Table 3~~). Similar observations were reported by Xu et al. (2020) who measured a ratio of ~2 for BBOA and around 1 for COA. However, since the ratio of *m/z* 60 to 73 for HOA (Table 3) is not significantly different from those of the various COA-related values, it cannot be used by itself to discriminate between these two types of organic aerosols (see also Fig. S3).

Table 3: Ratio of signal intensities at *m/z* 60 and 73 from mass spectra of different compounds and aerosol types. For BBOA, HOA, COA, and the cooking experiments, the average and standard deviation ~~was~~ were calculated from the available data. All mass spectra except for the cooking experiments were obtained from the AMS spectra database (Ulbrich et al., 2023).

	Ratio of signal intensities at *m/z* 60 and 73
BBOA-related	
Levoglucosan	3.71
BBOA	1.47 ± 0.53
HOA-related	
HOA	0.95 ± 1.12
COA-related	
Oleic acid	0.81
Stearic acid	0.87
Palmitic acid	0.89
COA	1.10 ± 0.13
Cooking experiments (our study) [a]	0.90 ± 0.08
Rapeseed oil	0.95

[a]excluding boiled dishes (low organic concentrations)

3.1.3 Discrimination of different aerosol types based on markers in their mass spectra

Ambient aerosol is usually a mixture of ~~various aerosols of~~ different aerosol types due to the contribution ~~by~~ of different aerosol sources and aging processes in the atmosphere. In order ~~T~~to identify the individual aerosol types and their contribution to the total aerosol, PMF is applied to the mass spectra of the measured organic aerosol fraction and the ~~obtained~~ factors obtained are attributed to ~~various~~ the different aerosol types using different indicators and ~~through~~ by comparison ~~to~~ with other available data. For this study, a new plot type ~~of diagram~~ was ~~applied~~ used to ~~verify~~ assess whether combinations of known and new indicators in the mass spectra are suitable to reliably ~~differentiate~~ discriminate between different aerosol types and to check whether PMF work~~ed~~ well ~~for~~ to separate~~ing~~ different aerosol contributions. While in some cases (like *f*60/*f*73, see Sect. 3.1.2) individual markers might be sufficient to reasonably differentiate between different aerosol types, using such a combination of indicators can give a more robust information also in cases where differences between individual markers are less pronounced between different aerosol types.

In these "rectangle plots"~~,~~ the values of two indicators for all available aerosol types are plotted against each other in an xy-~~diagram~~plot. The standard deviation or uncertainty for each indicator of a ~~certain~~ particular aerosol type is reflected in the x- and y-direction~~s~~ by a box to show the variability of the mass spectra for that ~~this~~ aerosol type. The different aerosol types are well separated with a selected combination of indicators if the~~re is no overlap of~~ boxes do not overlap. Indicators for individual aerosol types ~~might~~ can be the fraction of the signal intensity at a single *m/z* ~~from~~ out of the total organic signal, e.g. f_{44} for the signal fraction at *m/z* 44, a combination of such fractions, e.g. f_{55}/f_{57}, or ~~organic aerosol~~ elemental ratios of the organic aerosol, ~~like~~ such as *O/C* and *H/C*.

For the cooking experiments, the respective values were calculated as the average ~~from~~ of the three ~~repetitions~~replicates, while for the individual reference aerosol types~~,~~ the available mass spectra from the AMS spectra database (Ulbrich et al., 2023~~2~~) were averaged. In both cases t~~T~~he corresponding standard deviation is shown as a box ~~in both cases~~; if only one reference mass spectrum or one ~~repetition~~ replicate was available (e.g., rapeseed oil, RO), ~~only a marker is shown~~the variability observed during the respective measurement is used as the uncertainty in the rectangle plot. The boiled dishes experiments and one of the deep-frying

French fries experiments, in which the frying oil cooled down strongly due to too many French fries used ~~with the boiled dishes~~, were excluded from this analysis due to very low organic concentrations and resulting high uncertainties.

Plotting the two known COA markers, f_{55} and f_{55}/f_{57}, together in such a rectangle plot (Fig. ~~3~~4) shows that the mass spectra of ambient COA and from the cooking experiments are well separated from those of other aerosol types with this ~~selection~~ combination of markers. The values for COA and the cooking experiments are located in the ~~top~~ upper right corner with high f_{55} (> 0.06) and f_{55}/f_{57} (> 2) values. Alt~~T~~hough the COA and HOA mass spectra are often similar, when~~using~~ both markers are used in combination they are well separated from each other, except for the ~~experiment~~ charcoal grilled steaks experiment~~, grilled with charcoal~~ which is located within the HOA box. The ~~values of~~ f_{55} values for the cooking experiments are slightly lower than those ~~from~~ of the ambient COA while the f_{55}/f_{57} values are similar for both or slightly higher than those of the ambient COA. This could either be due to the difference between ambient and laboratory aerosol, as ambient aerosol can chemically change in the atmosphere, or because PMF is not able to completely separate the different aerosol types ~~completely~~; it could also simply reflect the fact that the cooking experiments represent single source processes, whereas the ambient COA data represent an aerosol that is a mixture of a large number of sources. The PMF results from the Christmas market measurements (Sect. 3.5) can be found in the same area of the rectangle plot, but partially outside the one-sigma range of the literature COA results. It is noteworthy that the box representing the results of the pure rapeseed oil measurements is shifted to slightly larger f_{55} values compared to those from the laboratory cooking experiments. This result suggests that although the correlation analysis shows a high similarity between the rapeseed oil and the cooking emission mass spectra, the cooking emissions contain other components in addition to rapeseed oil. Similarly, for pure oleic acid (taken from the AMS spectra database), f_{55} is significantly larger than the value found for the cooking related aerosols and rapeseed oil, probably due to the fact that the~~y~~ latter also contain other components. The rectangle plot of f_{55}/f_{57} versus f_{55} ~~rectangle plot~~ also shows that, based on this combination of COA markers for example, ~~e.g.~~ BBOA is not well separated from CCOA, CSOA and several OOA aerosol types~~, based on this combination of COA markers~~.

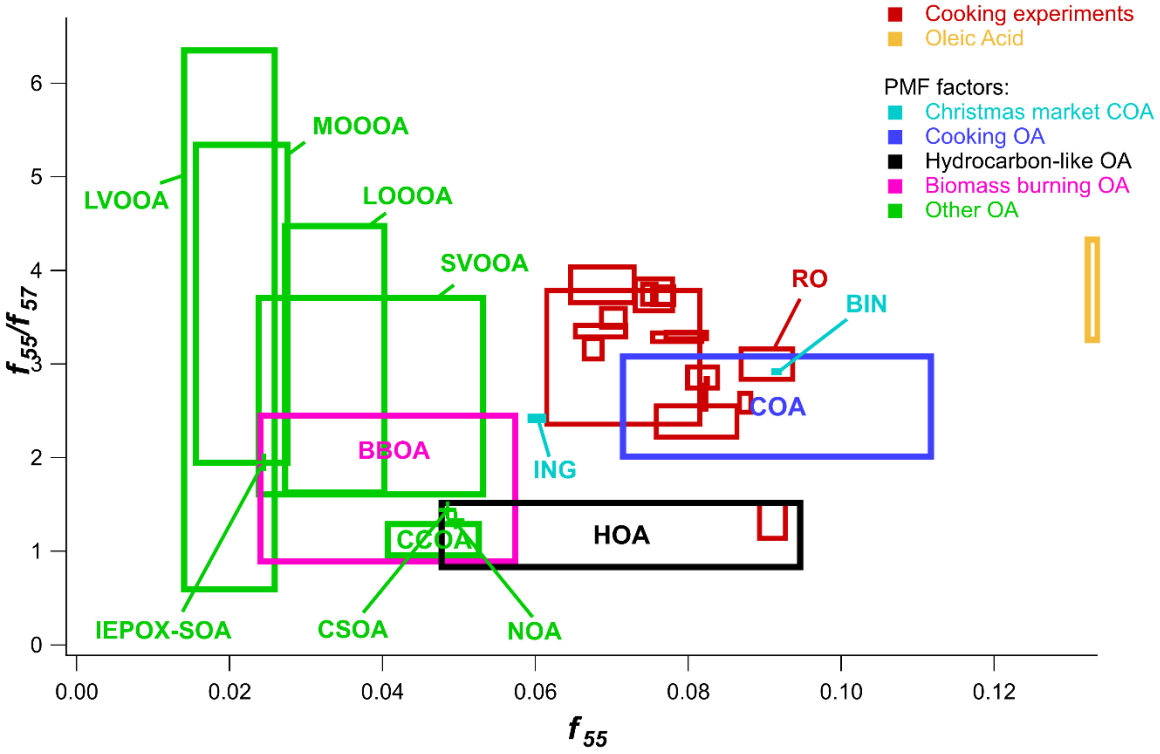

Figure 4: "Rectangle plot" of f_{55}/f_{57} combined with f_{55} for the cooking experiments and ~~various~~ different organic aerosol types from ambient measurements. The rectangles represent one~~the~~ standard deviation of the markers for the respective aerosol types as found in

mass spectra from the literature. The acronyms for the different aerosol types are listed in Table 2~~Table 2~~; RO stands for rapeseed oil; ING and BIN stand for the Christmas market measurements in Ingelheim and Bingen, respectively.

To determine whether the ~~ratio~~ f_{67}/f_{69} ratio is suitable as a COA marker, these ratios were plotted together with f_{55} in another "rectangle plot" (Fig. 5~~4~~). Also for this combination of markers, the cooking results are found in the upper right area of the plot, well separated from the other aerosol types. Only for the charcoal grilled steak experiment was an overlap found with the HOA box. The rapeseed oil results are found on the higher f_{55} side of the laboratory cooking experiments, as in the previous rectangle plot (Fig. 4)~~Although the laboratory results and ambient COA are well separated from most other aerosol types, there is an overlap with HOA for two of the laboratory experiments~~. ~~Therefore,~~ From these results we conclude that the ~~ratio~~ f_{67}/f_{69} ratio may~~might~~ be a marker for COA similar ~~as~~ to the ~~ratio~~ f_{55}/f_{57} ratio, but the influence of the fatty acid composition of the emitted oil or fat ~~needs to~~must be considered (see Sect. 3.1.2). Therefore, the ~~ratio of~~ f_{67}/f_{69} ratio should only be used as an additional marker for COA.

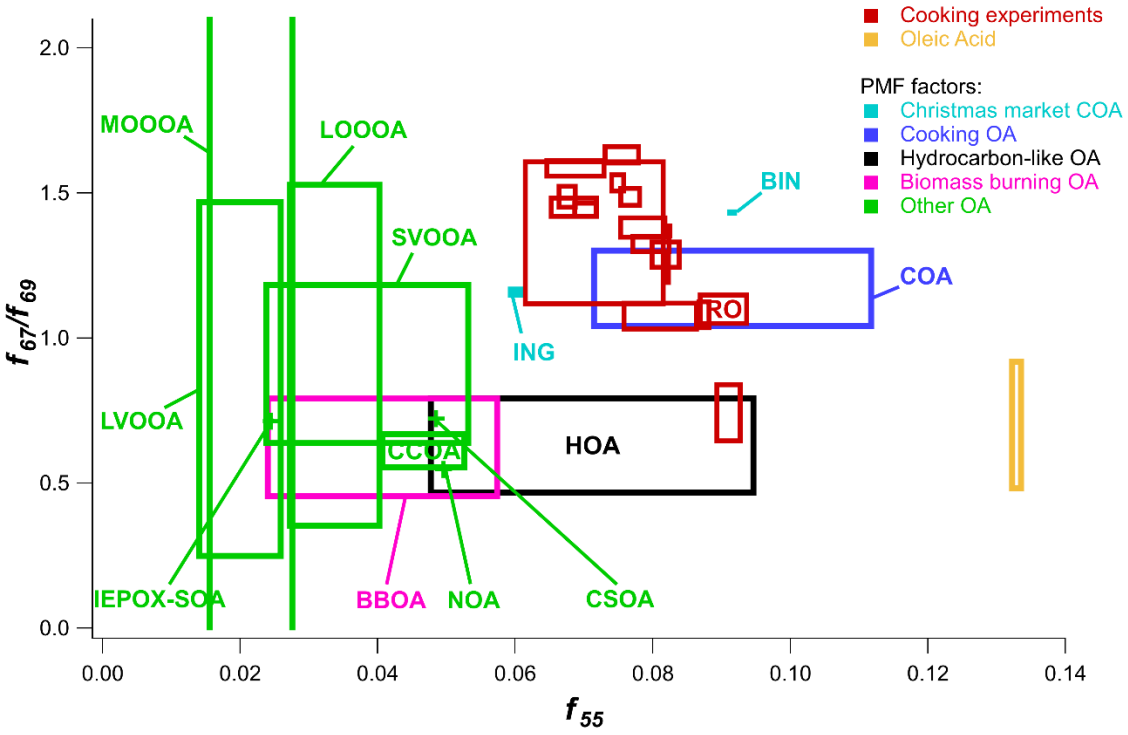

Figure 5~~4~~: "Rectangle plot" of f_{67}/f_{69} combined with f_{55} for the cooking experiments and ~~various~~ different organic aerosol types from ambient measurements. The rectangles represent one~~the~~ standard deviation of the markers for the respective aerosol types as found in mass spectra from the literature. The acronyms for the different aerosol types are listed in Table 2~~Table 2~~; RO stands for rapeseed oil; ING and BIN stand for the Christmas market measurements in Ingelheim and Bingen, respectively.

The high-resolution mass spectra from the cooking experiments were used to extract further information about the individual ions that contribute to the specific cooking-related mass spectra. Due to the strong fragmentation of organic molecules in the AMS analysis process, the individual ions measured by the instrument provide little information about the corresponding aerosol components. For this reason, AMS organics analysis typically reports ion families (i.e., groups of ions containing specific combinations of atomic contributions) rather than individual ions. For the *m/z* discussed in the previous "rectangle plots" (*m/z* 55, 57, 67, and 69), ions associated with the C_yH_y and C_xH_yO ion families are observed for the cooking experiments. In addition, ions of the $C_xH_yO_2$ family are found at very low abundance in the *m/z* 57 and *m/z* 69 signals.

Table 4 illustrates the contribution of different ion families to the individual marker *m/z* signals and corresponding ions. For each ion family at each *m/z*, in addition to the ~~"regular"~~main ion, an isotope ion containing ^{13}C is listed. These contribute approximately 2-3% of the respective family signal. For all marker *m/z*, the signal is dominated by the pure hydrocarbon ions (i.e., the ions from the C_xH_y family) with smaller relative contributions for *m/z* 55 and 57 (75% and 86%, respectively), in comparison to those for

m/z 67 and 69 (~100% and 96%, respectively). Consequently, the relative contribution of oxygen-containing ions is larger for *m*/z 55 and 57 and almost negligible for *m*/z 67. The uncertainties provided in Table 4 are the standard deviations for the individual relative ion family contributions, calculated from all cooking experiments. The uncertainty due to background subtraction and variations in background concentrations is much smaller than the variability between individual cooking experiments and is included in these values. In general, no significant difference in the relative contributions of the different ion families is observed across different cooking methods, with the exception of grilling, which shows a notable difference in the *m*/z 57 and *m*/z 69 composition. The contribution of the C_xH_yO family ions in the grilling experiments is significantly higher (18.1% for *m*/z 57 and 6.4% for *m*/z 69) than in the other experiments (12.4% for *m*/z 57 and 3.5% for *m*/z 69). This suggests that the grilling method results in an enhanced production of oxygen-containing substances, in comparison to the other cooking methods.

Table 4: Contribution of individual ion families and their associated ions to the ion signal at the four cooking-related marker *m*/z.

m/z	C_xH_y family		C_xH_yO family		$C_xH_yO_2$ family	
	ions	contribution	ions	contribution	ions	contribution
55	$^{13}CC_3H_6^+$, $C_4H_7^+$	75±4%	$^{13}CC_2H_2O^+$, $C_3H_3O^+$	25±4%	-	-
57	$^{13}CC_3H_8^+$, $C_4H_9^+$	86±5%	$^{13}CC_2H_4O^+$, $C_3H_5O^+$	14±5%	$^{13}CCO_2^+$, $C_2HO_2^+$	0.3±0.4%
67	$^{13}CC_4H_6^+$, $C_5H_7^+$	99.9±0.3%	$^{13}CC_3H_2O^+$, $C_3H_3O^+$	0.1±0.3%	-	-
69	$^{13}CC_4H_8^+$, $C_5H_9^+$	96±2%	$^{13}CC_3H_4O^+$, $C_4H_5O^+$	4±2%	$^{13}CC_2O_2^+$, $C_3HO_2^+$	0.3±0.3%

3.1.4 Relative ionization efficiency of cooking-related organic aerosol

The quantification of the aerosol species measured with the AMS is based on Eq. (2) (Canagaratna et al., 2007)

$$C_S = \frac{10^{12}\ MW_{NO_3}}{CE_S\ RIE_S\ IE_{NO_3}\ Q_{AMS}\ N_A} \sum_{all\ i} I_{S.i} \qquad (2)$$

~~converting~~ where the ion rates of species S, $I_{S,i}$, summed over all i *m*/z, are converted to mass concentrations C_S, with MW_{NO_3} the molecular weight of nitrate (in g mol^{-1}), Q_{AMS} the volumetric inlet flow rate (in cm^3 s^{-1}), N_A Avogadro's number and 10^{12} a unit conversion factor to µg m^{-3}. The remaining (unitless) factors in Eq. (2) are from calibrations or based on assumptions. The collection efficiency CE_S for the species S ~~gives~~ is the ratio of the particle mass measured by the AMS to the particle mass introduced into the inlet. It is mainly influenced by the particle phase, solid or liquid. The typical value for ambient aerosol is 0.5, which account~~sing~~ for mainly solid particles, a fraction of which bounces off the vaporizer without being vaporized. For the particles from the presented cooking experiments, a CE value of 1 was chosen, assuming that the emitted aerosol ~~mostly consisted mostly of~~ contained substantial amounts of liquid oil ~~droplets~~ (see Sect. 3.1.1), which ~~do not~~suppresses bounce (Matthew et al., 2008).

The ionization efficiency of nitrate IE_{NO_3}, determined in a calibration, is used as ~~a~~ the basis ~~to~~ for calculating~~e~~ the ionization efficiencies for other species, using the relative ionization efficiency of species S (RIE_S) relative to IE_{NO_3}. The default value for RIE_{Org} is 1.4, based on ~~multiple~~ laboratory experiments with ~~various~~ different types of organic species (Canagaratna et al., 2007). ~~As~~ Because COA concentrations ~~of COA~~ measured with the AMS in previous studies were found to be higher ~~compared to~~than those from parallel measurements with other instruments, ~~the~~ RIE_{COA} is assumed to be ~~larger~~ greater than 1.4 (Katz et al., 2021; Reyes-Villegas et al., 2018; Yin et al., 2015).

In this work, RIE_{COA} was determined ~~through~~ by comparing~~son of~~ the PM_1 mass concentration determined from the FMPS and OPC measurements (PM_1) ~~to~~ with the total AMS and black carbon mass concentration ($PM_{1,AMS+BC}$)~~,~~ measured in parallel. The

oven and boiling experiments were excluded from this analysis due to almost exclusively low measured organic mass concentrations (< 1 µg m^{-3}). The density ~~for~~ of the fine particles used to calculate PM_1 from the particle volume was in the range of 0.91 – 1.03 g cm^{-3} (Table S5), determined individually for each dish (see Sect. S1). These values are in good agreement with the densities for cooking emissions found by Katz et al. (2021) (0.95 – 1.0 g cm^{-3}), and, considering their uncertainty of 15%, also with that of rapeseed oil (0.91 g cm^{-3}), ~~in agreement~~consistent with our assumption that the particulate emissions from the cooking experiments ~~consisted mainly~~ contained substantial amounts of vaporized and recondensed~~of~~ oil or fatty acids (see Sect. 3.1.1). The measured PM_1 was~~consisted~~ mostly composed of organics (see Sect. 3.1.1; the contribution of BC was negligible); consequently, as expected, $PM_{1,AMS+BC}$ was higher for most of the cooking experiments compared to PM_1 when using the default RIE_{Org} = 1.4. To determine the RIE_{COA} for ~~the individual~~each experiment~~s~~ (or, more ~~specifically~~precisely, the product of RIE_{COA} and CE; we assume CE = 1), the $PM_{1,AMS+BC}$ time series was correlated with ~~the one~~that of PM_1 for each experiment separately and the RIE_{COA} was adjusted to obtain a slope of 1 for the correlation. For the grilling experiments, the RIE values were determined separately for the ~~experimental phases~~ "grilling" and "grill warm-up" experimental phases,~~with~~ the latter ~~ones~~ not being considered as RIE_{COA}. A typical example correlation for each cooking method is shown in Figure S4. The resulting RIE_{COA} values for the cooking experiments were in the range of 1.53 – 2.52 and thus frequently significantly ~~above~~ higher than the default value of 1.4 (Fig. 6~~5~~ and Table S5). The uncertainty for the determined RIE_{COA} value was estimated to be 38%, based on the method of Katz et al. (2021) with uncertainty propagation (see Sect. S3).

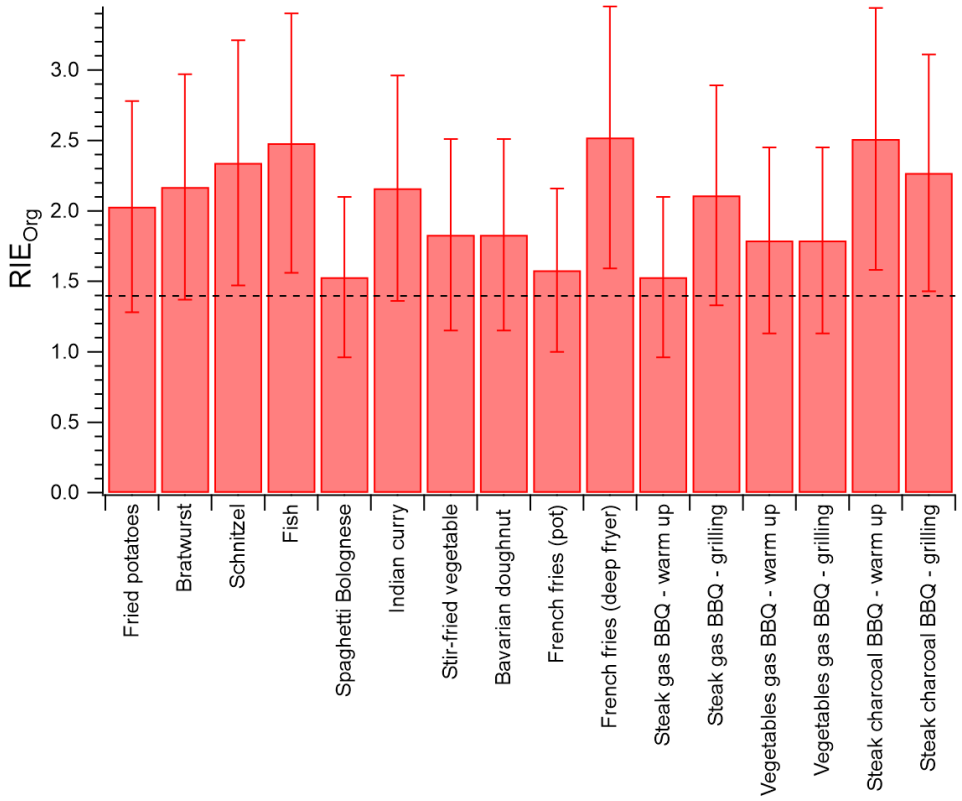

Figure 6~~5~~: RIE_{COA} obtained for the different cooking experiments. The default RIE_{Org} of 1.4 is shown as a dashed line.

In previous AMS studies of cooking ~~related~~ emissions, the ~~determined~~ RIE_{COA} determined was also ~~above~~ greater than 1.4. Reyes-Villegas et al. (2018) determined RIE values of 1.56 – 3.06 for cooking emissions from different types of dishes, comparable to our results, ~~through~~ by comparing~~son of~~ the measured concentrations (CE = 1) with ~~SMPS (~~scanning mobility particle sizer (SMPS) size distribution measurements (d_p = 18 – 514 nm)~~, comparable to our results~~. In contrast, ~~from indoor aerosol~~

~~measurements during cooking events,~~ Katz et al. (2021) found significantly ~~determined considerably~~ higher RIE_{COA} values of 4.26 – 6.50 from indoor aerosol measurements during cooking experiments with CE = 1, also ~~through~~ by comparison with SMPS data (d_p = 4 – 532 nm). A possible explanation for the ~~larger~~ higher values ~~from~~ of Katz et al. (2021) could be that the RIE_{COA} depends on the fatty acid composition of the oil or fat containing droplets. For oleic acid, the main fatty acid of rapeseed oil ~~which was~~ used in the present study and ~~the one~~that of Reyes-Villegas et al. (2018), Katz et al. (2021) obtained an RIE value of 3.18 ± 0.95, similar to the value of 3.0 measured by Xu et al. (2018), while for linoleic acid, the main component of soybean oil, ~~which~~ used by Katz et al. (2021) ~~used~~ for their cooking experiments, an RIE value of 5.77 ± 1.73 was found.

Summarizing the results ~~from~~ of the current and previous studies, we recommend ~~for measurements close to cooking emission sources~~ an RIE_{COA} ~~larger~~ greater than 1.4 for the COA fraction of the measured organic aerosol for measurements near cooking emission sources. Depending on the cooking oil, which ~~presumably has~~is expected to have a strong influence on the RIE_{COA} value, we suggest ~~for soy oil based cooking~~ an average RIE_{COA} of 5.16 ± 0.77 (average of all measurements with standard deviation) for soybean oil-based cooking, based on the measurements ~~by~~ of Katz et al. (2021), while for rapeseed oil-based cooking we recommend an average RIE_{COA} of 2.17 ± 0.48 (average of the averages ~~from~~ of both studies ~~and~~ with standard error), based on the ~~presented~~ measurements presented in ~~of~~ this study and ~~the ones~~those of ~~by~~ Reyes-Villegas et al. (2018). The individual values used for this estimate are listed in Table S5.

3.2 Emission dynamics related to temperature and cooking activities

In order ~~T~~to study the emission dynamics during cooking as a consequence of different activities, the concentration time series ~~determined~~ obtained for all dishes and for all measured variables were ~~inspected~~ examined in combination with the webcam recordings. For six emission variables, increases and changes over the ~~preparation~~ cooking time were identified: particle number concentration of smaller and larger particles measured by ~~the~~ CPC (PNC, d_p > 5 nm) and OPC ($PNC_{d>250\ nm}$), PM concentration (PM_1, $PM_{2.5}$, PM_{10}), BC, PAH, and organics mass concentrations (shown ~~exemplarily for the experiment "frying bratwurst"~~ in Fig. S~~4~~5 as an example for the "frying bratwurst" experiment). ~~From~~ Of these six, $PNC_{d>250nm}$, organics and PM mass concentrations are all ~~associated with~~related to the total emitted particle mass and therefore show similar emission dynamics. No increase above the detection limit was observed for the measured trace gas concentrations, except for NO_x during the grilling experiments and SO_2 during the charcoal grilling experiment.

~~For the six variables, t~~Two ~~kinds~~ types of systematic changes were observed for the six variables. First~~ly~~, the measured concentrations for these variables increased over the ~~preparation~~ cooking ~~period~~time, along with a~~n~~ general increase ~~of the~~in food and cookware temperature, as deduced from repeated manual temperature measurements with the IR camera. The emission concentrations usually started to increase only after a certain heating or cooking ~~period~~time, probably when the used oil and the food reached a certain temperature. Also, during ~~inactivity of~~ sufficiently long periods of inactivity ~~times~~, i.e. more than ~~approximately~~ about 30 – 60 s, the $PNC_{d>250\ nm}$ and organics mass concentrations increased, ~~as~~probably because certain ~~locations~~ parts of the food reached sufficiently high temperatures. Such increased particle mass and number emissions with higher temperature were also observed in previous studies, e.g. by Buonanno et al. (2009), Amouei Torkmahalleh et al. (2012), and Zhang et al. (2010).

The ~~R~~reason for this progressive increase ~~of~~ in concentration~~s~~ is presumably the increased~~ing~~ vaporization of substances with ~~rising~~ increasing temperatures. After emission, the vaporized substances cool down again, ~~finally resulting in~~eventually leading to increased particle number and mass concentration due to nucleation and re-condensation. ~~Accordingly~~Correspondingly, the emission concentrations decreased ~~when~~ as the power of the stove was ~~turned down~~reduced.

An increase ~~of~~ in BC and PAH mass concentrations ~~was~~ has only been observed ~~only~~ for high-temperature cooking methods ~~operating at high temperatures like~~ such as grilling or ~~in~~ the final ~~phase~~ stage of ~~preparing~~ stir-frying~~ied dishes~~. PAHs are formed at high temperatures, especially above 400 °C, and due to incomplete combustion, ~~like~~ such as during grilling, where BC is also formed ~~as well~~ (Jägerstad and Skog, 2005; Lijinsky, 1991; Omidvarborna et al., 2015). The described dependence of the measured concentrations on temperature is ~~shown~~ schematically illustrated in Fig. 7~~6~~. Due to the substantial heterogeneity of the temperature distribution throughout the food and cookware and the unknown location of the generation of emissions, this relationship can only be presented qualitatively.

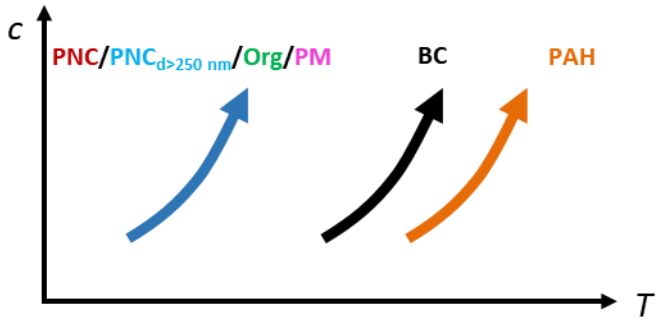

Figure 7~~6~~: Schematic diagram of the temperature (*T*) dependence of the emission concentrations (*c*) of six relevant species.

The second systematic observation ~~are~~ is the short-term~~ime~~ concentration changes associated with ~~different~~ various activities during cooking, ~~e.g.~~such as tilting the pan or ~~flipping~~ turning the food, which have not been studied in such detail before ~~so far~~. The activities leading to these short-term~~ime~~ changes are ~~schematically~~ shown schematically in Fig. ~~7~~ 8 ~~(symbols explained in Fig. S5)~~, grouped by emission variable~~s~~, with the increase factors by which the concentrations change from ~~right~~ just before the increase ~~up~~ to the corresponding maximum concentration. The factors are color-coded~~,~~ : ~~in~~ green for relative increases of less than~~below~~ one order of magnitude, ~~in~~ yellow for increases ~~above~~ of more than one order of magnitude, and ~~in~~ red for increases ~~above~~ of more than two orders of magnitude.

~~The e~~Presumably the emission concentrations ~~rise~~ increase briefly when hot material ~~of~~ from the cooked food is brought to the surface by stirring or similar activities, facilitating vaporization. This leads to increased particle formation and growth through condensation of these substances. ~~Furthermore~~In addition, contact ~~of~~ between cold, water-containing foods ~~with strongly~~and highly heated surfaces, such as the pan, grill, or hot oil, ~~leads to~~results in rapid vaporization of oil, various other substances, and~~, above all,~~ especially water, which can ~~cause~~ lead to bubbling of the oil. The ~~associated enhancement~~resulting increase in ~~of the~~ oil surface area presumably leads to increased vaporization of oil and mechanical formation of larger particles due to the bursting of oil bubbles. These processes ~~rapidly~~ decrease rapidly as the hot surface cools ~~down~~. Similarly, ~~short term~~momentary increases in concentration occur when droplets or components of the grilled food, as well as residues from cleaning the grate, fall onto hot surfaces, such as the charcoal, and quickly vaporize or burn. ~~Due to t~~The high temperatures at these locations~~,~~ also cause transient ~~concentration~~ increases ~~of~~ in BC and PAH concentrations ~~are generated~~. The ~~strongest~~ largest relative increases in ~~the~~ emission concentrations for almost all variables were observed when the oven was opened during baking, presumably due to the low concentrations before the oven was opened and the sudden release of emissions ~~which~~ that had accumulated ~~with~~in the oven.

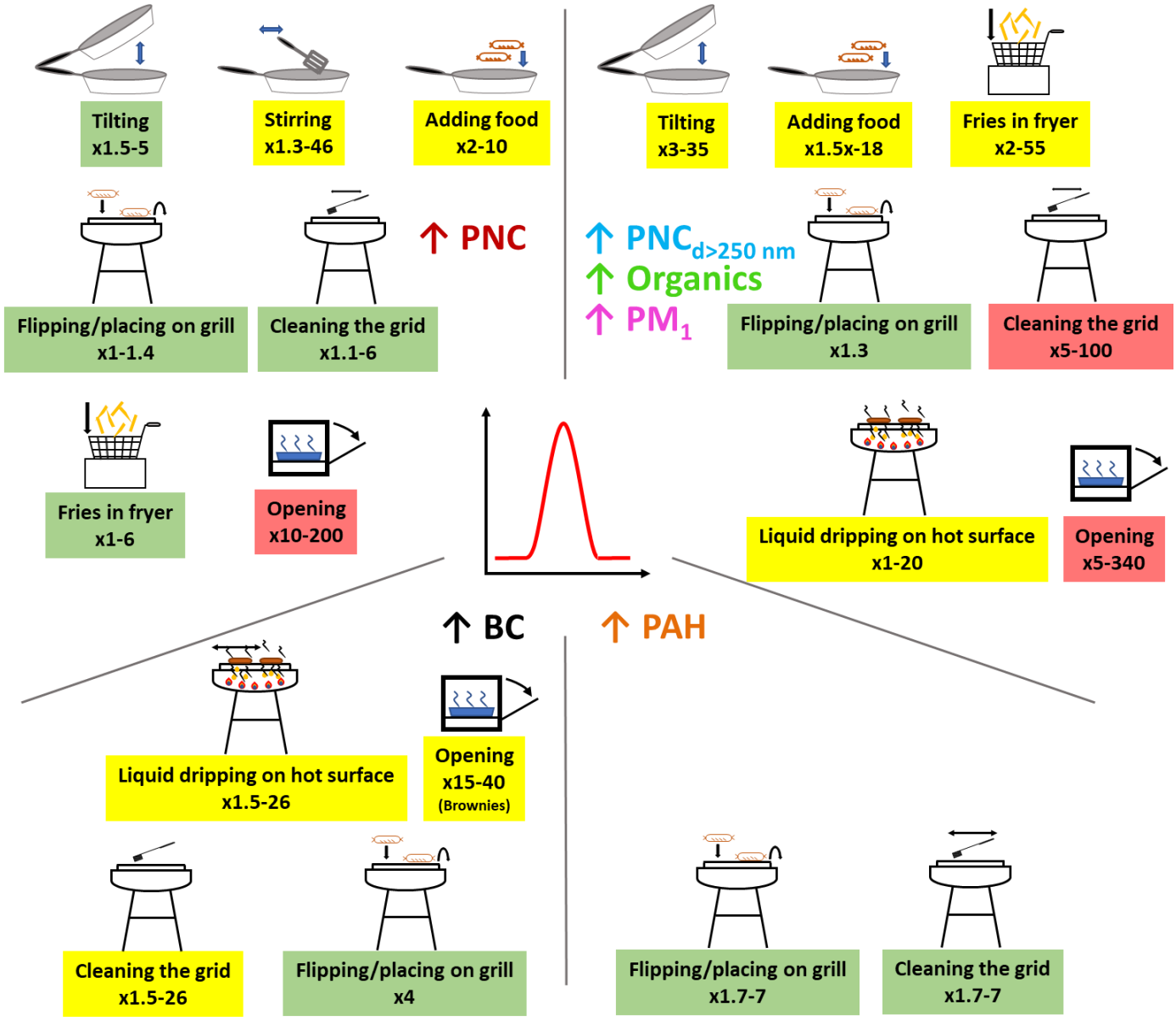

Figure ~~8~~7: Schematic diagram of the short-term~~time~~ concentration increases for the different variables due to various activities during the ~~preparation~~ cooking of the dishes ~~(see Fig. S4~~5 ~~for the meaning of the symbols)~~. PM_1 is shown as representative~~ly for~~ of PM. The range of factors by which ~~the~~ concentrations typically increase ~~are~~ is shown as numbers and color-coded, ~~in~~ green for small, ~~in~~ yellow for medium, and ~~in~~ red for high concentration increases.

3.3 Influence of ~~preparation~~ cooking method and cooking activities on the particle size distribution

The averaged particle number and volume size distributions of the emitted aerosols were similar for dishes with the same ~~preparation~~ cooking method in terms of particle mode position and intensity ~~of the particle mode~~. An overview of the mode diameters for the aerosols emitted during the ~~preparation~~ cooking of different dishes, grouped by ~~the preparation~~ cooking method or dish type, is shown in Table 5~~Table 4~~. The average standard deviation of the mode diameters from the three ~~repetitions~~ replicates was 5 nm for the particle number size distribution and 25 nm for the particle volume size distribution. Therefore, the observed differences between the distributions for the different ~~preparation~~ cooking methods were partially statistically significant.

The particle number distribution for most dishes was dominated by Aitken mode particles. The mode diameters ($d_{p,N}$) varied~~,~~ between 20 and 50 nm depending on the ~~preparation~~ cooking method~~, between 20 – 50 nm~~ (Fig. S6). During the warm-up phase of the grilling experiments, the size distribution was broader and plateau-like, presumably due to a combination of different particle

generation processes, ~~like~~ such as combustion of ~~leftovers from the~~ grid residues and incomplete combustion of ~~the~~ charcoal, but also dominated by Aitken mode particles (10 – 30 nm).

The average volume size distributions showed more variability for the different ~~preparation~~ cooking methods (Fig. S7). The distributions were mostly bimodal with an Aitken or accumulation mode and a coarse mode. ~~During~~ For baking and grilling with gas, the mode diameter of the fine particles was in the Aitken mode range ($d_{p,V}$ = 50 – 70 nm) while ~~during~~ for frying and grilling with charcoal the distribution was dominated by accumulation mode particles (200 – 300 nm). The coarse mode diameter was in the range of 2 – 3 µm.

Table ~~5~~4: Range of mode diameters from the averaged particle number and volume size distributions for particles emitted from ~~the~~ cooking ~~of~~ different dishes, sorted by mode diameter (dN/dlogd_p).

~~Preparation~~ Cooking method/ dish type	Dishes	Mode diameter dN/dlogd_p ($d_{p,N}$)	Mode diameter dV/dlogd_p ($d_{p,V}$)
Grill warm up (gas, charcoal)		20 ─ 30 nm	Gas: 50 ─ 60 nm, 2.5 ─ 3 µm Charcoal: 300 nm, 720 nm, 2.2 µm
Deep-frying in pot	French fries, Bavarian doughnut	20 ─ 30 nm	275 ─ 280 nm, 2 µm
Stir-frying with sauce	Spaghetti Bolognese, stir-fried vegetables, Indian curry	20 ─ 35 nm	205 ─ 220 nm, 2 ─ 3 µm
Grilling with gas	Vegetable skewers, steak	30 ─ 35 nm	60 ─ 70 nm, 2 ─ 5 µm
Baking	Baked potatoes, pizza, brownies	30 ─ 35 nm	45 ─ 70 nm, 2 ─ 3 µm
Stir-frying	Fried potatoes, bratwurst, schnitzel, fish	40 ─ 50 nm	205 ─ 220 nm, 2 ─ 3 µm
Deep-frying in deep fryer	French fries	50 nm	205 nm, 2 ─ 3 µm
Grilling with charcoal	Steak	50 nm	205 nm, 600 nm, 2.2 µm
Boiling	Boiled potatoes, rice, noodles	No clear result due to small concentrations	300 ─ 465 nm

Presumably, the observed mode diameter of the emitted fine (i.e., submicron) aerosol is most~~ly~~ ~~influenced~~ affected by the temperature of the prepared food and cookware. ~~With h~~Higher temperatures allow more oil and other substances ~~can~~ to vaporize, ~~leading to stronger~~resulting in greater particle growth and consequently larger particles. For example, particles from stir-fried dishes were larger ($d_{p,N}$ = 40 – 50 nm) than those from stir-fried dishes with sauce (20 – 35 nm) ~~as~~ because the addition of the sauce cooled ~~down~~ the food and pan and the sauce effectively covered the hottest part of the system, the ~~base~~ bottom of the pan. ~~Furthermore~~In addition, the ~~available~~ amount of material ~~which can~~available for vaporization ~~influences~~ affects the particle growth. For example, ~~during~~ frying, ~~has compared to baking,~~ more oil ~~is~~ available ~~which can~~to vaporize compared to baking, where it is limited to the dough components, ~~leading~~ resulting in~~to~~ larger particles. ~~During~~ Charcoal grilling ~~with charcoal, compared to gas, the~~ produces larger particles ~~were larger~~than gas grilling because ~~as~~ the incomplete combustion of charcoal ~~generates~~ produces smoke and~~, due to~~ the higher temperature~~,~~ allows additional ~~substances~~ material to~~can~~ vaporize, ~~also~~ including from the charcoal itself.

The coarse mode particles are generated by mechanical processes, presumably by the bursting of~~from~~ oil bubble~~s bursting~~. ~~During~~ When grilling with charcoal, the combustion of the charcoal also ~~leads to~~results in the emission of coarse particles. The particles emitted from the boiled dishes are ~~presumably~~ probably initially coarse particles from ~~water bubble~~the bursting of water bubbles

with droplets containing dissolved salt and other food components, which shrink to accumulation mode particles due to the low relative humidity ~~to accumulation mode particles~~.

~~In accordance~~Consistent with our measurements, similar dependencies ~~for the~~of mode diameter ~~of the~~on temperature and available amount of vaporizable material ~~which can vaporize were~~ have been observed in previous studies. With increasing cooking temperatures Amouei Torkmahalleh et al. (2012), Buonanno et al. (2009), and Zhang et al. (2010) measured particle size distributions with larger mode diameters. Furthermore, Buonanno et al. (2009) observed large number mode diameters ($d_{p,N}$ = 40 – 50 nm) for emissions from grilling (without oil on an electric or gas grill) of fatty foods, ~~like~~ such as cheese, bacon, and sausage, ~~larger number mode diameters ($d_{p,N}$ = 40 – 50 nm)~~ compared to those from cooking vegetables ($d_{p,N}$ = 30 nm) showing that the availability of easily vaporizable substances, ~~here~~ in this case fat or its decomposition products, leads to larger particles.

~~Apart from~~In addition to the ~~preparation~~ cooking method, which is mainly characterized by the cooking temperature and the availability of water, oil, or fat, individual activities during ~~the~~ cooking also influence the particle size distribution of the emitted aerosol. Such influences are ~~shown~~ illustrated in Fig. ~~8~~ 9 using the example of ~~deep~~ frying French fries in ~~the~~ a deep fryer, showing the number size distributions (15 - 30 s time periods, averaged over all ~~repetitions~~replicates) of emissions during different activities or ~~preparation~~ cooking phases. ~~Included are t~~The corresponding PM_1 mass concentrations for the same time periods are also shown; colored arrows ~~illustrate~~ indicate the temporal changes.

~~In the beginning~~Initially, the particle number concentration, size, and mass concentration increase as the frozen French fries are placed in the basket above the oil and then submerged in~~to~~ the oil (pink arrow). When the fries are ~~put~~ placed in~~to~~ the basket, the oil ~~starts~~ begins to bubble as small ~~parts~~ pieces of the fries and ice crystals ~~drop~~ fall into the hot oil and the water immediately vaporizes ~~immediately~~. The bubbling increases when the French fries are submerged in~~to~~ the oil as more water ~~rapidly~~ vaporizes quickly. The bubbles increase the surface area of the oil, which ~~lead to a larger oil surface, enhancing~~ increases the vaporization of the oil and ~~therefore~~ the ~~particle~~ formation and growth of particles. As a ~~consequence~~ result of the frozen French fries in the oil, the oil cools ~~down~~ and less oil vaporizes, resulting in a decrease in~~and consequently the~~ particle number concentration, size, and mass concentration ~~decrease~~ (green arrow). As the oil slowly heats up again towards the end of the cooking process, all variables increase again due to increased oil vaporization (yellow arrow).

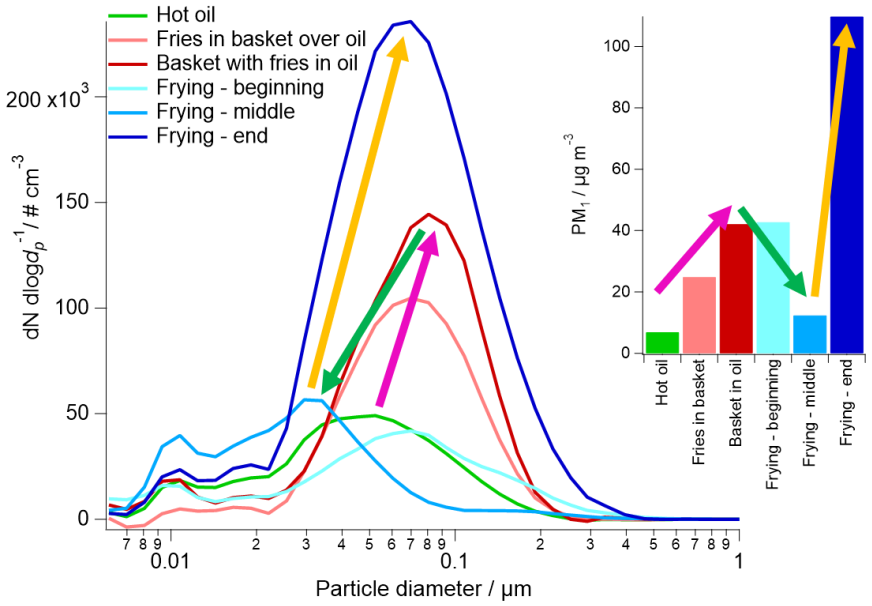

Figure ~~9~~8: Average number size distribution and PM_1 mass concentration for six different cooking activities ~~/~~ periods during the ~~preparation~~ cooking of French fries in ~~the~~ a deep fryer. The arrows ~~illustrate~~ indicate the temporal trends.

The example presented ~~example~~ illustrates the main parameters ~~which~~ that influence ~~the~~ particle emissions: 1. the temperature of the prepared food and cookware, 2. the oil surface, and 3. the available amount of vaporizable material, as also observed for the particle number concentration and mass concentration for ~~various~~ different variables (see Sect. 3.2). Similar dependencies were also observed during the ~~preparation~~ cooking of other dishes (Table 6~~Table 56~~). ~~Usually~~ In general, the mode diameter increased ~~over~~ during the ~~preparation~~ cooking ~~period~~time, as observed ~~e.g.~~for example during ~~the~~ heating of the oven and charcoal grilling ~~with charcoal~~. Presumably, the increase in temperature ~~increase~~ of the food and the cookware led to stronger vaporization of oil and other substances. Also, various activities during ~~the~~ food ~~preparation~~cooking ~~of the food~~ resulted in transient changes ~~of~~ in the size of the emitted particles, analogous to the changes ~~of the~~in emission intensity, as ~~presented~~ discussed in Sect. 3.2. In addition, when the grid of the grill was cleaned with a brush, the particle size increased, presumably because leftovers fell ~~off~~ from the grid onto the charcoal and burned or vaporized. A similar process was observed when steaks were cut on the grill and the meat juices ~~drops~~ vaporized ~~off~~ from the hot grid or charcoal, also resulting in~~leading to~~ larger particles ~~as well~~.

Table ~~6~~5: Overview of ~~the~~ particle mode diameter changes due to individual activities.

Process/activity	Mode diameter dN/dlogd_p	Reason
Charcoal ~~G~~grilling ~~on charcoal~~	35 nm → 170 nm	Temperature ~~I~~increase ~~of temperature~~ over time
Stir-frying	30 nm → 60 nm	Temperature ~~I~~increase ~~of temperature~~ over time
Heating of oven	17 nm → 40 nm	Temperature ~~I~~increase ~~of temperature~~ over time
Cleaning the grid of the grill	Increase by 5 – 10 nm	Food ~~leftovers~~ residues from the grid vaporized on hot surface
Cutting steaks on grill	Increase by 5 – 10 nm	Meat juices vaporized from hot surface

3.4 Quantification of cooking emissions: Emission factors

~~To be able~~In order to quantitatively estimate the emissions from cooking activities and their impact on air quality based on the mass of food prepared ~~food~~, emission factors (amount of emitted substance per kg of food prepared ~~food~~) were calculated for all dishes from this study and for all relevant variables (Table S6). The emission factors for PN (particle number, as measured by the CPC) and PM_1 ~~emission factors~~ are shown ~~exemplarily~~ in Fig. ~~9~~ 10 as examples for all dishes, grouped ~~by~~ according to the respective ~~preparation~~ cooking method. For other mass-based variables, ~~e.g.~~such as organics, the general trends are similar to those ~~of~~ for PM_1~~,~~ ~~which~~ and are described ~~in the following~~below.

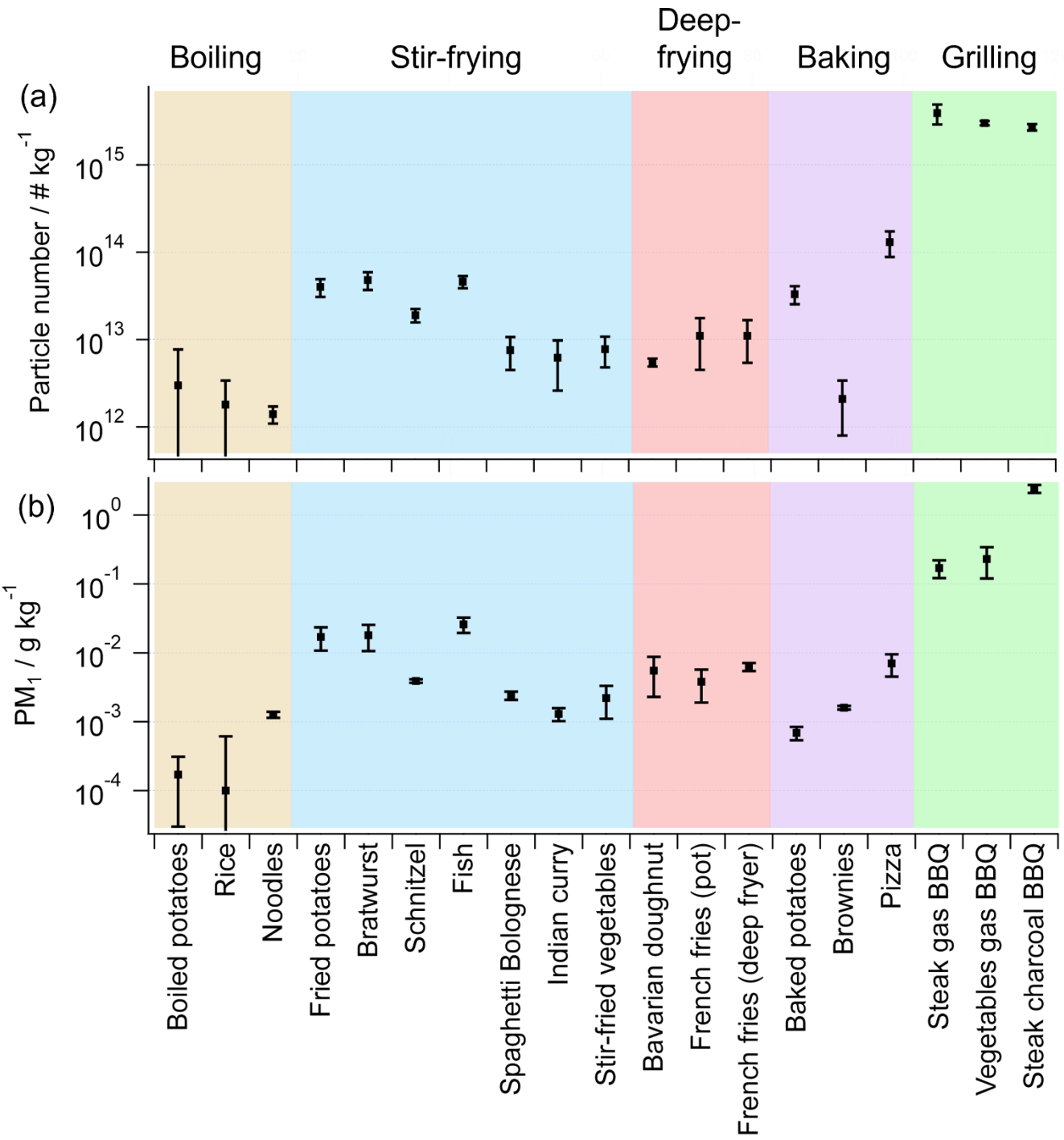

Figure ~~10~~9: Emission factors for (a) PN and (b) PM_1 for all dishes, with the standard deviation ~~from~~ of the three ~~repetitions~~ replicates as error bars. The values are grouped by ~~the preparation~~ cooking methods, highlighted ~~with~~ in different colors.

For dishes with the same ~~preparation~~ cooking method, the emission factors are similar and differ by at most one order of magnitude ~~apart from each other~~. The highest PN emission factors were observed for the grilling experiments with values up to $4 \cdot 10^{15}$ kg^{-1}~~,~~, while the emission factors for the oil-based or fat-containing dishes, including the ~~preparation~~ cooking methods stir-frying, deep-frying, and baking, are substantially smaller, ranging from $2.1 \cdot 10^{12} – 1.3 \cdot 10^{14}$ kg^{-1}. The smallest emission factors were observed for boiled dishes with values up to $3 \cdot 10^{12}$ kg^{-1}.

A similar trend was observed for PM_1 with the highest emission factors for the grilling experiments (0.2 – 2.4 g kg^{-1}) and one to two orders of magnitude ~~smaller~~ lower emission factors for stir-fried, deep-fried and baked dishes ($7 \cdot 10^{-4}$ – 0.026 g kg^{-1}). Again, the smallest emission factors were found for boiled dishes ($1 \cdot 10^{-4}$ – $1.3 \cdot 10^{-3}$ g kg^{-1}).

The $PN_{d>250\ nm}$ (number of particles measured by the OPC, i.e. with d_p >250 nm) emission factors range from $5 \cdot 10^{7}$ – $2 \cdot 10^{10}$ kg^{-1} for boiled and baked dishes, from more than $2 \cdot 10^{10}$ – $9 \cdot 10^{11}$ kg^{-1} for stir-fried, deep-fried, and gas-grilled dishes, and up to $2 \cdot 10^{13}$ kg^{-1} for the charcoal-grilled dish. BC and PAH emissions were ~~only~~ observed only for dishes where the cooking temperatures were sufficiently high for their formation, e.g. the grilling and stir-frying experiments (18 – 28,000 µg kg^{-1} and 3 – 208 µg kg^{-1}, respectively). Sulfate was ~~only~~ observed only for dishes ~~containing~~ with onions and for grilled dishes (6 – 354 µg kg^{-1}). ~~The~~ eEmission factors for all variables are listed in Table S6.

In ~~G~~general~~ly~~, the trends in the observed emission factors for the different ~~preparation~~ cooking methods were similar for the different measured variables. For mass-based or ~~-~~related variables (PM_1, organics, PAH, BC, and $PN_{d>250\ nm}$), the emission factors from the charcoal grilling experiment are ~~usually~~ typically one order of magnitude higher ~~compared to~~than those ~~of~~ from the gas grilling experiments. The incomplete combustion of the charcoal ~~leads to~~results in the additional emission of smoke ~~which includes~~containing larger particles and ~~in total~~a higher total emitted mass. The combustion of the charcoal during the ~~warm up~~heating of the grill already contributes ~~already~~ 34 – 52% of the total emissions for the whole cooking experiment, depending on the variable (PN, NO_x, organics: 34 – 40 %; PAH, $PM_{1/2.5/10}$, $PN_{d>250\ nm}$: 40 – 50 %; BC: 52 %). The emissions from grilling~~, compared to other preparation methods,~~ are one to two orders of magnitude higher than those from other cooking methods, presumably due to the burning of food ~~leftovers~~ residues ~~from~~ on the grid and ~~due to~~ the higher temperatures, which lead~~ing~~ to more vaporization of substances and ~~hence~~ thus to increased particle formation and growth due to re-condensation.

The emission factors for ~~the~~ stir-fried, deep-fried, and baked dishes were similar, ~~to each other as~~ since in these cases the emissions are ~~mostly~~ mainly due to the vaporization and re-condensation of oil and other substances, as well as mechanical processes ~~like~~ such as the vaporization of water, which lead~~sing~~ to oil bubbling and splashing. The lowest emissions were observed for boiled dishes, which was the only ~~applied preparation~~ cooking method used that did not involve ~~without any~~ oil or fatty food~~s involved~~. ~~For~~ In this ~~preparation~~ cooking method, the only source ~~for~~ of particles is the ~~bubble~~ bursting of bubbles, which results in ~~leading to~~ droplets ~~which~~ containing dissolved salt or other components.

That ~~O~~oil ~~-~~based cooking (e.g. deep-frying and stir-frying) ~~leading to~~results in higher particle number concentrations compared to water-based cooking (boiling and steaming) ~~was~~ has also been observed by See and Balasubramanian (2006), Wu et al. (2012), and Zhang et al. (2010). Similar observations were made for ~~the~~ emitted particle mass (Alves et al., 2014; See and Balasubramanian, 2006) and PAH emissions (Chen et al., 2007; Zhao et al., 2019).

For comparison with the results ~~from~~ of previous studies, PN and $PM_{2.5}$ emission rates (Table 7~~Table 6~~) were calculated for 1 kg of cooked food and 60 min of ~~preparation~~ cooking time (assuming that ~~the~~ food preparation takes one hour) for different ~~preparation~~ cooking methods. The emission rates determined from our experiments were mostly comparable to those obtained ~~from~~ in previous studies (He et al., 2004; Liao et al., 2006) or agreed with them within ~~an~~ one order of magnitude (Lee et al., 2001; Nasir and Colbeck, 2013). In contrast, ~~up to two orders of magnitude higher emission rates were reported by~~ Buonanno et al. (2009) reported emission rates up to two orders of magnitude higher for PN and ~~by~~ Olson and Burke (2006) for $PM_{2.5}$ ~~emissions~~.

Table 7~~6~~: PN and $PM_{2.5}$ emission rates for 1 kg of cooked food per ~~hour~~ 60 min ~~preparation~~ of cooking time, for different ~~preparation~~ cooking methods. Comparison of our results with those of previous studies.

	PN / kg^{-1} h^{-1}	$PM_{2.5}$ / mg kg^{-1} h^{-1}
Stir-frying		
This work	$5.2 \cdot 10^{13}$	23
Buonanno et al. (2011)	$4.5 \cdot 10^{15} – 5.4 \cdot 10^{15}$	
Nasir and Colbeck (2013)	$8 \cdot 10^{12}$	78
He et al. (2004)	$1.5 \cdot 10^{13}$	
Baking		
This work	$8.6 \cdot 10^{13}$	5
Nasir and Colbeck (2013)	$2.6 \cdot 10^{13}$	45
He et al. (2004)	$1.2 \cdot 10^{13}$	
Olson and Burke (2006)		600
Grilling		
This work		280 – 2700
Olson and Burke (2006)		10380
Deep-frying		
This work		10
Liao et al. (2006)		3.2 – 8
Lee et al. (2001)		70
Olson and Burke (2006)		3600

In the case of the study by Buonanno et al. (2011), these differences may be ~~caused by~~due to different measurement conditions, as the emissions in that study were measured in a closed kitchen with mechanical ventilation, at a distance of 2 m from the stove and not by capturing all emissions as in our study. In the case of the study by Olson and Burke (2006), who performed measurements with body-worn instruments to assess personal exposure, the massively ~~larger~~ higher emission rates they found compared to our and previous studies were presumably due to a combination of reasons, such as the influence of the high relative humidity on the measured particle mass, their assumptions about dilution of the emissions, and the use of peak concentrations for their calculation rather than averages over the entire experiment. ~~Firstly, the high relative humidity during cooking led to larger particles and consequently an overdetermination of particle concentrations due to increased light scattering in the nephelometers, which were used in their study to infer $PM_{2.5}$. In addition, the authors assumed that the emissions would be diluted equally in the whole apartment volume; however, as stated in their manuscript, inhomogeneous distribution of the emissions caused differences in the inferred emission rates depending on the measurement location (i.e. kitchen vs. living room). Finally, for their calculations of the emission rates they considered only the peak concentrations during cooking, while in the present study the whole cooking period was considered.~~

Overall, the comparison of emission rate measurements shows that the ~~obtained~~ emission rates obtained ~~are~~ depend~~ent~~ not only on the cooking conditions themselves, but also on the measurement (dilution) conditions and the method used to calculate the emission factors or rates. This ~~complicates the~~makes it difficult to compar~~eison of~~ different studies.

To obtain an idea ~~about~~ of the relevance of ~~the~~ emissions from cooking activities in relation to those from other emission sources, the emissions from the various ~~preparation~~ cooking methods were compared with emissions from traffic, biomass burning, burning of candles, and smoking. ~~To~~ For this ~~end~~purpose, ~~we calculated~~ the emissions from these sources were calculated for activities

over a period of one hour ~~each~~, i.e. for the one-time ~~preparation~~ cooking of a ~~dish~~ meal ("cooking"), for driving a car over a distance of 100 km ("~~traffic~~driving a car"), for smoking two cigarettes ("smoking"), and for ~~biomass~~ wood burning-based heating a room of 50 m^2 ("~~biomass burning~~wood home heating") or for burning a candle ("candle burning") for one hour. The emission factors for the various activities were taken from the literature~~, as~~ and are summarized in Table S7. As these activities are ~~chosen~~ partially arbitrarily chosen, this comparison only serves as a rough classification of cooking emissions compared to those of other emission sources.

The calculated emissions for the dishes with the same ~~preparation~~ cooking method were averaged for four variables: ~~PN,~~ PM_1, PN, BC, and PAH (Fig. 1~~0~~1 ~~and Fig. S8~~7~~6~~), and their standard deviation is used as the uncertainty. For the emissions from other sources, the ranges of emissions calculated from the emission factors found in the literature are presented as bars to reflect the variability of the emission levels.

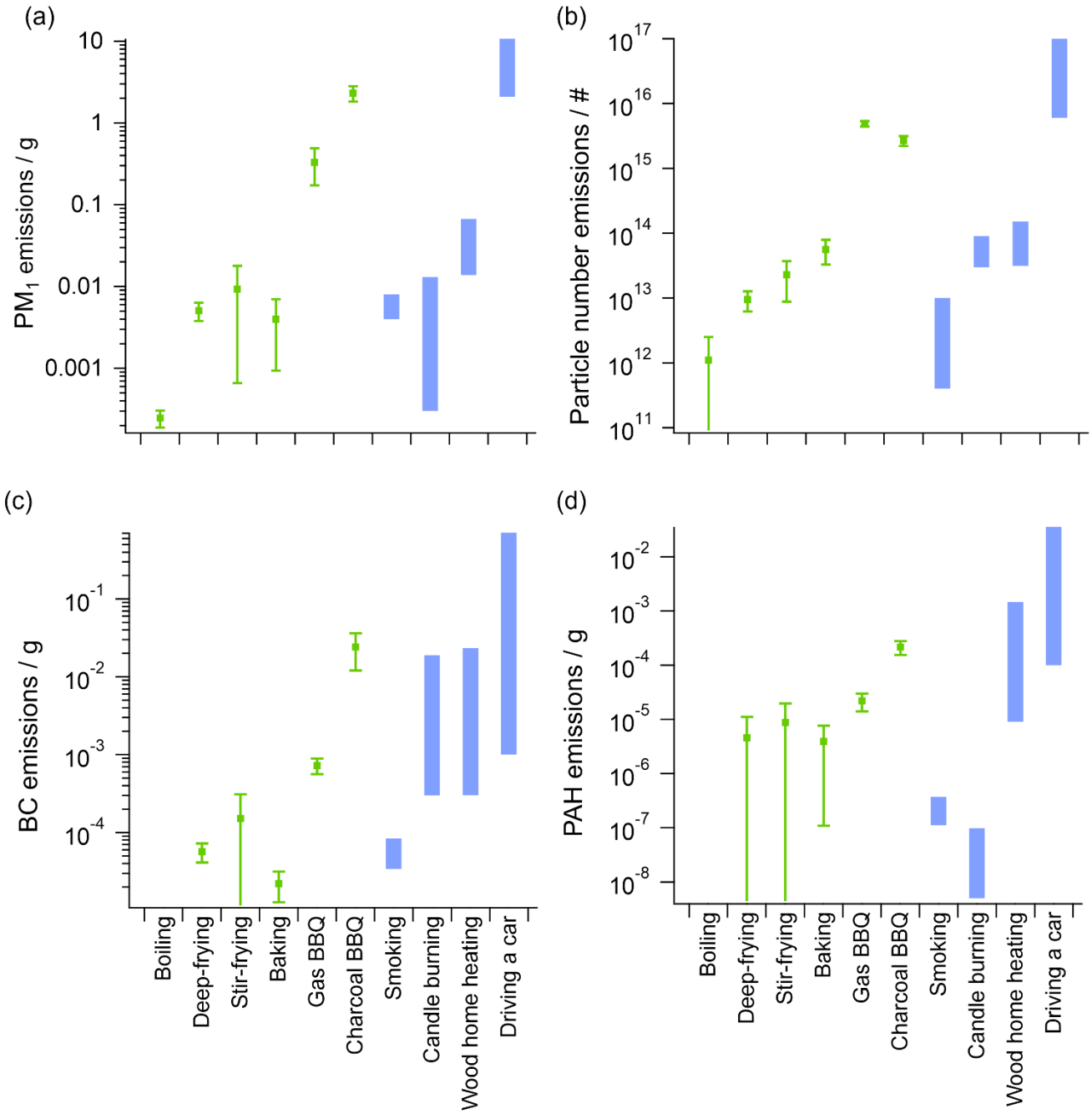

Figure 1110: Total emissions per unit activity of (a) PM_1 mass, and (b) particle number, (c) black carbon mass, and (d) PAH mass for cooking one dish, averaged for the different preparation cooking types methods with the standard deviation as error bars, and comparison with emissions from various other activities during one hour, shown as bars indicating the variability found in the literature.

For the mass-based variables (PM_1, BC, PAH), the highest cooking emissions, which were from charcoal grilling, are in the same range as those observed from traffic car driving, indicating the potential for a significant local impact of grilling on air quality. This assumption is supported by a study of by Kaltsonoudis et al. (2017), which shows that during a Greek holiday, when traditionally meat is traditionally grilled everywhere in all over the city, the contribution of COA reached up to 85% of the measured organic aerosol.

Stir-frying, deep-frying, and baking, all oil-based preparation cooking methods, show have emissions of similar order of magnitude to each other, typically on at the lower end of emissions from biomass wood burning-based room heating, and on at the upper end of emissions from candle burning and cigarette smoking. This finding is consistent with observations from ambient measurements, which show that COA can easily make up account for similar proportions of total organics as traffic- and biomass wood burning-related organic aerosols, especially particularly in urban environments (e.g., Mohr et al., 2012; Struckmeier et al., 2016). In indoor environments, cooking is one of the major emission sources leading to high emissions of fine particulate matter emissions, in terms of number and mass wise, even exceeding the emissions due to from light smoking (Abdullahi et al., 2013; Zhou et al., 2016; He et al., 2004).

Boiling, on the other hand, causes results in much smaller lower emissions, which are at the lower end or even below those of smoking and candle burning. Thus, Uunlike oil-based preparation cooking methods, boiling therefore will usually typically be not a major contributor have no strong contribution to the total ambient aerosol load, which is in line consistent with the conclusion that ambient COA consists mainly of externally mixed (Freutel et al., 2013) oil or fatty acids containing droplets (Allan et al., 2010).

3.5 Ambient measurements at two Christmas markets

At both Christmas markets, substantial increases in aerosol concentrations increases were measured during the opening hours compared to the background (i.e., the hours when the markets were closed) for the same six species which that were also relevant during in the laboratory measurements: PNC and $PNC_{d>250\ nm}$, PM, BC, PAH, and organics mass concentrations (Fig. S98 and Fig. S109). In Aaddition ally, CO_2 and particulate chloride concentrations increased, especially particularly at the market in Ingelheim, both presumably due to wood burning of wood at the market (Fachinger et al., 2018; Levin et al., 2010; Williams et al., 2012). A summary of the measured concentrations (represented shown in box plots) for time periods inside within and outside the of opening hours is shown in Fig. 121, which illustrates the increase of in concentrations due to the Christmas market emissions.

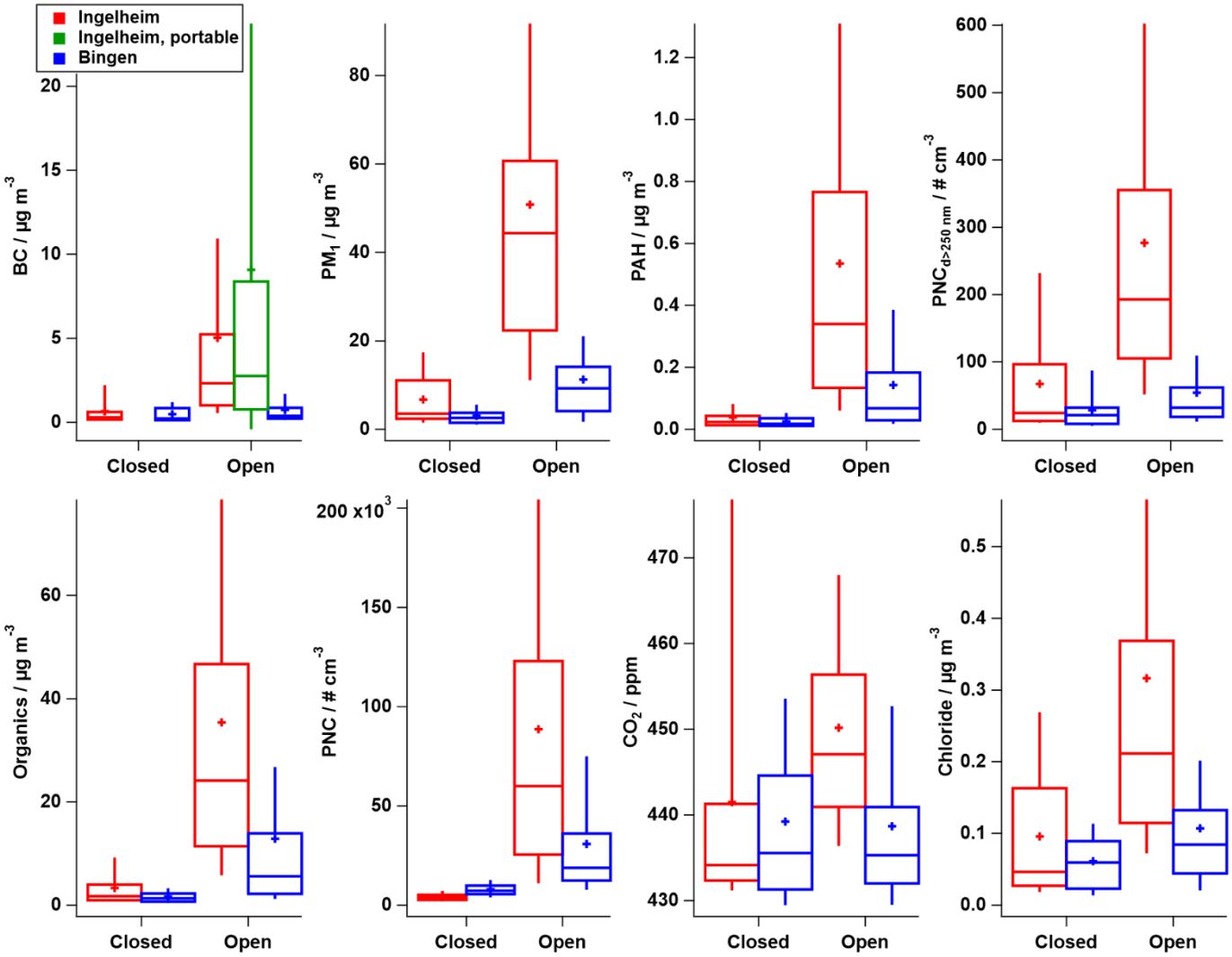

Figure 12~~11~~: Pollutant concentrations measured during (open) and outside (closed) ~~the~~ opening hours ~~for~~ of the Christmas markets in Ingelheim (red and green) and Bingen (blue). For each variable, the average concentration is shown as cross, the 25th and 75th percentiles as a box, ~~with~~ the median as a horizontal bar, and the 10th and 90th percentiles as whiskers.

In Ingelheim, the median PNC and the mass concentrations of organics, PM_1 and PAH ~~mass concentrations~~ were ~~larger during the opening hours by~~ more than one order of magnitude higher during the opening hours than during ~~compared to~~ the background period. The median $PNC_{d>250\ nm}$, BC, and particulate chloride mass concentrations were ~~enhanced~~ increased by a factor of 4 – 8. The median CO_2 volume mixing ratio was ~~larger by~~ 13 ppm higher. In Bingen, the median concentration enhancements due to ~~the~~ Christmas market emissions were smaller: for organics, PM_1, and PAH mass concentrations by a factor of 3.5 – 4.5, for the other variables by a factor of 1.5 – 2.5, except for CO_2, which did not show an increase during the opening hours.

The different concentration levels between ~~both~~ the two locations during ~~the~~ opening hours are presumably due to two reasons. First, the monitoring site in Ingelheim ~~the measurement location~~ was very close (a few meters) to the food stands, while ~~in Bingen~~ the distance to the ~~next~~ nearest food stand in Bingen was about 25 m. Second, the Christmas market in Ingelheim was larger, with more visitors and more densely packed food stands ~~which stood more densely~~. In ~~G~~generall~~y~~, the measurements show that emissions from a Christmas market ~~might~~ can lead to substantial increases in pollutant concentration~~s enhancements~~ at ~~a~~ the local level.

In Ingelheim, ~~the~~ BC mass concentrations were additionally measured with a portable aethalometer (Fig. 1~~1~~2, green box plot for BC) while repeatedly walking across the Christmas market during ~~the~~ opening hours in order to estimate the personal exposure of

market visitors. The median ~~value measured during~~of these mobile measurements across the market was similar to the median ~~value from~~of the stationary measurements directly downwind the market. This indicates that the ~~measured~~ concentrations measured at a single location ~~at~~ on the downwind edge are representative ~~for~~ of the ~~overall~~ market as a whole. At the same time, the average concentration measured with the portable instrument (9.1 µg m^{-3}) was almost twice as high as the average of the stationary measurements (5.0 µg m^{-3}). Thus, visitors ~~of~~ to the market ~~can~~ may be exposed to much higher transient BC concentrations, presumably when ~~they~~ walking near ~~close by~~ fire-places or other strong sources, thereby increasing their personal exposure.

3.5.1 PMF analysis of the AMS organics data

For detailed information ~~about~~ on the contribution of different aerosol types, the AMS organics mass spectra were analyzed using positive matrix factorization (PMF), separately for both Christmas markets. For both markets, BBOA, COA, and OOA (~~which is~~ usually associated with aged background aerosol)~~,~~ were identified as aerosol types from the most reasonable PMF solution (Figs. S10~~11~~ and S11~~12~~). The challenge ~~during~~ in this analysis was that two emission sources, cooking and biomass burning, were close to each other with similar activity times, while a requirement for the PMF algorithm to separate different aerosol types ~~of aerosols~~ is a characteristic temporal variation~~,~~ that is different for each aerosol type. This resulted in an incomplete separation of the OOA factor for the measurements in Ingelheim with considerable OOA concentration increases during the opening hours of the market, while for this background -related aerosol type rather constant concentrations independent of the opening times are expected (as seen in Bingen).

The mass spectra of COA, BBOA, and OOA are similar for both ~~locations~~ sites and ~~exhibit~~ show the typical markers for ~~the respective~~each aerosol type~~s~~. In the mass spectra of OOA the most intense signal is at *m/z* 44 (CO_2^+)~~,~~ ~~originating from~~due to thermal decomposition of oxidized organic compounds (Ng et al., 2010). BBOA could be identified by the elevated signal intensities at *m/z* 60 and 73, whose ratio of 2.6 at both markets points to levoglucosan (see Sect. 3.1.2), ~~which is a~~ resulting from ~~of~~ the pyrolysis of cellulose (Schneider et al., 2006). In the COA mass spectra, the highest signal intensities are at *m/z* 41 and 55, and the signal ratio of *m/z* 55 and 57 is 2.6, which is consistent with the results ~~from~~ of previous studies (Mohr et al., 2012; Sun et al., 2011; Xu et al., 2020) and our laboratory studies (Sect. 3.1.2). ~~The c~~Correlation with corresponding reference mass spectra (averaged from the available mass spectra from the AMS database, see Table S3) supported the assignment of the identified factors, with correlation coefficients of 0.93 and 0.97 for COA, 0.98 and 0.95 for OOA, and 0.83 and 0.77 for BBOA~~,~~ for Ingelheim and Bingen, respectively.

~~The~~ COA and BBOA concentrations ~~were~~ increased significantly ~~enhanced~~ during the opening hours, while ~~the~~ OOA concentrations remained almost constant (OOA for Ingelheim not ~~regarded~~ considered here due to incomplete separation). The average concentrations of COA (CE = 1; RIE = 2.27; see Sect. 3.5.2) were 3.5/0.14 µg m^{-3} and 2.5/0.05 µg m^{-3} and of BBOA (CE = 0.5; RIE = 1.4) were 17.1/0.54 µg m^{-3} and 2.4/0.21 µg m^{-3} during/outside ~~the~~ opening hours for Ingelheim and Bingen, respectively. In Bingen, the OOA concentration (CE = 0.5; RIE = 1.4) ~~were~~ was mostly below 2 µg m^{-3} ~~over~~ during the whole measurement period, suggesting that this PMF factor can be attributed to the background aerosol. The observed step~~wise~~ changes ~~of the~~in OOA concentration (Fig. S10~~11~~) were due to changes in wind direction ~~changes~~. The fraction of OOA at both Christmas markets during the opening hours was similar ~~with~~ at 15 % and 17 %, while the one of BBOA ~~amounts to~~was 71 % and 40 % and the one of COA ~~to~~ was 14 % and 43 % for Ingelheim and Bingen, respectively. The higher proportion of BBOA ~~fraction~~ in Ingelheim ~~might~~ may be due to a second wood-fired barrel ~~at~~ 25 m ~~distance to~~away from MoLa on two afternoons and a flame-grilled salmon stand with an open wood fire within the circle of food stands ~~circle~~ where MoLa was located.

3.5.2 Validation of laboratory measurements using the Christmas market data

To assess whether the results ~~from~~ of the laboratory experiments are also applicable to ambient measurements, we used the Christmas market data to verify ~~different~~ several aspects of our results. Due to the higher fraction of COA measured during the Christmas market opening hours in Bingen (43 %) compared to Ingelheim (14 %) the analysis was ~~only~~ performed only with the data set collected in Bingen.

The dishes prepared at the Christmas market which were also ~~studied~~ investigated in the laboratory are fried bratwurst ~~frying~~, ~~deep frying~~fried French fries (in a deep fryer), and steaks grilled on a gas grill. A linear correlation of the average COA mass spectrum from the PMF analysis of the Christmas market data with the mass spectra of the above ~~mentioned~~ three dishes showed a very high similarity between the spectra (Pearson's r = 0.99), as did the correlation with ~~the one~~those of rapeseed oil (r = 0.98) and oleic acid (r = 0.93). The ratio of f_{67}/f_{69} for this COA mass spectrum was 1.4, similar to the ratios of previously measured ambient COA (1.2 ± 0.1) and ~~the~~ laboratory measurements (1.1 – 1.6), supporting our ~~suggestion~~ proposal of f_{67}/f_{69} as an additional COA marker (see Sect. 3.1.2).

To verify whether the densities for the organic fraction derived from the cooking emission experiments can be applied to ambient measurements, the densities for the three Christmas market-related dishes as well as for the COA PMF factor from the market measurements ~~at the market~~ were calculated based on the formula of Kuwata et al. (2012). The density of COA ~~with~~ at 0.94 g cm^{-3} is ~~in agreement~~consistent with the densities for the three dishes (0.94 – 0.98 g cm^{-3}, Table S5). This finding, together ~~along~~ with the high mass spectral similarity discussed above, suggests that the observed ambient COA is ~~mostly consisted~~ composed to a substantial amount of vaporized and re-condensed oil or decomposed fats.

~~In order t~~To validate whether the RIE_{COA} values determined from laboratory measurements are applicable to ambient measurements of cooking -related aerosols, PM_1 (from FMPS and OPC measurements, Sect. S1) was compared ~~to~~ with PM_1 calculated from BC and AMS species ($PM_{1,AMS+BC}$) for two different ~~value~~ sets of RIE_{COA} and CE_{COA} values: i) the ~~default~~ standard AMS values, i.e. RIE_{COA} = 1.4 and CE_{COA} = 0.5 (Fig. 1~~3~~2a); and ii) average values derived from the laboratory measurements of the three Christmas market-related dishes (RIE_{COA} = 2.27 and CE_{COA} = 1; Fig. 1~~3~~2b). In a~~A~~dditionally, the ~~fractions~~ proportions of the different aerosol species ~~of~~ in the Christmas market PM_1 emissions (after background subtraction) are shown as pie charts in Fig. 1~~2~~3, ~~as pie charts which were~~ calculated by applying ~~for COA~~ the ~~respective~~ corresponding RIE and CE values to the COA. In both cases, default RIE and CE values were used for the other AMS species including BBOA and OOA (i.e., assuming externally mixed COA; Freutel et al., 2013). As illustrated in Fig. 13, the correlations between the two types of PM_1 values are characterized by a considerable amount of scatter, particularly in the lower PM_1 concentration range. This is likely due to the fact that several sources for cooking-related PM_1 as well as for other types of organic aerosol are in close proximity to the measurement location, resulting in significant variability in the data from the instruments used to determine PM_1. This is also reflected in the poor correlation coefficients for both approaches to calculate PM_1 from AMS and BC data (r^2 = 0.56 and 0.58 with the default and laboratory values for RIE_{COA} and CE_{COA}, respectively). ~~According to~~ Figure~~.~~ 1~~3~~2a~~,~~ illustrates that $PM_{1,AMS+BC}$ ~~seems~~ appears to be overestimated for higher PM_1 concentrations when ~~using~~ the default values are employed.~~,~~ In contrast, when~~while with~~ RIE_{COA} and CE_{COA} ~~taken~~ are derived from the laboratory results, ~~the~~ PM_1 values scatter more around ~~align fit reasonably well with~~ the one-to-one line (Figure~~.~~ 1~~3~~2b), suggesting ~~a better~~improved mass closure. ODR fitting of the two pairs of PM_1 data with the intercept forced through the origin yields $PM_{1,AMS+BC}$ = 1.71 * PM_1 and $PM_{1,AMS+BC}$ = 0.68 * PM_1, respectively, for the default and the laboratory values. These results indicate a slight improvement in the agreement between the two sets of data when the laboratory RIE_{COA} and CE_{COA} values were employed.~~, though~~However, ~~no definitive answer can be given due to the low correlation coefficient in both cases (r = 0.56 and 0.58 with the default and laboratory values, respectively) as a result of the strong scatter in the correlations, probably due to the proximity of the sources to the measurement site~~. The pie charts ~~highlight~~ show the effect of the different RIE and CE values on

the calculated fraction of COA of the emitted Christmas market PM_1. Using the default values, the COA fraction would be 26% ~~larger~~ higher compared to ~~that when~~ using the laboratory values, showing the importance of choosing correct RIE and CE values for COA.

In ~~G~~general~~ly~~, the result of this comparison is ~~in agreement~~consistent with ~~those of~~ previous ambient measurements of cooking emissions, which also suggest a higher RIE_{COA} value than the ~~default~~ standard RIE_{Org} of 1.4 (Katz et al., 2021; Reyes-Villegas et al., 2018).

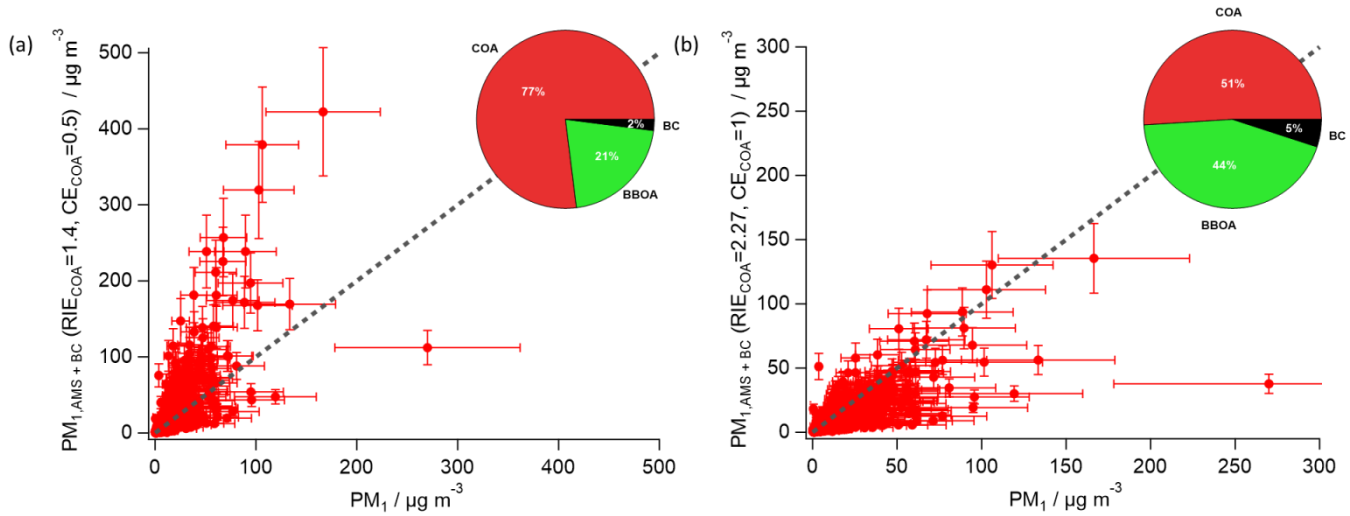

Figure 1312: Comparison of measured $PM_{1,AMS+BC}$ with PM_1 ~~with~~ using (a) RIE_{COA} = 1.4, CE_{COA} = 0.5 and (b) RIE_{COA} = 2.27, CE_{COA} = 1 for the COA fraction. The 1:1 line serves as a guid~~eance~~ for the eye. The pie charts show the calculated PM_1 composition of the Christmas market emissions (i.e., only for opening ~~times~~hours, after background subtraction).

Based on the results of the laboratory experiments as well as those of previous studies, no strong contribution of BC ~~was expected~~ from cooking emissions was expected (Zhang et al., 2010; Zhao et al., 2007), and the observed BC was assumed to originate mainly from biomass burning. In fact~~deed~~, the ratio of BBOA (RIE = 1.4 and CE = 0.5) to BC mass concentrations was on average ~~was~~ 3.3 during the Christmas market opening ~~times~~hours, which is well within the range of 1.7 – 33 observed for open biomass burning (Reid et al., 2005) and close to the ratios of 4.0 and 3.16 measured ~~for mainly domestic heating in urban environments~~ by Crippa et al. (2013) and Elser et al. (2016) for mainly residential heating in urban environments.

The applicability of the laboratory emission factors (see Sect. 3.4) to ambient measurements was verified by testing whether they ~~can~~ could reproduce the concentrations measured during the Christmas market in a simple model. For this purpose, the emission factors determined in the laboratory for the variables PN, PM_1, and organics were used for the dishes which were prepared at the Christmas market ~~were used~~ (fried bratwurst ~~frying~~, ~~deep frying~~ French fries fried in ~~the~~ a deep fryer, and steaks from ~~the~~ a gas grill) ~~for the variables PN, PM_1, and organics~~. Here, we assume that the emission factors obtained in the laboratory for the marinated steak are not strongly different from those for the non-marinated steak, which was used for cooking on the Christmas market. The emission factors for ~~G~~gas grilling ~~rather than~~ were used instead of those for charcoal grilling ~~emission factors were used here since~~, because PMF is likely to allocate ~~apportions~~ part of the charcoal grilling to the biomass burning factor, ~~causing~~ leading to an underestimation~~e~~ of the respective COA emissions.

The emissions per hour (EM) needed to generate the measured concentrations were calculated using the average concentration during the opening hours ($\overline{c_{CM}}$) minus the average background concentration ($\overline{c_{BG}}$) and the volumetric flow rate Q_{CM} with which the emissions were diluted (Eq. (3)). The volumetric flow rate Q_{CM} was estimated based on the average wind speed (1.15 m s^{-1}, mostly from the west), the height of the houses ~~(8 m)~~ surrounding the square (8 m), ~~up~~ to which we assumed the emissions would

be diluted, and the width of the street ~~that runs~~ running from west to east, which transport~~sing~~ most of the air mass, resulting in Q_{CM} = 5 · 10^5 m^3 h^{-1} (138 m^3 s^{-1}). ~~Finally, u~~Using the emission factors *EF* from the laboratory experiments, we calculated ~~which~~ the amount of food (m) that would ~~be~~ need~~ed~~ to be cooked per hour ~~in order~~ to generate the calculated emissions per hour (Eq. (4)).

$$EM = (\overline{c_{CM}} - \overline{c_{BG}}) \cdot Q_{CM} \quad (3)$$

$$m = \frac{EM}{EF} \quad (4)$$

Finally, assuming that a bratwurst has a mass of 150 g, a schnitzel has a mass of 180 g, and a unit of French fries has a mass of 250 g, the calculated masses were converted into food units to make the results more tangible. ~~As~~ Since the emission factors were determined from cooking activities, ~~we considered~~ only the COA-related fraction of the measured Christmas market emissions was considered for the mass-based variables PM_1 and organic mass concentration. The COA concentration was calculated using RIE_{COA} = 2.27 and CE_{COA} = 1 and considering only the ~~emissions of the~~ Christmas market emissions (background subtracted). For PM_1, the fraction ~~that is~~ related to COA ~~amounts to~~is 51% (Fig. 1~~3~~2b), and for the total measured AMS organics ~~to~~ it is 54%. ~~As~~ Since it is not possible to determine the COA ~~-~~related fraction for PN based on the ~~results for~~ PM_1 results, we ~~estimated~~ assumed that the COA related fraction for PN would be somewhere between 20% and 80% and performed the calculations for these two extreme scenarios.

Figure 14~~Figure 13~~ shows, for the three selected ~~chosen~~ variables, the ~~amount~~ number of ~~of~~ food units ~~which~~ that would ~~be~~ need~~ed~~ to be cooked ~~of the respective single dishes~~ per hour of each dish ~~in order~~ to account for the observed emissions. For the mass-based variables, the calculated ~~masses for~~numbers of steaks were ~~12~~67 – ~~17~~94 ~~kg h^{-1}~~ per hour, and for bratwurst and French fries, the numbers were at least ~~one~~ an order of magnitude ~~higher~~ higher ~~with~~ at ~~115~~ 770 – ~~538~~ 2150 ~~kg h^{-1}~~ units per hour. For PN, the calculated numbers of food units ~~amount~~ for the chosen COA fraction range of 20% to 80% ~~was~~ were ~~similar~~ smaller ~~as~~than those for the mass-based variables for ~~with 0.6 – 2.4 kg h^{-1} of~~ steaks ~~with~~at 3 – 13 units per hour and similar to those for the mass-based variables ~~with~~at ~~47 – 803 kg h^{-1} of~~ 310 - 1250 units of bratwurst and 800 – 3200 units of French fries. These calculated ~~masses~~ units of food prepared per hour are ~~all~~ in a realistic order of magnitude, assuming a reasonable mix of different types of food being prepared and the overall emissions being dominated by those from grilling steaks ~~(especially for the steak dish)~~, suggesting that the laboratory-derived emission factors for PN, PM_1, and organics are applicable to ambient measurements within an acceptable range of uncertainty.

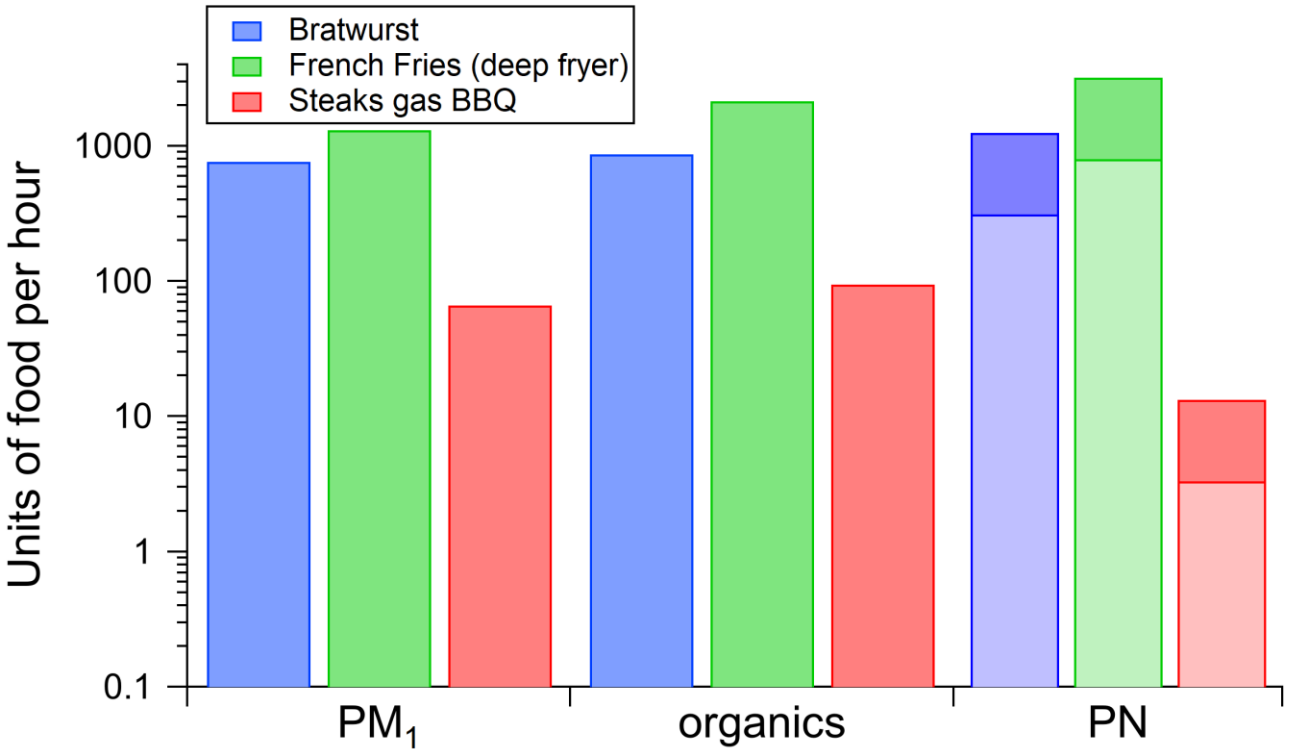

Figure 1413: ~~Amount~~ Units of food ~~which needs to~~that must be prepared per hour to generate the same concentrations (after background subtraction) as measured at the Christmas market in Bingen, calculated based on the emission~~s~~ factors for three different dishes and ~~on~~ the local aerosol transport conditions. For each variable~~,~~ the ~~respective~~ corresponding COA fraction was calculated with RIE_{COA} = 2.27 and CE_{COA} = 1 and for PN a COA fraction range of 20% (light bar) ~~to~~ and 80% (dark bar) was assumed.

4 Conclusion

In a comprehensive laboratory study, various aspects of cooking~~-related~~ emissions were ~~studied~~ investigated in real time with multiple instruments, including the chemical composition of PM_1 and particle size distributions, as well as emission dynamics and ~~the~~ quantification of emissions through the calculation of emission factors. In addition, the influence of cooking activities on ~~the~~ ambient aerosol was investigated at two German Christmas markets.

From the laboratory experiments, it was found that the measured particle number concentrations as well as several mass-based variables (PM, BC, PAH, organics) were strongly affected by the cooking activities. Measurements with the AMS ~~indicate~~ suggest that the PM_1 fraction of the measured emissions ~~was mostly composed~~ contains a substantial fraction of vaporized and recondensed oil or fatty acids, as shown ~~through~~ by comparing~~son of~~ the mass spectra of the measured emissions with ~~the one~~that of rapeseed oil, the used cooking oil. Therefore, we ~~assume~~ believe that particle formation and growth is ~~mainly~~ to a large degree the result of oil vaporization or fat decomposition and re-condensation of the emitted vapors.

~~Through~~ By comparing~~-comparison of~~ the AMS-measured organics mass concentrations with the size-distribution-derived mass concentration~~s derived from size distributions~~, we found that higher values ~~for the~~of RIE_{COA} (1.53 – 2.52) compared to the ~~default~~ standard value of 1.4 are required ~~for~~ to correctly determine~~ation of~~ the mass concentrations of cooking-related organic aerosols. These results confirm and extend the findings of previous studies. ~~As a~~In conclusion, we recommend the use~~using~~ of different RIE_{COA} values depending on the cooking oil, since it ~~has an~~ influence~~s on~~ the RIE_{COA}: for cooking with rapeseed oil, an RIE_{COA} of

2.17 ± 0.48 based on this study and the one by Reyes-Villegas et al. (2018), and for ~~soy-oil-based~~ cooking with soybean oil, an RIE_{COA} of 5.16 ± 0.77 based on the measurements by Katz et al. (2021).

~~Furthermore~~In addition, to support the AMS data analysis of organic aerosol types, a new ~~diagram~~ plot type is presented that ~~enables a simple~~provides an easy and quick way to check whether PMF has succeeded in separating different aerosol types using known markers, and also to identify and validate new markers, e.g. for real-time identification of aerosol types. By ~~U~~using ~~the~~ data ~~of~~ from multiple measurement campaigns, the variability of the mass spectra for individual aerosol types is ~~accounted for~~taken into account and this provides the opportunity to evaluate how well the separation of aerosol types works~~,~~ based on the selected markers. Here~~,~~ we have identified and evaluated the ratio $f_{67}/f_{69} > 1$ as an additional COA marker. The presented examples show the importance of combining markers or indicators to achieve a robust separation from other aerosol types, ~~like~~ such as for COA f_{55} (> 0.06) and f_{55}/f_{57} (> 2) for separation especially from HOA.

The relevant parameters that influenc~~eing~~ the amount of cooking emissions are the cooking temperature, the use of oil, the ingredients, and the activities during the cooking process. These are mostly dependent on the ~~preparation~~ cooking method; ~~hence~~ therefore we observed similar results for dishes with similar ~~preparation~~ cooking methods. A change ~~of~~ in the concentrations of the relevant variables (PM, BC, PAH, organics) as well as ~~of~~ in the particle size could be attributed to changes ~~of~~ in the temperature of the food and the cookware as well as to different activities during the ~~preparation~~cooking. ~~Due to rising~~As the temperature increases, more substances vaporize and condense, ~~leading to~~resulting in higher emissions ~~as well as~~and larger particles. ~~The emission of~~ BC and PAH emissions ~~were was~~ observed only at higher temperatures, e.g. towards the end of the cooking ~~preparation~~. ~~Different~~ Various activities lead to transient changes in concentration and particle size ~~changes as~~ because they 1. facilitate the vaporization of substances, e.g., ~~through~~ by stirring or tilting the pan, 2. increase the amount of vaporizable material, e.g., by cleaning the grill grid, or 3. suddenly release accumulated emissions, e.g., by opening the oven.

The ~~used~~ ingredients used ~~themselves~~ also have a strong influence on the aerosol composition. The emissions from boiled dishes differ from ~~the emissions~~those of other dishes ~~mostly~~ mainly due to the ~~broad~~ large absence of oil and fatty ingredients. Another example is the occurrence of sulfur-containing species in the emitted aerosol for dishes with fried onions.

~~For~~ In order to quantify~~ication of~~ the emissions, emission factors ~~were determined~~ for all relevant variables were determined individually for all dishes. The highest emissions were released ~~from preparing~~during the ~~preparation~~cooking of dishes on a gas and a charcoal grill due to the highest cooking temperatures, the burning of food ~~leftovers~~ residues from the grid, and, in the case of charcoal grilling, ~~due to~~ additional emissions from the ~~charcoal~~ burning of the charcoal itself. The emission levels from ~~cooking~~ the ~~preparation~~cooking of stir-fried, deep-fried, and baked dishes were similar to each other as oil or fatty ingredients were ~~used for all dishes~~present. The ~~preparation~~ cooking of boiled dishes resulted in the ~~release of the~~ lowest emissions ~~as~~ because no oil was used and no or only little amounts of fatty ingredients were available, limiting the amount of vaporizable substances. Furthermore, a comparison ~~to~~ with other relevant indoor and ~~ambient~~ outdoor emission sources showed that grilling one dish emits similar amounts of particles as driving 100 km ~~by~~ in a car, and emissions from oil-based cooking, ~~like~~ such as frying, are ~~of~~ similar ~~order of~~in magnitude ~~as such~~to those from domestic ~~biomass~~ wood burning over a comparable time ~~interval~~period.

~~The a~~Average PM_1 concentrations during the opening hours ~~at~~ of a Christmas market were found to be as high as 51 µg m^{-3}. Locally, visitors could be exposed to even higher concentrations, as shown ~~for~~ by the BC concentrations measured with a portable aethalometer ~~across~~ on the market, which were on average twice as high as those of the stationary measurements immediately downwind of the market. ~~T~~Although this is not a 24-hour ~~h~~ average ~~value~~, these elevated concentrations show that events ~~like~~ such as Christmas markets have a strong ~~influence~~ impact on local air quality.

This result, together with those from the laboratory measurements, shows that cooking activities contribute substantially to indoor and ambient aerosol. The amount of emissions is mainly determined by the ~~preparation~~ cooking method, with barbecues ~~as especially~~being a particularly strong emission source.

Author contribution. JP and FD ~~conceptualized~~ designed the measurements. JP ~~carried out~~performed the experiments, analyzed the MoLa data with support from FF, and ~~prepared~~ drafted the paper with contributions from FD, FF, a~~u~~nd SB.

Competing interests. The authors declare that they have no conflict of interest.

Acknowledgements. We thank Thomas Böttger and the mechanical workshop for technical support. The authors thank David Troglauer, Lasse Moormann, and Philipp Schuhmann for ~~support during~~assistance with the laboratory measurements. We also thank the organizers of the Christmas markets for the ~~possibility~~ opportunity to perform our measurements. ~~Furthermore, w~~We ~~acknowledge~~ thank the Max Planck Institute for Chemistry for funding ~~of~~ this work.

References

Abbatt, J. P. D. and Wang, C.: The atmospheric chemistry of indoor environments, Environ. Sci.: Processes Impacts, 22, 25–48, https://doi.org/10.1039/c9em00386j, 2020.

Abdullahi, K. L., Delgado-Saborit, J. M., and Harrison, R. M.: Emissions and indoor concentrations of particulate matter and its specific chemical components from cooking: A review, Atmos. Environ., 71, 260–294, https://doi.org/10.1016/j.atmosenv.2013.01.061, 2013.

Alfarra, M. R., Coe, H., Allan, J. D., Bower, K. N., Boudries, H., Canagaratna, M. R., Jimenez, J. L., Jayne, J. T., Garforth, A. A., Li, S.-M., and Worsnop, D. R.: Characterization of urban and rural organic particulate in the Lower Fraser Valley using two Aerodyne Aerosol Mass Spectrometers, Atmos. Environ., 38, 5745–5758, https://doi.org/10.1016/j.atmosenv.2004.01.054, 2004.

Allan, J. D., Williams, P. I., Morgan, W. T., Martin, C. L., Flynn, M. J., Lee, J., Nemitz, E., Phillips, G. J., Gallagher, M. W., and Coe, H.: Contributions from transport, solid fuel burning and cooking to primary organic aerosols in two UK cities, Atmos. Chem. Phys., 10, 647–668, https://doi.org/10.5194/acp-10-647-2010, 2010.

Alves, C. A., Duarte, M., Nunes, T., Moreira, R., and Rocha, S.: Carbonaceous particles emitted from cooking activities in Portugal, Glob. Nest J., 16, 411–419, https://doi.org/10.30955/gnj.001313, 2014.

Alves, C. A., Evtyugina, M., Cerqueira, M., Nunes, T., Duarte, M., and Vicente, E.: Volatile organic compounds emitted by the stacks of restaurants, Air Qual. Atmos. Health., 8, 401–412, https://doi.org/10.1007/s11869-014-0310-7, 2015.

Amouei Torkmahalleh, M., Goldasteh, I., Zhao, Y., Udochu, N. M., Rossner, A., Hopke, P. K., and Ferro, A. R.: PM2.5 and ultrafine particles emitted during heating of commercial cooking oils, Indoor Air, 22, 483–491, https://doi.org/10.1111/j.1600-0668.2012.00783.x, 2012.

Baron, P. A., Kulkarni, P., and Willeke, K. (Eds.): Aerosol measurement: Principles, techniques, and applications, 3rd ed., Engineering professional collection, John Wiley & Sons, Inc., New York, 883 pp., 2011.

Boelens, M., Valois, P. J. de, Wobben, H. J., and van der Gen, A.: Volatile flavor compounds from onion, J. Agric. Food Chem., 19, 984–991, https://doi.org/10.1021/jf60177a031, 1971.

Buonanno, G., Johnson, G., Morawska, L., and Stabile, L.: Volatility characterization of cooking-generated aerosol particles, Aerosol Sci. Technol., 45, 1069–1077, https://doi.org/10.1080/02786826.2011.580797, 2011.

Buonanno, G., Morawska, L., and Stabile, L.: Particle emission factors during cooking activities, Atmos. Environ., 43, 3235–3242, https://doi.org/10.1016/j.atmosenv.2009.03.044, 2009.

Canagaratna, M. R., Jayne, J. T., Jimenez, J. L., Allan, J. D., Alfarra, M. R., Zhang, Q., Onasch, T. B., Drewnick, F., Coe, H., Middlebrook, A., Delia, A., Williams, L. R., Trimborn, A. M., Northway, M. J., DeCarlo, P. F., Kolb, C. E., Davidovits, P., and Worsnop, D. R.: Chemical and microphysical characterization of ambient aerosols with the aerodyne aerosol mass spectrometer, Mass Spectrom. Rev., 26, 185–222, https://doi.org/10.1002/mas.20115, 2007.

Chafe, Z. A., Brauer, M., Klimont, Z., van Dingenen, R., Mehta, S., Rao, S., Riahi, K., Dentener, F., and Smith, K. R.: Household cooking with solid fuels contributes to ambient PM2.5 air pollution and the burden of disease, Environ. Health Perspect., 122, 1314–1320, https://doi.org/10.1289/ehp.1206340, 2014.

Chen, Y., Ho, K. F., Ho, S. S. H., Ho, W. K., Lee, S. C., Yu, J. Z., and Sit, E. H. L.: Gaseous and particulate polycyclic aromatic hydrocarbons (PAHs) emissions from commercial restaurants in Hong Kong, J. Environ. Monit., 9, 1402–1409, https://doi.org/10.1039/b710259c, 2007.

Cheng, S., Wang, G., Lang, J., Wen, W., Wang, X., and Yao, S.: Characterization of volatile organic compounds from different cooking emissions, Atmos. Environ., 145, 299–307, https://doi.org/10.1016/j.atmosenv.2016.09.037, 2016.

Christie, W. W.: The Lipid Web, https://www.lipidmaps.org/resources/lipidweb/lipidweb_html/index.html, last access: 18 September 2023.

Crippa, M., DeCarlo, P. F., Slowik, J. G., Mohr, C., Heringa, M. F., Chirico, R., Poulain, L., Freutel, F., Sciare, J., Cozic, J., Di Marco, C. F., Elsasser, M., Nicolas, J. B., Marchand, N., Abidi, E., Wiedensohler, A., Drewnick, F., Schneider, J., Borrmann, S., Nemitz, E., Zimmermann, R., Jaffrezo, J.-L., Prévôt, A. S. H., and Baltensperger, U.: Wintertime aerosol chemical composition and source apportionment of the organic fraction in the metropolitan area of Paris, Atmos. Chem. Phys., 13, 961–981, https://doi.org/10.5194/acp-13-961-2013, 2013.

Diffey, B. L.: An overview analysis of the time people spend outdoors, Br. J. Dermatol., 164, 848–854, https://doi.org/10.1111/j.1365-2133.2010.10165.x, 2011.

Drewnick, F., Böttger, T., Weiden-Reinmüller, S.-L. v. d., Zorn, S. R., Klimach, T., Schneider, J., and Borrmann, S.: Design of a mobile aerosol research laboratory and data processing tools for effective stationary and mobile field measurements, Atmos. Meas. Tech., 5, 1443–1457, https://doi.org/10.5194/amt-5-1443-2012, 2012.

Elser, M., Huang, R.-J., Wolf, R., Slowik, J. G., Wang, Q., Canonaco, F., Li, G., Bozzetti, C., Daellenbach, K. R., Huang, Y., Zhang, R., Li, Z., Cao, J., Baltensperger, U., El-Haddad, I., and Prévôt, A. S. H.: New insights into $PM_{2.5}$ chemical composition and sources in two major cities in China during extreme haze events using aerosol mass spectrometry, Atmos. Chem. Phys., 16, 3207–3225, https://doi.org/10.5194/acp-16-3207-2016, 2016.

Faber, P., Drewnick, F., Veres, P. R., Williams, J., and Borrmann, S.: Anthropogenic sources of aerosol particles in a football stadium: Real-time characterization of emissions from cigarette smoking, cooking, hand flares, and color smoke bombs by high-resolution aerosol mass spectrometry, Atmos. Environ., 77, 1043–1051, https://doi.org/10.1016/j.atmosenv.2013.05.072, 2013.

Fachinger, F., Drewnick, F., Gieré, R., and Borrmann, S.: Communal biofuel burning for district heating: Emissions and immissions from medium-sized (0.4 and 1.5 MW) facilities, Atmos. Environ., 181, 177–185, https://doi.org/10.1016/j.atmosenv.2018.03.014, 2018.

Fachinger, J. R. W., Gallavardin, S. J., Helleis, F., Fachinger, F., Drewnick, F., and Borrmann, S.: The ion trap aerosol mass spectrometer: field intercomparison with the ToF-AMS and the capability of differentiating organic compound classes via MS-MS, Atmos. Meas. Tech., 10, 1623–1637, https://doi.org/10.5194/amt-10-1623-2017, 2017.

Freutel, F., Schneider, J., Drewnick, F., Weiden-Reinmüller, S.-L. v. d., Crippa, M., Prévôt, A. S. H., Baltensperger, U., Poulain, L., Wiedensohler, A., Sciare, J., Sarda-Estève, R., Burkhart, J. F., Eckhardt, S., Stohl, A., Gros, V., Colomb, A., Michoud, V., Doussin, J. F., Borbon, A., Haeffelin, M., Morille, Y., Beekmann, M., and Borrmann, S.: Aerosol particle measurements at three stationary sites in the megacity of Paris during summer 2009: meteorology and air mass origin dominate aerosol particle composition and size distribution, Atmos. Chem. Phys., 13, 933–959, https://doi.org/10.5194/acp-13-933-2013, 2013.

Gao, J., Cao, C., Wang, L., Song, T., Zhou, X., Yang, J., and Zhang, X.: Determination of size-dependent source emission rate of cooking-generated aerosol particles at the oil-heating stage in an experimental kitchen, Aerosol Air Qual. Res., 13, 488–496, https://doi.org/10.4209/aaqr.2012.09.0238, 2013.

Goldstein, A. H., Nazaroff, W. W., Weschler, C. J., and Williams, J.: How do indoor environments affect air pollution exposure?, Environ. Sci. Technol., 55, 100–108, https://doi.org/10.1021/acs.est.0c05727, 2021.

Hallgren, B., Ryhage, R., Stenhagen, E., Sömme, R., and Palmstierna, H.: The mass spectra of methyl oleate, methyl linoleate, and methyl linolenate, Acta Chem. Scand., 13, 845–847, https://doi.org/10.3891/acta.chem.scand.13-0845, 1959.

He, C., Morawska, L., Hitchins, J., and Gilbert, D.: Contribution from indoor sources to particle number and mass concentrations in residential houses, Atmos. Environ., 38, 3405–3415, https://doi.org/10.1016/j.atmosenv.2004.03.027, 2004.

He, L.-Y., Lin, Y., Huang, X.-F., Guo, S., Xue, L., Su, Q., Hu, M., Luan, S.-J., and Zhang, Y.-H.: Characterization of high-resolution aerosol mass spectra of primary organic aerosol emissions from Chinese cooking and biomass burning, Atmos. Chem. Phys., 10, 11535–11543, https://doi.org/10.5194/acp-10-11535-2010, 2010.

IPCC: Climate Change 2021: The Physical Science Basis, Cambridge University Press, Cambridge, New York, 2021.

Jägerstad, M. and Skog, K.: Genotoxicity of heat-processed foods, Mutat. Res., 574, 156–172, https://doi.org/10.1016/j.mrfmmm.2005.01.030, 2005.

Kaltsonoudis, C., Kostenidou, E., Louvaris, E., Psichoudaki, M., Tsiligiannis, E., Florou, K., Liangou, A., and Pandis, S. N.: Characterization of fresh and aged organic aerosol emissions from meat charbroiling, Atmos. Chem. Phys., 17, 7143–7155, https://doi.org/10.5194/acp-17-7143-2017, 2017.

Katragadda, H. R., Fullana, A., Sidhu, S., and Carbonell-Barrachina, Á. A.: Emissions of volatile aldehydes from heated cooking oils, Food Chemistry, 120, 59–65, https://doi.org/10.1016/j.foodchem.2009.09.070, 2010.

Katz, E. F., Guo, H., Campuzano-Jost, P., Day, D. A., Brown, W. L., Boedicker, E., Pothier, M., Lunderberg, D. M., Patel, S., Patel, K., Hayes, P. L., Avery, A., Hildebrandt Ruiz, L., Goldstein, A. H., Vance, M. E., Farmer, D. K., Jimenez, J. L., and DeCarlo, P. F.: Quantification of cooking organic aerosol in the indoor environment using aerodyne aerosol mass spectrometers, Aerosol Sci. Technol., 55, 1099–1114, https://doi.org/10.1080/02786826.2021.1931013, 2021.

Klein, F., Platt, S. M., Farren, N. J., Detournay, A., Bruns, E. A., Bozzetti, C., Daellenbach, K. R., Kilic, D., Kumar, N. K., Pieber, S. M., Slowik, J. G., Temime-Roussel, B., Marchand, N., Hamilton, J. F., Baltensperger, U., Prévôt, A. S. H., and El Haddad, I.: Characterization of Gas-Phase Organics Using Proton Transfer Reaction Time-of-Flight Mass Spectrometry: Cooking Emissions, Environ. Sci. Technol., 50, 1243–1250, https://doi.org/10.1021/acs.est.5b04618, 2016.

Kreyling, W. G., Semmler-Behnke, M., and Möller, W.: Health implications of nanoparticles, J. Nanopart. Res. (Journal of Nanoparticle Research), 8, 543–562, https://doi.org/10.1007/s11051-005-9068-z, 2006.

Kuwata, M., Zorn, S. R., and Martin, S. T.: Using elemental ratios to predict the density of organic material composed of carbon, hydrogen, and oxygen, Environ. Sci. Technol., 46, 787–794, https://doi.org/10.1021/es202525q, 2012.

Lee, S. C., Li, W.-M., and Lo Yin Chan: Indoor air quality at restaurants with different styles of cooking in metropolitan Hong Kong, Sci. Total Environ., 279, 181–193, https://doi.org/10.1016/S0048-9697(01)00765-3, 2001.

Levin, E. J. T., McMeeking, G. R., Carrico, C. M., Mack, L. E., Kreidenweis, S. M., Wold, C. E., Moosmüller, H., Arnott, W. P., Hao, W. M., Collett, J. L., and Malm, W. C.: Biomass burning smoke aerosol properties measured during Fire Laboratory at Missoula Experiments (FLAME), J. Geophys. Res., 115, https://doi.org/10.1029/2009jd013601, 2010.

Liao, C.-M., Chen, S.-C., Chen, J.-W., and Liang, H.-M.: Contributions of Chinese-style cooking and incense burning to personal exposure and residential PM concentrations in Taiwan region, Sci. Total Environ., 358, 72–84, https://doi.org/10.1016/j.scitotenv.2005.03.026, 2006.

Lijinsky, W.: The formation and occurrence of polynuclear aromatic hydrocarbons associated with food, Mutat. Res. - Genet. Toxicol., 259, 251–261, https://doi.org/10.1016/0165-1218(91)90121-2, 1991.

Liu, T., Wang, Z., Huang, D. D., Wang, X., and Chan, C. K.: Significant production of secondary organic aerosol from emissions of heated cooking oils, Environ. Sci. Technol. Lett., 5, 32–37, https://doi.org/10.1021/acs.estlett.7b00530, 2018.

Liu, T., Li, Z., Chan, M., and Chan, C. K.: Formation of secondary organic aerosols from gas-phase emissions of heated cooking oils, Atmos. Chem. Phys., 17, 7333–7344, https://doi.org/10.5194/acp-17-7333-2017, 2017a.

Liu, T., Liu, Q., Li, Z., Huo, L., Chan, M., Li, X., Zhou, Z., and Chan, C. K.: Emission of volatile organic compounds and production of secondary organic aerosol from stir-frying spices, Sci. Total Environ., 599-600, 1614–1621, https://doi.org/10.1016/j.scitotenv.2017.05.147, 2017b.

Liu, Y., Ma, H., Zhang, N., and Li, Q.: A systematic literature review on indoor PM2.5 concentrations and personal exposure in urban residential buildings, Heliyon, 8, e10174, https://doi.org/10.1016/j.heliyon.2022.e10174, 2022.

Marć, M., Śmiełowska, M., Namieśnik, J., and Zabiegała, B.: Indoor air quality of everyday use spaces dedicated to specific purposes-a review, Environ. Sci. Pollut. Res., 25, 2065–2082, https://doi.org/10.1007/s11356-017-0839-8, 2018.

Martin, W. J., Ramanathan, T., and Ramanathan, V.: Household air pollution from cookstoves: Impacts on health and climate, in: Climate Change and Global Public Health. Respiratory Medicine, Humana,Cham, 369–390, https://doi.org/10.1007/978-3-030-54746-2_17.

Marval, J. and Tronville, P.: Ultrafine particles: A review about their health effects, presence, generation, and measurement in indoor environments, Build. Environ., 216, 108992, https://doi.org/10.1016/j.buildenv.2022.108992, 2022.

Matthew, B. M., Middlebrook, A. M., and Onasch, T. B.: Collection Efficiencies in an Aerodyne Aerosol Mass Spectrometer as a Function of Particle Phase for Laboratory Generated Aerosols, Aerosol Science and Technology, 42, 884–898, https://doi.org/10.1080/02786820802356797, 2008.

McLafferty, F. W. and Turecek, F.: Interpretation of Mass Spectra, 4th ed., University Science Books, Melville, 371 pp., 1993.

Mohr, C., DeCarlo, P. F., Heringa, M. F., Chirico, R., Slowik, J. G., Richter, R., Reche, C., Alastuey, A., Querol, X., Seco, R., Peñuelas, J., Jiménez, J. L., Crippa, M., Zimmermann, R., Baltensperger, U., and Prévôt, A. S. H.: Identification and quantification of organic aerosol from cooking and other sources in Barcelona using aerosol mass spectrometer data, Atmos. Chem. Phys., 12, 1649–1665, https://doi.org/10.5194/acp-12-1649-2012, 2012.

Mohr, C., Huffman, A., Cubison, M. J., Aiken, A. C., Docherty, K. S., Kimmel, J. R., Ulbrich, I. M., Hannigan, M., and Jimenez, J. L.: Characterization of primary organic aerosol emissions from meat cooking, trash burning, and motor vehicles with high-resolution aerosol mass spectrometry and comparison with ambient and chamber observations, Environ. Sci. Technol., 43, 2443–2449, https://doi.org/10.1021/es8011518, 2009.

Nasir, Z. A. and Colbeck, I.: Particulate pollution in different housing types in a UK suburban location, Sci. Total Environ., 445-446, 165–176, https://doi.org/10.1016/j.scitotenv.2012.12.042, 2013.

Ng, N. L., Canagaratna, M. R., Zhang, Q., Jimenez, J. L., Tian, J., Ulbrich, I. M., Kroll, J. H., Docherty, K. S., Chhabra, P. S., Bahreini, R., Murphy, S. M., Seinfeld, J. H., Hildebrandt, L., Donahue, N. M., DeCarlo, P. F., Lanz, V. A., Prévôt, A. S. H., Dinar, E., Rudich, Y., and Worsnop, D. R.: Organic aerosol components observed in Northern Hemispheric datasets from Aerosol Mass Spectrometry, Atmos. Chem. Phys., 10, 4625–4641, https://doi.org/10.5194/acp-10-4625-2010, 2010.

Olson, D. A. and Burke, J. M.: Distributions of PM2.5 source strengths for cooking from the Research Triangle Park particulate matter panel study, Environ. Sci. Technol., 40, 163–169, https://doi.org/10.1021/es050359t, 2006.

Omidvarborna, H., Kumar, A., and Kim, D.-S.: Recent studies on soot modeling for diesel combustion, Renew. Sust. Energ. Rev., 48, 635–647, https://doi.org/10.1016/j.rser.2015.04.019, 2015.

Paatero, P. and Tapper, U.: Positive matrix factorization: A non-negative factor model with optimal utilization of error estimates of data values, Environmetrics, 5, 111–126, https://doi.org/10.1002/env.3170050203, 1994.

Pope, C. A. and Dockery, D. W.: Health effects of fine particulate air pollution: lines that connect, J. Air Waste Manag. Assoc., 56, 709–742, https://doi.org/10.1080/10473289.2006.10464485, 2006.

Pope, C. A., Burnett, R. T., Thurston, G. D., Thun, M. J., Calle, E. E., Krewski, D., and Godleski, J. J.: Cardiovascular mortality and long-term exposure to particulate air pollution: epidemiological evidence of general pathophysiological pathways of disease, Circulation, 109, 71–77, https://doi.org/10.1161/01.CIR.0000108927.80044.7F, 2004.

Reid, J. S., Koppmann, R., Eck, T. F., and Eleuterio, D. P.: A review of biomass burning emissions part II: intensive physical properties of biomass burning particles, Atmos. Chem. Phys., 5, 799–825, https://doi.org/10.5194/acp-5-799-2005, 2005.

Reyes-Villegas, E., Bannan, T., Le Breton, M., Mehra, A., Priestley, M., Percival, C., Coe, H., and Allan, J. D.: Online chemical characterization of food-cooking organic aerosols: Implications for source apportionment, Environ. Sci. Technol., 52, 5308–5318, https://doi.org/10.1021/acs.est.7b06278, 2018.

Robinson, E. S., Gu, P., Ye, Q., Li, H. Z., Shah, R. U., Apte, J. S., Robinson, A. L., and Presto, A. A.: Restaurant impacts on outdoor air quality: Elevated organic aerosol mass from restaurant cooking with neighborhood-scale plume extents, Environ. Sci. Technol., 52, 9285–9294, https://doi.org/10.1021/acs.est.8b02654, 2018.

Rogge, W. F., Hildemann, L. M., Mazurek, M. A., Cass, G. R., and Simoneit, B. R. T.: Sources of fine organic aerosol. 1. Charbroilers and meat cooking operations, Environ. Sci. Technol., 25, 1112–1125, https://doi.org/10.1021/es00018a015, 1991.

Schneider, J., Weimer, S., Drewnick, F., Borrmann, S., Helas, G., Gwaze, P., Schmid, O., Andreae, M. O., and Kirchner, U.: Mass spectrometric analysis and aerodynamic properties of various types of combustion-related aerosol particles, Int. J. Mass Spectrom., 258, 37–49, https://doi.org/10.1016/j.ijms.2006.07.008, 2006.

See, S. W. and Balasubramanian, R.: Physical Characteristics of Ultrafine Particles Emitted from Different Gas Cooking Methods, Aerosol Air Qual. Res., 6, 82–92, https://doi.org/10.4209/aaqr.2006.03.0007, 2006.

Shiraiwa, M., Ueda, K., Pozzer, A., Lammel, G., Kampf, C. J., Fushimi, A., Enami, S., Arangio, A. M., Fröhlich-Nowoisky, J., Fujitani, Y., Furuyama, A., Lakey, P. S. J., Lelieveld, J., Lucas, K., Morino, Y., Pöschl, U., Takahama, S., Takami, A., Tong, H., Weber, B., Yoshino, A., and Sato, K.: Aerosol health effects from molecular to global scales, Environ. Sci. Technol., 51, 13545–13567, https://doi.org/10.1021/acs.est.7b04417, 2017.

Struckmeier, C., Drewnick, F., Fachinger, F., Gobbi, G. P., and Borrmann, S.: Atmospheric aerosols in Rome, Italy: sources, dynamics and spatial variations during two seasons, Atmos. Chem. Phys., 16, 15277–15299, https://doi.org/10.5194/acp-16-15277-2016, 2016.

Sun, Y.-L., Zhang, Q., Schwab, J. J., Demerjian, K. L., Chen, W.-N., Bae, M.-S., Hung, H.-M., Hogrefe, O., Frank, B., Rattigan, O. V., and Lin, Y.-C.: Characterization of the sources and processes of organic and inorganic aerosols in New York city with a high-resolution time-of-flight aerosol mass apectrometer, Atmos. Chem. Phys., 11, 1581–1602, https://doi.org/10.5194/acp-11-1581-2011, 2011.

Takhar, M., Li, Y., and Chan, A. W. H.: Characterization of secondary organic aerosol from heated-cooking-oil emissions: evolution in composition and volatility, Atmos. Chem. Phys., 21, 5137–5149, https://doi.org/10.5194/acp-21-5137-2021, 2021.

Thomas, R. J.: Particle size and pathogenicity in the respiratory tract, Virulence, 4, 847–858, https://doi.org/10.4161/viru.27172, 2013.

Ulbrich, I. M., Canagaratna, M. R., Zhang, Q., Worsnop, D. R., and Jimenez, J. L.: Interpretation of organic components from Positive Matrix Factorization of aerosol mass spectrometric data, Atmos. Chem. Phys., 9, 2891–2918, https://doi.org/10.5194/acp-9-2891-2009, 2009.

Ulbrich, I. M., Handschy, A., Lechner, M., and Jimenez, J.L.: High-Resolution AMS Spectral Database, http://cires.colorado.edu/jimenez-group/HRAMSsd/, last access: 18 September 2023.

von der Weiden, S.-L., Drewnick, F., and Borrmann, S.: Particle Loss Calculator – a new software tool for the assessment of the performance of aerosol inlet systems, Atmos. Meas. Tech., 2, 479–494, https://doi.org/10.5194/amt-2-479-2009, 2009.

Wallace, L. and Ott, W.: Personal exposure to ultrafine particles, J. Expo. Sci. Environ. Epidemiol., 21, 20–30, https://doi.org/10.1038/jes.2009.59, 2011.

Wallace, L. A., Emmerich, S. J., and Howard-Reed, C.: Source strengths of ultrafine and fine particles due to cooking with a gas stove, Environ. Sci. Technol., 38, 2304–2311, https://doi.org/10.1021/es0306260, 2004.

Wang, Q., He, X., Zhou, M., Huang, D. D., Qiao, L., Zhu, S., Ma, Y.-g., Wang, H.-l., Li, L., Huang, C., Huang, X. H. H., Xu, W., Worsnop, D., Goldstein, A. H., Guo, H., and Yu, J. Z.: Hourly measurements of organic molecular markers in urban Shanghai, China: Primary organic aerosol source identification and observation of cooking aerosol aging, ACS Earth Space Chem., 4, 1670–1685, https://doi.org/10.1021/acsearthspacechem.0c00205, 2020.

WHO: WHO global air quality guidelines: Particulate matter (PM2.5 and PM10), ozone, nitrogen dioxide, sulfur dioxide and carbon monoxide, WHO European Centre for Environment and Health, Bonn, 285 pp., 2021.

WHO: Household air pollution, https://www.who.int/news-room/fact-sheets/detail/household-air-pollution-and-health, last access: 27 July 2023.

Williams, A., Jones, J. M., Ma, L., and Pourkashanian, M.: Pollutants from the combustion of solid biomass fuels, Prog. Energy Combust. Sci., 38, 113–137, https://doi.org/10.1016/j.pecs.2011.10.001, 2012.

Wu, C. L., Chao, C. Y. H., Sze-To, G. N., Wan, M. P., and Chan, T. C.: Ultrafine particle emissions from cigarette smouldering, incense burning, vacuum cleaner motor operation and cooking, Indoor Built Environ., 21, 782–796, https://doi.org/10.1177/1420326X11421356, 2012.

Xu, J., Wang, P., Li, T., Shi, G., Wang, M., Huang, L., Kong, S., Gong, J., Yang, W., Wang, X., Geng, C., Han, B., and Bai, Z.: Exposure to source-specific particulate matter and health effects: a review of epidemiological studies, Curr. Pollution Rep. (Current Pollution Reports), 381, 705, https://doi.org/10.1007/s40726-022-00235-6, 2022.

Xu, W., He, Y., Qiu, Y., Chen, C., Xie, C., Lei, L., Li, Z., Sun, J., Li, J., Fu, P., Wang, Z., Worsnop, D. R., and Sun, Y.: Mass spectral characterization of primary emissions and implications in source apportionment of organic aerosol, Atmos. Meas. Tech., 13, 3205–3219, https://doi.org/10.5194/amt-13-3205-2020, 2020.

Xu, W., Lambe, A., Silva, P., Hu, W., Onasch, T., Williams, L., Croteau, P., Zhang, X., Renbaum-Wolff, L., Fortner, E., Jimenez, J. L., Jayne, J., Worsnop, D., and Canagaratna, M.: Laboratory evaluation of species-dependent relative ionization efficiencies in the Aerodyne Aerosol Mass Spectrometer, Aerosol Sci. Technol., 52, 626–641, https://doi.org/10.1080/02786826.2018.1439570, 2018.

Yeung, L. L. and To, W. M.: Size distributions of the aerosols emitted from commercial cooking processes, Indoor Built Environ., 17, 220–229, https://doi.org/10.1177/1420326X08092043, 2008.

Yin, J., Cumberland, S. A., Harrison, R. M., Allan, J., Young, D. E., Williams, P. I., and Coe, H.: Receptor modelling of fine particles in southern England using CMB including comparison with AMS-PMF factors, Atmos. Chem. Phys., 15, 2139–2158, https://doi.org/10.5194/acp-15-2139-2015, 2015.

Yu, Y., Guo, S., Wang, H., Shen, R., Zhu, W., Tan, R., Song, K., Zhang, Z., Li, S., Chen, Y., and Hu, M.: Importance of Semivolatile/Intermediate-Volatility Organic Compounds to Secondary Organic Aerosol Formation from Chinese Domestic Cooking Emissions, Environ. Sci. Technol. Lett., 9, 507–512, https://doi.org/10.1021/acs.estlett.2c00207, 2022.

Zhang, Q., Gangupomu, R. H., Ramirez, D., and Zhu, Y.: Measurement of ultrafine particles and other air pollutants emitted by cooking activities, Int. J. Environ. Res. Public Health., 7, 1744–1759, https://doi.org/10.3390/ijerph7041744, 2010.

Zhang, Z., Zhu, W., Hu, M., Wang, H., Chen, Z., Shen, R., Yu, Y., Tan, R., and Guo, S.: Secondary organic aerosol from typical chinese domestic cooking emissions, Environ. Sci. Technol. Lett., 8, 24–31, https://doi.org/10.1021/acs.estlett.0c00754, 2021.

Zhao, W., Hopke, P. K., Norris, G., Williams, R., and Paatero, P.: Source apportionment and analysis on ambient and personal exposure samples with a combined receptor model and an adaptive blank estimation strategy, Atmos. Environ., 40, 3788–3801, https://doi.org/10.1016/j.atmosenv.2006.02.027, 2006.

Zhao, Y., Liu, L., Tao, P., Zhang, B., Huan, C., Zhang, X., and Wang, M.: Review of effluents and health effects of cooking and the performance of kitchen ventilation, Aerosol Air Qual. Res., 19, 1937–1959, https://doi.org/10.4209/aaqr.2019.04.0198, 2019.

Zhao, Y., Hu, M., Slanina, S., and Zhang, Y.: Chemical compositions of fine particulate organic matter emitted from Chinese cooking, Environ. Sci. Technol., 41, 99–105, https://doi.org/10.1021/es0614518, 2007.

Zhou, L., Liu, T., Yao, D., Guo, H., Cheng, C., and Chan, C. K.: Primary emissions and secondary production of organic aerosols from heated animal fats, Science of The Total Environment, 794, 148638, https://doi.org/10.1016/j.scitotenv.2021.148638, 2021.

Zhou, Z., Liu, Y., Yuan, J., Zuo, J., Chen, G., Xu, L., and Rameezdeen, R.: Indoor PM2.5 concentrations in residential buildings during a severely polluted winter: A case study in Tianjin, China, Renew. Sust. Energ. Rev., 64, 372–381, https://doi.org/10.1016/j.rser.2016.06.018, 2016.

Zhu, W., Guo, S., Zhang, Z., Wang, H., Yu, Y., Chen, Z., Shen, R., Tan, R., Song, K., Liu, K., Tang, R., Liu, Y., Lou, S., Li, Y., Zhang, W., Zhang, Z., Shuai, S., Xu, H., Li, S., Chen, Y., Hu, M., Canonaco, F., and Prévôt, A. S. H.: Mass spectral characterization of secondary organic aerosol from urban cooking and vehicular sources, Atmos. Chem. Phys., 21, 15065–15079, https://doi.org/10.5194/acp-21-15065-2021, 2021.

Particulate emissions from cooking activities: emission factors, emission dynamics, and mass spectrometric analysis for different preparation methods

Julia Pikmann[1], Frank Drewnick[1], Friederike Fachinger[1], Stephan Borrmann[1,2]

[1]Particle Chemistry Department, Max Planck Institute for Chemistry, Mainz, 55128, Germany
[2]Institute for Atmospheric Physics, Johannes Gutenberg University Mainz, Mainz, 55128, Germany

Correspondence to: Frank Drewnick (frank.drewnick@mpic.de)

Abstract.

As most people, especially in developed countries, spend most of their time indoors, they are strongly exposed to indoor aerosol, which potentially can lead to adverse health effects. A major source of indoor aerosols are cooking activities releasing large amounts of particulate emissions, in terms of both number and mass ~~-wise~~, with often complex composition. To investigate the characteristics of cooking emissions and what influences these ~~parameters, which influences on these characteristics~~ emissions, we conducted a comprehensive study, ~~in form of a measurement series~~ cooking 19 dishes with different ingredients and preparation methods. The emissions were monitored in real time with multiple online instruments, that ~~measuring~~ measured both physical and chemical particle properties as well as trace gas concentrations. With the same instrumentation, the influence of cooking emissions on the ambient aerosol load was studied at two German Christmas markets. In contrast to previous studies, which often focus on individual aspects or emission variables, this broad and coherent approach allows comparison between the influence of different parameters (e.g., ingredients, preparation method, cooking temperature, cooking activities) on the emissions.

For six variables~~,~~ we found evidence of ~~observed changes~~emissions ~~during~~ from ~~the~~ cooking: particle number concentration of smaller (particle diameter d_p > 5 nm) and larger particles (d_p > 250 nm), PM (PM_1, $PM_{2.5}$, PM_{10}), BC, PAH and organic~~s~~ aerosol mass concentration~~s~~. Generally, similar emission characteristics were observed for dishes with the same preparation method mainly due to similar cooking temperature and use of oil. The ~~emission~~ temporal dynamics in the emissions of the ~~above~~aforementioned~~-mentioned~~ variables, as well as the sizes of the emitted particles, were mostly influenced by the cooking temperature and the activities during cooking. The emissions were quantified via emission factors, with the highest values for grilled dishes, one to two orders of magnitude smaller ones for oil-based cooking (baking, stir-frying, deep-frying) and the smallest for boiled dishes.

For the identification of cooking emissions with the Aerodyne Aaerosol M~~m~~ass S~~s~~pectrometer (AMS), and more generally for the identification of new AMS markers for individual organic aerosol types, we propose a new ~~diagram~~ plot type ~~where~~ that takes into account the mass spectral variability ~~of the mass spectra of different~~for individual aerosol types ~~is considered~~. Combining our results and those ~~from~~ of previous studies for the quantification of cooking -related organic aerosols with the AMS, we recommend ~~using values for~~the use of ~~the~~ relative ionization efficiency values higher ~~which are larger~~ than the default value for organics (RIE_{Org} = 1.4): for rapeseed oil -based cooking 2.17 ± 0.48 and for soy oil -based cooking 5.16 ± 0.77.

1 Introduction

Aerosols influence the earth's climate as well as air quality and human health (IPCC, 2021; WHO, 2021). According to calculations of the WHO (World Health Organization) air pollution leads to 6.7 million premature deaths every year and almost half of them were attributed to indoor air pollution (WHO). People tend to spend an increasing fraction of their time indoors, especially in developed countries with about 90%; they are therefore exposed over long periods to the indoor aerosol and the therein contained

pollutants (Diffey, 2011; Goldstein et al., 2021; Liu et al., 2022). Inhaled, these pollutants can cause the formation of radicals leading to oxidative stress and formation of oxygenated species which can induce inflammation processes (Kreyling et al., 2006). The resulting impacts on health are versatile and include respiratory diseases, cardiovascular diseases, allergies, infectious diseases, and cancer (Pope et al., 2004; Pope and Dockery, 2006; Shiraiwa et al., 2017; Xu et al., 2022).

The composition of the indoor aerosol is influenced by the atmospheric aerosol infiltrating through ventilation and leaks as well as by multiple emission sources indoors (Abbatt and Wang, 2020; Marval and Tronville, 2022). Aerosols can be generated through evaporation of substances from furnishing, building materials, and consumer products. The human body itself is a direct and indirect source of aerosols due to perspiration, breathing, talking etc. Furthermore, different activities at home (like cleaning and moving around) lead to resuspension and emission of aerosol particles. Combustion processes like cigarette smoking, candle or wood burning also cause strong indoor emissions (Abbatt and Wang, 2020).

Cooking is considered one of the most important indoor sources, an activity which often occurs on a daily basis at home as well as on larger scales in e.g. restaurants. In a study evaluating the personal exposure to indoor aerosol, cooking was identified as the largest contributor to indoor PM (particulate matter) (Zhao et al., 2006). The indoor PM concentrations can increase tremendously depending on the cooking activity with $PM_{2.5}$ concentrations (PM of aerodynamic diameter with $d_p < 2.5$ µm) of up to 1400 µg m^{-3} (Abdullahi et al., 2013). In developing countries where solid fuels are often used for cooking the health burden through the stronger emissions is even higher (Chafe et al., 2014; Martin et al; Nasir and Colbeck, 2013).

Cooking activities also have an impact on the ambient aerosol. In urban areas cooking contributes 5-30% of the organic aerosol in fine particles during the typical meal times, as shown by various measurements, including measurements with the AMS (aerosol mass spectrometer; Crippa et al., 2013; Mohr et al., 2012; Struckmeier et al., 2016), TAG (thermal desorption aerosol gas chromatography−mass spectrometry; Wang et al., 2020) and filter measurements (Rogge et al., 1991). During mapping measurements in the proximity of restaurants, performed by Robinson et al. (2018) with an AMS, most measured organic aerosol plumes were attributed to cooking emissions with concentrations of up to 100 µg m^{-3}, showing the potential of cooking emissions to affect local air quality.

During cooking, a large fraction of the emitted particle mass is in fine particles ($PM_{2.5}$), while the particle number concentrations of the emissions are dominated by ultrafine particles ($d_p < 100$ nm). Accordingly, the number and mass size distributions are dominated by Aitken and accumulation mode particles, respectively (Buonanno et al., 2009; Marval and Tronville, 2022; Wallace et al., 2004; Wallace and Ott, 2011; Yeung and To, 2008). When inhaled, these particles can enter deep into the lungs to the alveoli. Especially the ultrafine particles, due to their larger specific surface, can cause stronger reactions or inflammation processes in the body, compared to larger particles with the same total mass (Baron et al., 2011; Marval and Tronville, 2022; Thomas, 2013).

A large variety of substances is emitted during cooking including volatile organic compounds and particulate matter. The major constituents are saturated and unsaturated fatty acids, glycerides, as well as sugars and their decomposition products, like levoglucosan. Furthermore, aromatics, PAHs (polycyclic aromatic hydrocarbons), and aldehydes might be emitted, many of which are hazardous to health (Abdullahi et al., 2013; Cheng et al., 2016; Klein et al., 2016; Liu et al., 2018; Zhao et al., 2007; Zhao et al., 2019).

Studies of individual aspects of emissions from cooking activities have shown that the composition and quantity of the emissions are affected by various parameters, like the preparation method, ingredients, cooking temperature, and used fuel type (e.g., Zhang et al., 2010). The particle sizes as well as number and mass concentrations increase with increasing temperature during cooking (Amouei Torkmahalleh et al., 2012; Buonanno et al., 2009; Klein et al., 2016; Zhang et al., 2010). The comparison of different preparation methods like steaming, boiling, baking, deep-frying, stir-frying, and grilling showed that the lowest emissions were observed from steaming and boiling while the strongest were from grilling, followed by deep- and stir-frying (Alves et al., 2015;

Lee et al., 2001; Olson and Burke, 2006). The differences are mainly due to the different cooking temperatures and the use of oil. For example, See and Balasubramanian (2006) measured the particle size distribution of emissions from cooking tofu with five different preparation methods and observed a 24-fold increase in particle number concentration compared to the background during deep-frying compared to a 1.5-fold increase during steaming. Another aspect which is relevant for the amount of particulate emissions is the smoke point of the used oil. Studies measuring the emissions from heating different oils showed that for oils with high smoke points, as sunflower and soy oil, compared to olive oil with a lower smoke point, the emissions were 4 – 9 times lower (Amouei Torkmahalleh et al., 2012; Gao et al., 2013).

In addition to primary aerosol particles, cooking emissions contain substantial amounts of VOCs (e.g., Katragadda et al., 2010; Klein et al., 2016), S/IVOCs (Yu et al., 2022), and aldehydes (Takhar et al., 2021), which are potential precursors for secondary organic aerosol (SOA) formation. SOA production rates from cooking-related gaseous emissions have been determined using oxidation flow reactors that simulate defined intervals of atmospheric aging. These experiments have shown that the amount of SOA from cooking processes compared to the primary aerosol emissions ranges from similar values to more than an order of magnitude higher amounts (Liu et al., 2018; Yu et al., 2022; Zhou et al., 2021) and is strongly dependent on the cooking method (Zhu et al., 2021).

The analysis of cooking emissions is challenging due to the high complexity of the emitted substance mixture, as well as the high emission dynamics with strong concentration variability ~~in concentrations~~ during ~~the~~ cooking. ~~Especially~~ In particular the ingredients and the preparation method have a strong influence on the emissions (Abdullahi et al., 2013; Marć et al., 2018; Zhang et al., 2010). In addition, the sampling approach itself (e.g., sampling location or dilution of samples) and the analysis procedure (e.g., focusing on peak levels or integrating over the entire cooking process) can have a strong influence on the resulting emission data.

As shown above, there are several studies in the literature that focus on individual aspects of particulate or gas phase emissions from cooking. Few of these studies focus on the emission dynamics during cooking and their dependence on, for example, cooking related activities. Others focus on physical particle characteristics of the emitted aerosol or on the chemical composition of the emissions. Even within those studies that provide emission factors for different aerosol properties (e.g., particle number or mass), substantial differences in the experimental setup often prevent direct comparability of emission factors obtained in different studies. ~~So far~~To date, there are very few systematic studies that have both ~~covering~~ investigated the influence of different cooking parameters on the emissions ~~while~~ and measur~~ed~~~~ing~~ a large variety of chemical and physical aerosol properties in parallel.

Therefore, we conducted a comprehensive study of cooking emissions by performing a measurement series cooking 19 dishes with different ingredients and preparation methods. During the cooking, various chemical and physical properties of the emitted primary aerosol were monitored in real time with our mobile laboratory (MoLa, used in stationary measurement mode in the laboratory), including PM, organics and non-refractory inorganics, BC and PAH mass concentrations as well as the particle number concentration and size distribution. These online measurements allowed for the analysis of the emission dynamics during the cooking and of the influence of different cooking activities during the preparation on the emissions.

The emissions were quantified and emission factors related to the amount of food were determined for all relevant variables. Based on the laboratory measurements, we investigated how the identification of cooking emissions with the AMS and generally the identification of new AMS markers can be further improved using a new diagram type. Furthermore, the influence of cooking emissions on ambient aerosol was studied at two German Christmas markets with MoLa. Based on these measurements, we examined the applicability of the laboratory-derived emission factors to ambient data.

2 Methods and instrumentation

2.1 Laboratory study design and experimental procedure

For a systematic study, 19 different dishes were cooked in the laboratory (Table 1~~Table 1~~). The concept was to prepare dishes often-cooked in Central Europe (Germany) while including different classes of ingredients and preparation methods, i.e. boiling, stir-frying, deep-frying, baking, and grilling with gas and charcoal. Each dish was cooked with an amount for approximately four persons and all ingredients were weighed before preparation (Table S1). Rapeseed oil was used for the preparation of all dishes except for the boiled dishes, frozen pizza, and brownies. Only salt and pepper were used as seasoning if not stated otherwise in Table S1.

Table 1: List of prepared dishes for the laboratory study (for details see Table S1).

Preparation method	Dishes
Boiling	Boiled potatoes, rice, noodles
Stir-frying	Fried potatoes, bratwurst, schnitzel, fish, spaghetti Bolognese, stir-fried vegetables, Indian curry
Deep-frying	French fries (in pot), French fries (deep fryer), Bavarian doughnut (in pot)
Baking	Baked potatoes, frozen pizza, brownies
Grilling on gas grill	Steaks, vegetable skewers
Grilling on charcoal grill	Steaks

Each dish was cooked three times on the same day to assess the variability of the emissions due to variations in ingredients and performance of the cooking process between the repetitions. Background measurements were performed over 20 min right before the start of the cooking. Between repetitions, we waited for the aerosol concentration to return to a stable background level; if necessary, the room was ventilated. The cooking process was recorded using a webcam (HD Pro Webcam C920, Logitech, Switzerland) to apportion individual concentration changes to activities during the cooking. Furthermore, the surface temperature of the cooked food and of the cookware were~~as~~ measured repeatedly (typically every few min) at selected locations ~~(typically every few min)~~ with an IR thermometer (Fluke 568, Fluke Corporation, USA). During the baking experiments, the temperature of the air inside the oven was monitored continuously using the same thermometer with a thermocouple as sensor. The ambient temperature around the kitchen setup was not measured. We estimate that it ranged ~~between~~from about 18 °C ~~and~~to 25 °C, depending on the ~~outdoor ambient~~ outside temperature~~s~~.

The measurements were performed in an experimental hall with a custom-made kitchen setup consisting of a regular household electric stove with oven (30540 P, Privileg, Germany) and a fume hood above (CH 44060-60 GA, Respekta®, Germany) which was connected to an exhaust ventilation (Fig.1). The exhaust flow rate Q_E was 7.5 m^3 min^{-1}. To quantitatively capture the cooking emissions, the space between the stove and the fume hood was encased by four plexiglass walls and only the front glass was left partially open, leaving a gap of ca. 50 cm to be able to access the cookware. For the oven and barbecue experiments, additional screens were used for a complete capture of the emissions. From the pipe of the exhaust ventilation above the fume hood the cooking emissions were sub-sampled, diluted (1:13) with a dilution system (VKL 10 E, Palas, Germany) using dry, particle-free compressed air (1 bar), and transferred to the instruments inside our mobile laboratory MoLa. As the dilution with dry air led to low relative humidity (< 7 %) we measured dry particles, which might differ in particle size (and, therefore, mass) from particles measured without dilution close to the source. The particle loss within the setup was calculated using the particle loss calculator (von der Weiden et al., 2009) and found to be negligible for the particle size range relevant in this study.

The stir-fried dishes were prepared in a Teflon-coated frying pan, the boiled dishes in a stainless-steel pot, and the deep-fried dishes in a stainless-steel pot or a deep fryer (FT 2400.9, 2300 W, 2.5 L oil, Tevion, Germany). For the barbecue experiments, a gas and a charcoal grill were used.

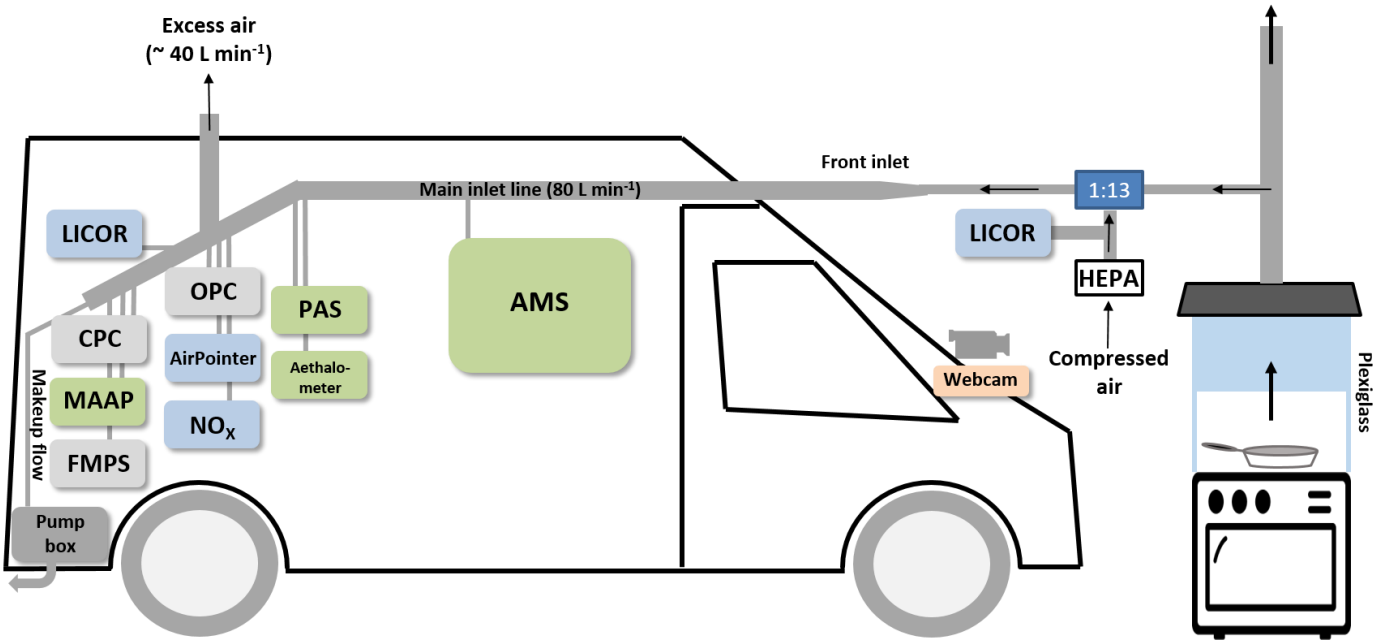

Figure 1: Scheme of the laboratory setup for the cooking experiments (MoLa scheme adapted from Drewnick et al., 2012). HEPA: high-efficiency particulate air filter. For details regarding the instrumentation, see Table S2.

2.2 Ambient measurements at two German Christmas markets

Measurements to assess the influence of cooking emissions on the local air quality under ambient conditions were performed at two Christmas markets in Germany:

- Ingelheim (05.12. until 08.12.2019)

  The Christmas market in Ingelheim (ca. 35000 inhabitants) was located around the Burgkirche; the mobile laboratory MoLa was situated directly behind a circle of seven food stands, offering burgers, French fries, flame-grilled salmon, waffles, vegan food, and mulled wine, at the eastern edge of the market. A barrel for wood fire was placed on the 07. and 08.12.2019 at a distance of 25 m from MoLa and another barrel in the middle of the food stands circle next to MoLa (distance approximately 10 m) during all evenings. More food stands and wood fire barrels were distributed over the market, which covered an area of ca. 100 m by 50 m. The opening hours were 06.12. 5 PM until 10 PM, 07.12. 3 PM until 10 PM, and 08.12. 3 PM until 9 PM.

- Bingen (13.12. until 15.12.2019)

  The Christmas market in Bingen (ca. 25000 inhabitants) was spread over the city center. MoLa was located at the eastern edge of the Bürgermeister Neff Square, an open area of ca. 50 m by 25 m, with the closest food stand at a distance of 25 m. The six food stands on the square, offering Langos, French fries, bratwurst, barbecue, crepes, raclette, tarte flambée, sweets, and mulled wine, were arranged in a half circle. On the 14.12. a suckling pig was grilled over an open wood fire next to the western edge of the square. Furthermore, on the 14. and 15.12. a barrel for wood fire was placed in the middle of the square and another barrel on a crossing road at the western edge of the square. The opening hours were 13.12. 4 PM until 9 PM, 14.12. 11 AM until 9 PM, and 15.12. 11 AM until 7 PM.

The inlet height for the MoLa instrumentation was at 5 m above ground level. We measured mostly dry particles as the elevated temperature within MoLa led to low relative humidity (< 32 %) in the inlet lines. During the measurements in Ingelheim, we additionally measured with a portable aethalometer (microAeth® MA200, AethLabs, USA) the black carbon mass concentrations during random walks across the market.

The temperatures during the measurements at both locations were in the range of 4 – 11 °C and light occasional rain showers occurred. The wind direction in Ingelheim was mainly from south-southwest with wind speeds of 1 – 4 m s^{-1} and in Bingen from west with wind speeds of 0.5 – 2 m s^{-1}, which resulted in the mobile laboratory being downwind of the Christmas markets most of the time.

2.3 Instrumentation

Within the mobile laboratory (MoLa) various instruments were used to measure different aerosol properties like the particle number concentration (measured with a condensation particle counter CPC for particles with d_p > 5 nm and with an optical particle counter OPC for particles with d_p > 250 nm) and particle size distribution (d_p = 5.6 nm – 32 µm, measured with two different instruments: the fast mobility particle sizer FMPS and the OPC), the mass concentration for the fractions PM_1, $PM_{2.5}$, PM_{10} and the chemical components black carbon (BC) and PAH in the PM_1 fraction as well as trace gas concentrations of NO_x, O_3, SO_2, CO, and CO_2. The HR-ToF-AMS (high-resolution time-of-flight aerosol mass spectrometer) was applied to measure the non-refractory chemical composition of PM_1 and was operated in V-mode for maximum sensitivity, with a time resolution of 15 s for the laboratory measurements and 30 s for the Christmas market measurements. An overview of the MoLa instruments, the measured variables, time resolutions, and measurement uncertainties is provided in Table S2; for further details regarding MoLa see Drewnick et al. (2012).

2.4 Data processing

All data processing was performed with Igor Pro (versions 6 – 8, WaveMetrics, Inc., USA). The data from the laboratory (Christmas market) measurements were averaged on a common 15 s (30 s) time base. All data were corrected for sampling time delays, checked for invalid data due to e.g. internal calibrations, and normalized to standard conditions (T = 20 °C, p = 1013.25 hPa). In the further analysis of the cooking experiments, the sampling dilution (1:13) was considered. From the combined FMPS and OPC size distribution data the PM_1, $PM_{2.5}$, and PM_{10} mass concentrations were calculated (SI Sect. S1). The time averaged data from the individual experiments were averaged over the three repetitions (if not stated otherwise), such that the corresponding standard deviation reflects the variability between the repetitions. For the Christmas market measurements, the periods with opened and closed market, respectively, were averaged separately over all days.

To calculate the cooking emissions from the laboratory data, the averaged background concentrations (c_{Back}) measured before each experiment were subtracted from the concentrations measured during the cooking (c_{Cook}). Identified trends in the background concentrations were corrected accordingly. Emission factors (EF) were calculated to estimate the total emissions from cooking per kilogram food according to Eq. (1) from the average concentration of the respective variable ($c_{Avg} = c_{Cook} - c_{Back}$), the volume flow rate of the exhaust Q_E (7.5 m^3 min^{-1}), the preparation time t, the dilution factor D (13), and the mass of the ingredients m.

$$EF = \frac{c_{Avg} \cdot Q_E \cdot t \cdot D}{m} \quad (1)$$

The analysis of the high-resolution AMS data was performed with the software tools SQUIRREL 1.63I and PIKA 1.23I within Igor Pro following the standard procedures (Canagaratna et al., 2007). The ionization efficiency of the AMS as well as the relative

ionization efficiencies for ammonium (4.21) and sulfate (1.31) were determined in calibrations before and after the measurements.

For the laboratory data, a collection efficiency (CE) of 1 was applied ~~as~~ because we assumed that the emitted particles were mostly composed of liquid components.~~,~~ This assumption is valid only for the laboratory measurements and is based on the observation that BC and other co-emitted (non-organic) components contribute only about 1% to the total submicron aerosol mass (see Table S6). Using this approach, we can determine ~~and for each dish~~ the relative ionization efficiency for organics (RIE_{COA}) ~~was determined~~for each dish ~~separately~~ (see Sect. 3.1.4). For the Christmas market data, the standard values for the CE (0.5) and RIE_{Org} (1.4) were applied (Canagaratna et al., 2007) except for the cooking organic aerosol fraction, as described in Sect. 3.5.1.

For the comparison of the measured mass spectra with ~~the ones~~those of different organic aerosol types from previous studies (Table 2~~Table 2~~), all available high-resolution mass spectra of the respective aerosol types were taken from the AMS spectra database (Ulbrich et al., 2009; Ulbrich et al., 2022), as listed in Table S3.

Positive matrix factorization (PMF, Paatero and Tapper, 1994) was performed on the AMS organic high resolution mass spectra up to *m/z* 116 using the PMF Evaluation Tool (PET) v3.07C (Ulbrich et al., 2009, see SI Sect. S2 for details).

Table 2: List of organic aerosol types and their acronyms.

Acronym	Aerosol type
COA	Cooking organic aerosol
BBOA	Biomass burning organic aerosol
HOA	Hydrocarbon-like organic aerosol
OOA	Oxygenated organic aerosol
LVOOA	Low-volatile oxygenated organic aerosol
SVOOA	Semi-volatile oxygenated organic aerosol
LOOOA	Less oxidized oxygenated organic aerosol
MOOOA	More oxidized oxygenated organic aerosol
NOA	Nitrogen-enriched organic aerosol
CCOA	Coal combustion organic aerosol
CSOA	Cigarette smoke-related organic aerosol
IEPOX-SOA	Isoprene-epoxydiol-derived secondary organic aerosol

3 Results and discussion

3.1 Chemical analysis of cooking emissions with HR-ToF-AMS

3.1.1 Average chemical composition and correlation of mass spectra

The mass spectra of the non-refractory PM_1 cooking emissions from different dishes show high similarity between each other. On average, the measured aerosol consisted mainly of organics (96.7 – 99.9 %) with minor contributions of nitrate (< LOD – 2.8 %), ammonium (< LOD – 0.5 %), sulfate (< LOD – 1.8 %), and chloride (< LOD – 0.4 %). Most ions of the organic fraction were attributed to the C_xH_y family (77.8 – 91.8 %) indicating a weakly oxidized aerosol. The remaining ions were mostly oxygen containing ions ($C_xH_yO_1$: 6.5 – 17.4 %; $C_xH_yO_{>1}$: < LOD – 6.2 %) with a small fraction attributed to the C_xH_yN family (< LOD – 2.3 %) and C_x family (0.1 – 0.8 %). For two dishes, Indian curry and spaghetti Bolognese, small fractions of the ions were attributed to the C_xS family (0.1 %) and also the sulfate fraction was slightly elevated (0.3 – 0.7 %), presumably due to the emission of sulfur-containing substances from onions in the food (Boelens et al., 1971).

To obtain quantitative information on how similar the emissions from different experiments are, linear correlations between all ~~the~~ averaged normalized organic mass spectra (unit mass resolution) of the emissions from all dishes were calculated (Fig. 2). Additionally, the mass spectrum of emissions from heated rapeseed oil (Fig. S1) was included in this ~~analysis~~ comparison. ~~as~~This choice of a comparison spectrum is based on the fact that ~~-~~rapeseed oil was used for all dishes where oil was required. Most spectra show a high degree of similarity between each other and with the spectrum of rapeseed oil (Pearson's $r > 0.94$), suggesting~~and we conclude~~ that the emissions ~~consisted mostly~~ are associated with oil, which might have ~~of~~ vaporized and re-condensed ~~oil~~. Consistently, the mass spectra of emissions from boiled dishes and steaks grilled with charcoal are less similar to those of the rest: For the boiled dishes no oil was used and for the steaks the mass spectrum is strongly influenced by the emissions from the charcoal itself. Additionally, the correlations of the cooking mass spectra with the ones of various fatty acids (palmitic, stearic, oleic, and linoleic acid), all measured with the AMS (Ulbrich et al., not shown in Fig. 2) show the highest similarity with the one of oleic acid (r = 0.85 – 0.94), the main component of rapeseed oil and many other cooking oils. These observations suggest that a substantial fraction of cooking-related emissions are fatty acids, either from the used cooking oils or from components of the prepared food. This is consistent with the fact that oil components may vaporize and recondense, and fats contained in the food

may produce condensable fatty acids after decomposition. In contrast, peptides and carbohydrates are more likely to decompose into products that either remain in the gas phase or do not vaporize under the cooking conditions.

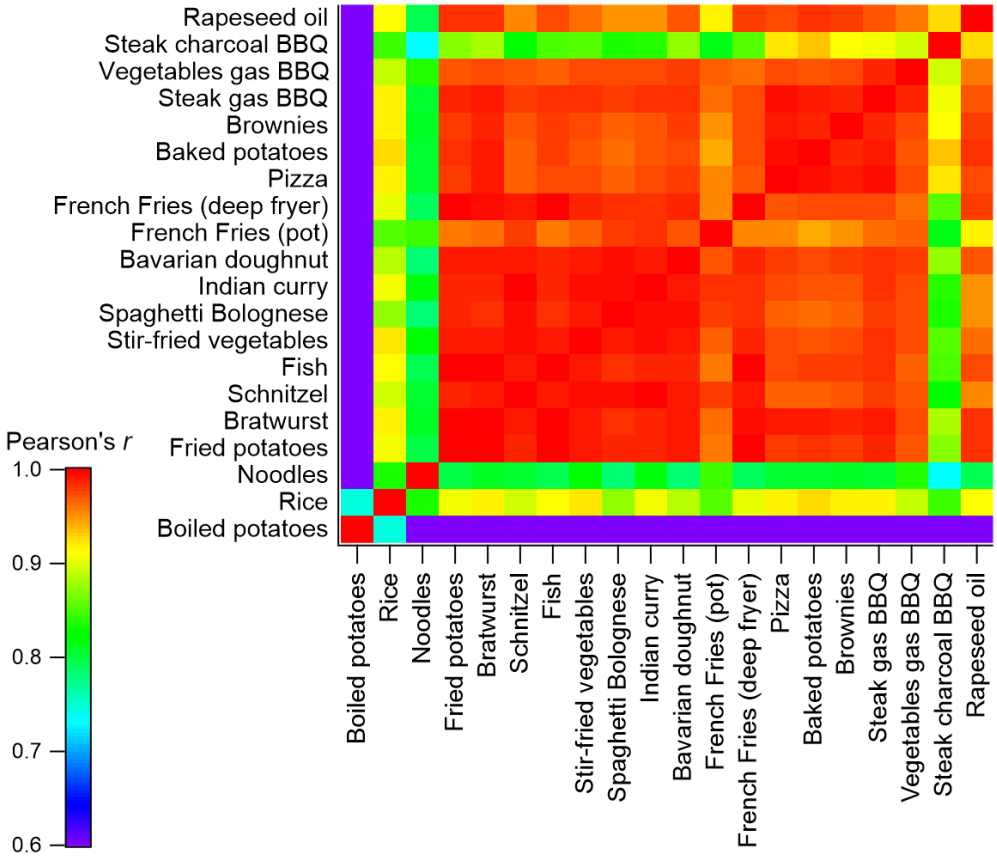

Figure 2: Linear correlation of the averaged mass spectra of cooking emissions for all laboratory experiments and pure rapeseed oil, color-coded based on the respective correlation coefficient (Pearson's *r*).

Furthermore, correlations of the cooking mass spectra from this study with mass spectra of different organic aerosol types from previous studies were calculated (Fig. S2). The latter, obtained through PMF analysis of field measurement data, were taken from the AMS spectra database (Ulbrich et al. 2023) and averaged over all available spectra for the respective aerosol type (see Table S3 for list of used mass spectra). The highest similarity of mass spectra related to oil- or fat- containing dishes was observed with the average COA mass spectrum (r = 0.92 ─ 0.98); therefore, we ~~assume~~ conclude that also during field measurements, the mass spectra of ~~detected~~ cooking-related emissions are significantly influenced by the mass spectral patterns~~mostly consisted~~ of vaporized and re-condensed oil or fatty acids. Furthermore, a strong correlation was observed between the mass spectra from the steak charcoal grilling experiment with the one of HOA, presumably due to the contribution of charcoal combustion to the overall emissions in this case.

3.1.2 Characteristics of mass spectra from cooking emissions

The main characteristics of the mass spectra from the cooking experiments are ~~agree with those of previous studies (Allan et al., 2010; Mohr et al., 2009; Mohr et al., 2012),~~ exemplarily shown in Fig. ~~S~~3 for the "frying bratwurst" experiment. The highest signal intensities were found at *m/z* 41 and 55, except for the boiled dish experiments. These signals are due to emissions of unsaturated hydrocarbons, presumably unsaturated fatty acids (He et al., 2010; Mohr et al., 2009). The most prominent ion series in the mass spectra are $C_nH_{2n+1}^+$ and $C_mH_{2m+1}CO^+$ (*m/z* 29, 43, 57, 71, …), and $C_nH_{2n-1}^+$ and $C_mH_{2m-1}CO^+$ (*m/z* 41, 55, 69, 83, …) from alkanes,

alkenes, and oxygenated substances like acids, especially fatty acids. In addition, the ion series $C_nH_{2n-3}^+$ (*m/z* 67, 81, 95, 107, …) and $C_6H_5C_nH_{2n}^+$ (*m/z* 77, 91, 105) indicate the presence of cycloalkanes and aromatic hydrocarbons (Alfarra et al., 2004; He et al., 2010; McLafferty and Turecek, 1993; Mohr et al., 2009).

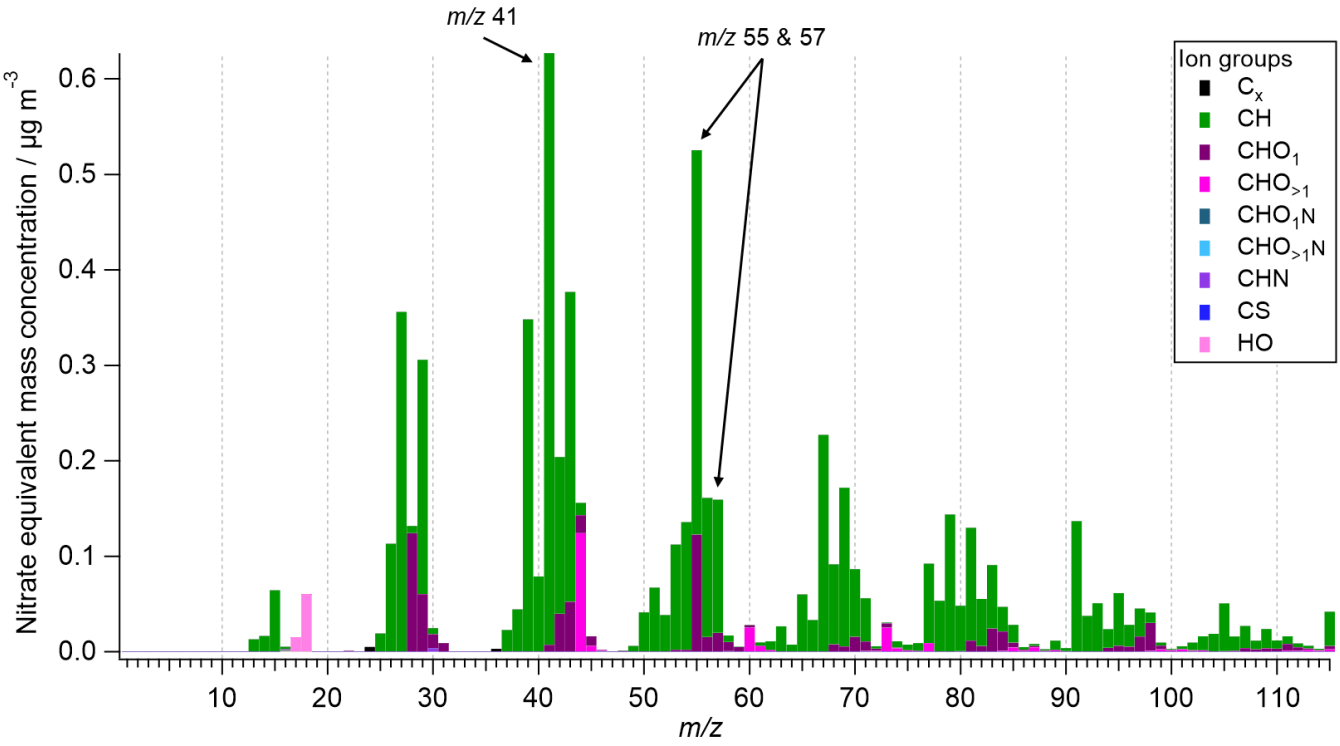

Figure 3: Unit-resolution mass spectrum of emitted organic aerosol from frying bratwurst with important *m/z* marked.

An ~~well known~~ indicator~~ion~~ for COA is a high ratio of *m/z* 55 to *m/z* 57 in the mass spectra.~~, typically above two (Mohr et al., 2012; Sun et al., 2011; Xu et al., 2020).~~ ~~For the presented~~In our experiments, the observed ratio was 2.3 ─ 4.5, except for the boiled potatoes and the steaks grilled with charcoal with 1.3 and 1.7, presumably due to the fact that the respective emissions are not dominated by vaporized oil and decomposed fats. This is in good agreement with the observation of ratios of typically above two for COA-related mass spectra (Mohr et al., 2012; Sun et al., 2011; Xu et al., 2020).

As another meaningful marker for cooking-related organic aerosol ~~is~~we identified the ~~comparison of the mass spectra with those of other typical aerosol types from the AMS spectra data base (Ulbrich et al.) indicates that a~~ ratio of *m/z* 67 to *m/z* 69 in the spectra~~above 1 might be another potential COA marker~~. ~~This ratio for HOA, BBOA, LVOOA, and SVOOA is ranging from 0.63 to 0.88 (Table S4).~~ For ~~the~~ our cooking experiments, th~~is~~e ratio was in the range of 1.1 – 1.6, again excluding the boiled potatoes and the steaks over charcoal grilling experiments with 0.81 and 0.7, respectively. The ratio for COA obtained from previous PMF analyses of ambient measurements is 1.2 ± 0.1 (Ulbrich et al.), while from direct measurements of cooking aerosols differing results were obtained. For emissions from Chinese cooking, heating sunflower, soy, corn, and rapeseed oil, and frying sausages and French fries with rapeseed and sunflower oil, the ratio was above 1 (Faber et al., 2013; He et al., 2010; Liu et al., 2017a; Liu et al., 2017b; Xu et al., 2020), while Allan et al. (2010) and Zhang et al. (2021) measured ratios below 1 from heating or cooking with rapeseed, sunflower, peanut, and corn oil; further it was below or close to 1 for barbecue emissions, frying meat, heating olive and palm oil, and lard (Kaltsonoudis et al., 2017; Liu et al., 2018; Xu et al., 2020). ~~This ratio f~~For HOA, BBOA, LVOOA, and SVOOA, ~~is~~ratios ranging from 0.63 to 0.88 were observed (Table S4).

Considering these studies, we conclude that the ratio of *m/z* 67 to *m/z* 69 in the mass spectra is dependent on the fatty acid composition and the fraction of polyunsaturated fatty acids in the measured aerosol. For saturated and monounsaturated fatty acids the ion series $C_nH_{2n-1}^+$ and $C_mH_{2m-1}CO^+$ (*m/z* 41, 55, **69**, 83, …) are more prominent, while for polyunsaturated fatty acids the ion series $C_nH_{2n-3}^+$ (*m/z* **67**, 81, 95, 107, …) is dominant (Christie; Hallgren et al., 1959). For oils from rapeseed, sunflower, and corn the fraction of polyunsaturated fatty acids is above 25% and the ratio of *m/z* 67 to *m/z* 69 is mainly above 1. For oils with lower fractions of polyunsaturated fatty acids, like palm or olive oil, and animal fats, like lard, the ratio is below 1. Thus, the ratio of *m/z* 67 to *m/z* 69 might be an indicator for the composition of the oil used for cooking.

~~Emissions from biomass burning are mostly identified by the high signal intensity at *m/z* 60 and 73 which is due to the fragments $C_2H_4O_2^+$ and $C_3H_5O_2^+$ of levoglucosan generated by pyrolysis of cellulose (Schneider et al., 2006).~~ During the laboratory cooking experiments, ~~also~~ elevated signal intensities for *m/z* 60 and 73 ~~these ions~~ were observed~~, however less intense than for biomass burning aerosols~~. We found t~~T~~hese ~~elevated~~ enhanced signal intensities ~~were~~ also ~~measured~~ for emissions from pure heated rapeseed oil and they were also observed in reference mass spectra of the fatty acids oleic, stearic, and palmitic acid (AMS spectra database, Ulbrich et al. 2023). ~~Typically~~Frequently, in AMS mass spectra, high signal intensities at *m/z* 60 and 73 are an indication of biomass burning aerosol, due to the fragments $C_2H_4O_2^+$ and $C_3H_5O_2^+$ of levoglucosan generated by pyrolysis of cellulose (Schneider et al., 2006).~~,~~ Elevated signal intensities at these *m/z* in cooking-related aerosols, however, ~~therefore~~ likely originate~~and therefore in these cases likely originate~~ from fatty acids rather than from levoglucosan, i.e. the ion structure contains a carboxyl group rather than a diol (Fachinger et al., 2017), leading to a different fragmentation pattern. Thus, ~~A~~a possibility to differentiate between biomass burning and cooking emissions ~~therefore~~ might be the ratio of *m/z* 60 to 73. The ratios for pure levoglucosan and BBOA are 3.7 and 1.5, respectively, while the ratios from the cooking experiments, excluding the boiled dishes due to low organic concentrations and high uncertainty, ambient COA, and fatty acids are at most 1.1 (Table 3~~Table 3~~). Similar observations were reported by Xu et al. (2020) who measured a ratio of ~2 for BBOA and around 1 for COA. However, since the ratio of *m/z* 60 to 73 for HOA (Table 3) is not significantly different from those of the various COA-related values, it cannot be used by itself to differentiate between these two types of organic aerosols (see also Fig. S3).

Table 3: Ratio of signal intensities at *m/z* 60 and 73 from mass spectra of different compounds and aerosol types. For BBOA, HOA, COA, and the cooking experiments the average and standard deviation was calculated from the available data. All mass spectra except for the cooking experiments were obtained from the AMS spectra database (Ulbrich et al., 2023).

	Ratio of signal intensities at *m/z* 60 and 73
BBOA-related	
Levoglucosan	3.71
BBOA	1.47 ± 0.53
HOA-related	
HOA	0.95 ± 1.12
COA-related	
Oleic acid	0.81
Stearic acid	0.87
Palmitic acid	0.89
COA	1.10 ± 0.13
Cooking experiments (our study) [a]	0.90 ± 0.08
Rapeseed oil	0.95

[a]excluding boiled dishes (low organic concentrations)

3.1.3 Discrimination of different aerosol types based on markers in their mass spectra

Ambient aerosol is usually a mixture of various aerosols of different types due to the contribution by different aerosol sources and aging processes in the atmosphere. To identify individual aerosol types and their contribution to the total aerosol, PMF is applied to the mass spectra of the measured organic aerosol fraction and the obtained factors are attributed to various aerosol types using different indicators and through comparison to other available data. For this study, a new type of diagram was applied to verify whether combinations of known and new indicators in the mass spectra are suitable to reliably differentiate between different aerosol types and to check whether PMF worked well for separating different aerosol contributions. While in some cases (like *f*60/*f*73, see Sect. 3.1.2) individual markers might be sufficient to reasonably differentiate between different aerosol types, using such a combination of indicators can give a more robust information also in cases where differences between individual markers are less pronounced between different aerosol types.

In these "rectangle plots", the values of two indicators for all available aerosol types are plotted against each other in an xy-diagram. The standard deviation or uncertainty for each indicator of a certain aerosol type is reflected in x- and y-direction by a box to show the variability of the mass spectra for this aerosol type. The different aerosol types are well separated with a selected combination of indicators if there is no overlap of boxes. Indicators for individual aerosol types might be the fraction of the signal intensity at a single *m/z* from the total organic signal, e.g. f_{44} for the signal fraction at *m/z* 44, a combination of such fractions, e.g. f_{55}/f_{57}, or organic aerosol elemental ratios, like *O/C* and *H/C*.

For the cooking experiments, the respective values were calculated as average from the three repetitions, while for the individual reference aerosol types, available mass spectra from the AMS spectra database (Ulbrich et al., 2022) were averaged. The corresponding standard deviation is shown as box in both cases; if only one reference mass spectrum or one repetition was available (e.g., rapeseed oil, RO), ~~only a marker is shown~~the variability observed during the respective measurement is used as the uncertainty in the rectangle plot. The experiments with the boiled dishes and one of the deep-frying French fries experiments, in which the frying oil cooled down strongly due to too many French fries used, were excluded from this analysis due to very low organic concentrations and resulting high uncertainties.

Plotting the two known COA markers, f_{55} and f_{55}/f_{57}, together in such a rectangle plot (Fig. ~~3~~4) shows that the mass spectra of ambient COA and from the cooking experiments are well separated from those of other aerosol types with this ~~selection~~ combination of markers. The values for COA and the cooking experiments are in the top right corner with high f_{55} (> 0.06) and f_{55}/f_{57} (> 2) values. Though COA and HOA mass spectra are often similar, using both markers in combination they are well separated from each other, except for the experiment steaks grilled with charcoal which is located within the HOA box. The values of f_{55} for the cooking experiments are slightly lower than those from ambient COA while the f_{55}/f_{57} values are similar for both or slightly higher than those of the ambient COA. This could either be due to the difference between ambient and laboratory aerosol, as ambient aerosol can chemically change in the atmosphere, or because PMF is not able to separate the different aerosol types completely; it could also simply reflect the fact that the cooking experiments represent single source processes, whereas the ambient COA data represent an aerosol that is a mixture of a large number of sources. The PMF results from the Christmas market measurements (Sect. 3.5) can be found in the same area of the rectangle plot, but partially outside the one-sigma range of the literature COA results. It is noteworthy that the box representing the results of the pure rapeseed oil measurements is shifted to slightly larger f_{55} values compared to those from the laboratory cooking experiments. This result suggests that although the correlation analysis shows a high similarity between the rapeseed oil and the cooking emission mass spectra, the cooking emissions contain other components in addition to rapeseed oil. Similarly, for pure oleic acid (taken from the AMS spectra database), f_{55} is significantly larger than the value found for the cooking related aerosols and rapeseed oil, probably due to the fact that the latter also contain other components. The f_{55}/f_{57} versus f_{55} rectangle plot also shows that e.g. BBOA is not well separated from CCOA, CSOA and several OOA aerosol types based on this combination of COA markers.

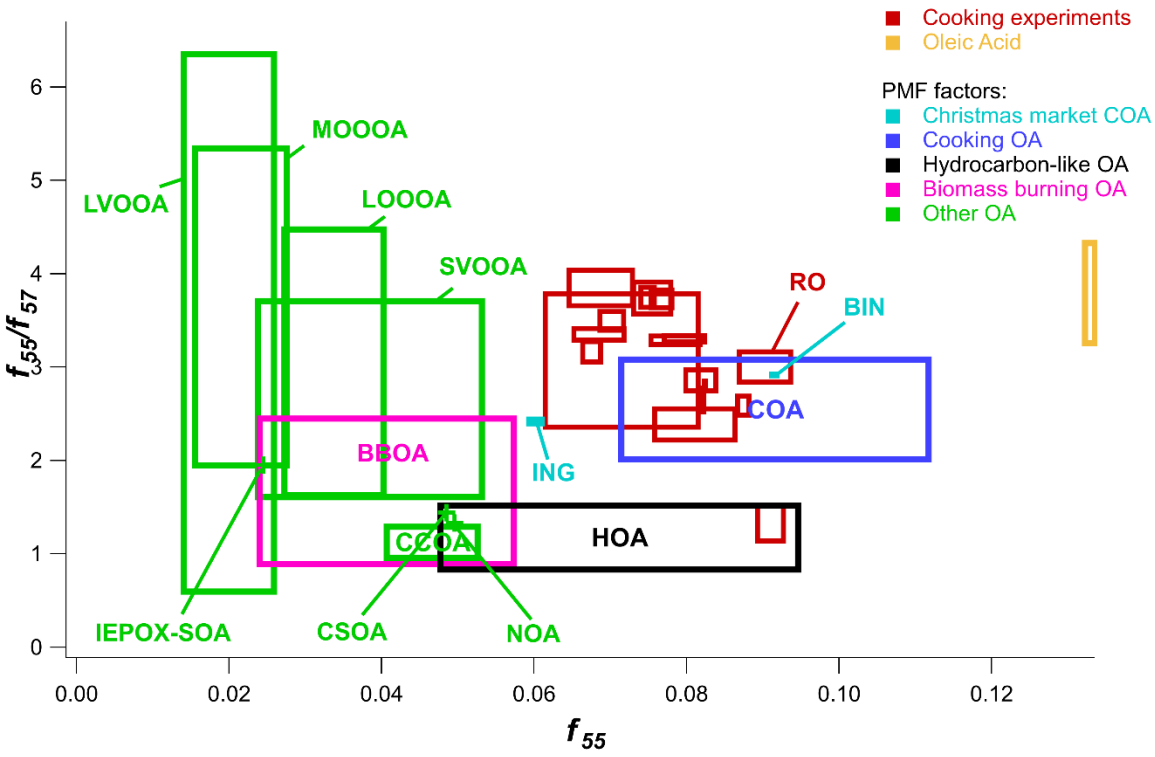

Figure ~~4~~3: "Rectangle plot" of f_{55}/f_{57} combined with f_{55} for the cooking experiments and various organic aerosol types from ambient measurements. The rectangles represent one~~the~~ standard deviation of the markers for the respective aerosol types as found in mass spectra from the literature. The acronyms for the different aerosol types are listed in Table 2~~Table 2~~; RO stands for rapeseed oil; ING and BIN stand for the Christmas market measurements in Ingelheim and Bingen, respectively.

To determine whether the ratio f_{67}/f_{69} is suitable as COA marker, these ratios were plotted together with f_{55} in another "rectangle plot" (Fig. 5~~4~~). Also for this combination of markers, the cooking results are found in the upper right area of the plot, well separated from the other aerosol types. Only for the charcoal grilled steak experiment was an overlap found with the HOA box. The rapeseed oil results are found on the higher f_{55} side of the laboratory cooking experiments, as in the previous rectangle plot (Fig. 4). ~~Although the laboratory results and ambient COA are well separated from most other aerosol types, there is an overlap with HOA for two of the laboratory experiments. Therefore~~From these results~~,~~ we conclude that the ratio f_{67}/f_{69} might be a marker for COA similar as the ratio f_{55}/f_{57}, but the influence of the fatty acid composition of the emitted oil or fat needs to be considered (see Sect. 3.1.2). Therefore, the ratio of f_{67}/f_{69} should only be used as additional marker for COA.

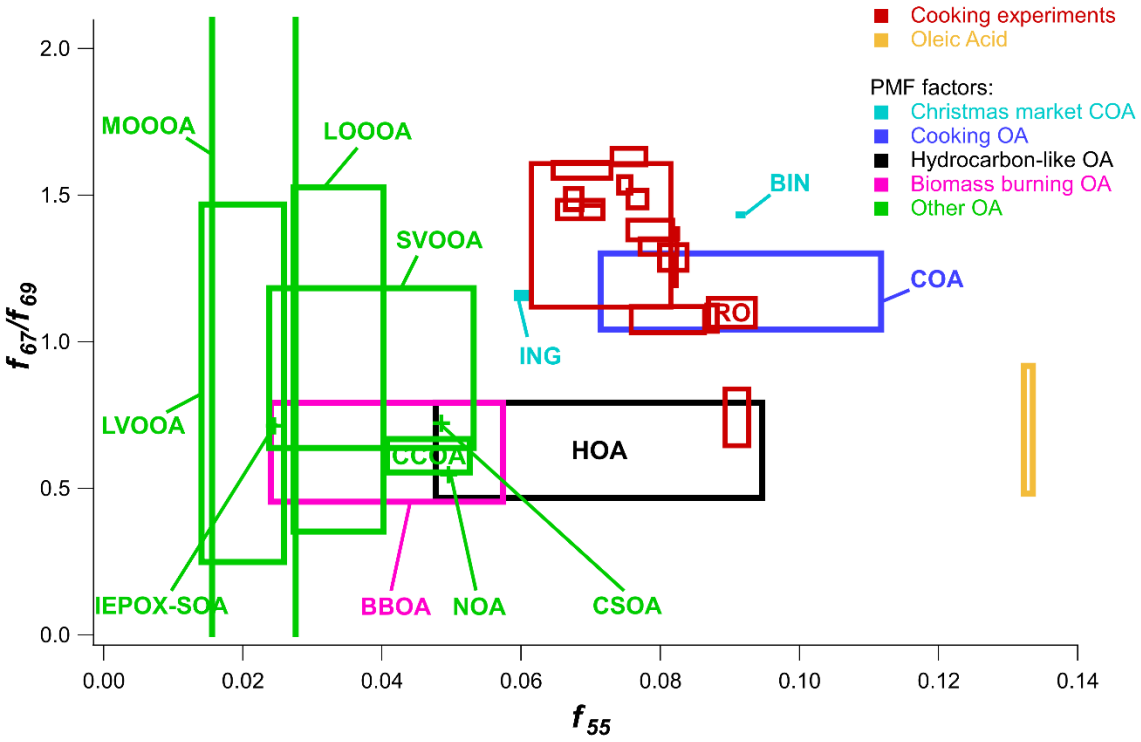

Figure 5~~4~~: "Rectangle plot" of f_{67}/f_{69} combined with f_{55} for the cooking experiments and various organic aerosol types from ambient measurements. The rectangles represent one~~the~~ standard deviation of the markers for the respective aerosol types as found in mass spectra from the literature. The acronyms for the different aerosol types are listed in Table 2~~Table 2~~; RO stands for rapeseed oil ING and BIN stand for the Christmas market measurements in Ingelheim and Bingen, respectively.

The high-resolution mass spectra from the cooking experiments were used to extract further information about the individual ions that contribute to the specific cooking-related mass spectra. Due to the strong fragmentation of organic molecules in the AMS analysis process, the individual ions measured by the instrument provide little information about the corresponding aerosol components. For this reason, AMS organics analysis typically reports ion families (i.e., groups of ions containing specific combinations of atomic contributions) rather than individual ions. For the *m/z* discussed in the previous "rectangle plots" (*m/z* 55, 57, 67, and 69), ions associated with the C_yH_y and C_xH_yO ion families are observed for the cooking experiments. In addition, ions of the $C_xH_yO_2$ family are found at very low abundance in the *m/z* 57 and *m/z* 69 signals.

Table 4 illustrates the contribution of different ion families to the individual marker *m/z* signals and corresponding ions. For each ion family at each *m/z*, in addition to the main ion, an isotope ion containing ^{13}C is listed. These contribute approximately 2-3% of the respective family signal. For all marker *m/z*, the signal is dominated by the pure hydrocarbon ions (i.e., the ions from the C_xH_y family) with smaller relative contributions for *m/z* 55 and 57 (75% and 86%, respectively), in comparison to those for *m/z* 67 and 69 (~100% and 96%, respectively). Consequently, the relative contribution of oxygen-containing ions is larger for *m/z* 55 and 57

and almost negligible for *m/z* 67. The uncertainties provided in Table 4 are the standard deviations for the individual relative ion family contributions, calculated from all cooking experiments. The uncertainty due to background subtraction and variations in background concentrations is much smaller than the variability between individual cooking experiments and is included in these values. In general, no significant difference in the relative contributions of the different ion families is observed across different cooking methods, with the exception of grilling, which ~~has a notable effect on the~~shows a notable difference in the *m/z* 57 and *m/z* 69 composition. The contribution of the C_xH_yO family ions in the grilling experiments is significantly higher (18.1% for *m/z* 57 and 6.4% for *m/z* 69) than in the other experiments (12.4% for *m/z* 57 and 3.5% for *m/z* 69). This suggests that the grilling method results in an enhanced production of oxygen-containing substances, in comparison to the other cooking methods.

Table 4: Contribution of individual ion families and their associated ions to the ion signal at the four cooking-related marker *m/z*.

m/z	C_xH_y family		C_xH_yO family		$C_xH_yO_2$ family	
	ions	contribution	ions	contribution	ions	contribution
55	$^{13}CC_3H_6^+$, $C_4H_7^+$	75±4%	$^{13}CC_2H_2O^+$, $C_3H_3O^+$	25±4%	-	-
57	$^{13}CC_3H_8^+$, $C_4H_9^+$	86±5%	$^{13}CC_2H_4O^+$, $C_3H_5O^+$	14±5%	$^{13}CCO_2^+$, $C_2HO_2^+$	0.3±0.4%
67	$^{13}CC_4H_6^+$, $C_5H_7^+$	99.9±0.3%	$^{13}CC_3H_2O^+$, $C_3H_3O^+$	0.1±0.3%	-	-
69	$^{13}CC_4H_8^+$, $C_5H_9^+$	96±2%	$^{13}CC_3H_4O^+$, $C_4H_5O^+$	4±2%	$^{13}CC_2O_2^+$, $C_3HO_2^+$	0.3±0.3%

3.1.4 Relative ionization efficiency of cooking-related organic aerosol

The quantification of the aerosol species measured with the AMS is based on Eq. (2) (Canagaratna et al., 2007)

$$C_S = \frac{10^{12}\ MW_{NO_3}}{CE_S\ RIE_S\ IE_{NO_3}\ Q_{AMS}\ N_A} \sum_{all\ i} I_{S.i} \quad (2)$$

converting the ion rates of species S, $I_{S,i}$, summed over all i *m/z*, to mass concentrations C_S, with MW_{NO_3} the molecular weight of nitrate (in g mol^{-1}), Q_{AMS} the volumetric inlet flow rate (in cm^3 s^{-1}), N_A Avogadro's number and 10^{12} a unit conversion factor to µg m^{-3}. The remaining (unitless) factors in Eq. (2) are from calibrations or based on assumptions. The collection efficiency CE_S for the species S gives the ratio of particle mass measured by the AMS to the particle mass introduced to the inlet. It is mainly influenced by the particle phase, solid or liquid. The typical value for ambient aerosol is 0.5 accounting for mainly solid particles, a fraction of which bounces off the vaporizer without being vaporized. For particles from the presented cooking experiments, a CE value of 1 was chosen assuming that the emitted aerosol ~~mostly consisted of~~ contained substantial amounts of liquid oil ~~droplets~~ (see Sect. 3.1.1) which suppresses~~do not~~ bounce (Matthew et al., 2008).

The ionization efficiency of nitrate IE_{NO_3}, determined in a calibration, is used as a basis to calculate the ionization efficiencies for other species, using the relative ionization efficiency of species S (RIE_S) relative to IE_{NO_3}. The default value for RIE_{Org} is 1.4 based on multiple laboratory experiments with various types of organic species (Canagaratna et al., 2007). As concentrations of COA measured with the AMS in previous studies were found to be higher compared to those from parallel measurements with other instruments, the RIE_{COA} is assumed to be larger than 1.4 (Katz et al., 2021; Reyes-Villegas et al., 2018; Yin et al., 2015).

In this work, RIE_{COA} was determined through comparison of the PM_1 mass concentration determined from the FMPS and OPC measurements (PM_1) to the total AMS and black carbon mass concentration ($PM_{1,AMS+BC}$), measured in parallel. The oven and boiling experiments were excluded from this analysis due to almost exclusively low measured organic mass concentrations (< 1 µg m^{-3}). The density for the fine particles used to calculate PM_1 from the particle volume was in the range of 0.91 – 1.03 g cm^{-3} (Table S5), determined individually for each dish (see Sect. S1). These values are in good agreement with the densities for

cooking emissions found by Katz et al. (2021) (0.95 – 1.0 g cm^{-3}), and, considering their uncertainty of 15%, also with that of rapeseed oil (0.91 g cm^{-3}), in agreement with our assumption that the particulate emissions from the cooking experiments ~~consisted mainly of~~ contained substantial amounts of vaporized and recondensed oil or fatty acids (see Sect. 3.1.1).

The measured PM_1 consisted mostly of organics (see Sect. 3.1.1; contribution of BC was negligible); consequently, as expected, $PM_{1,AMS+BC}$ was higher for most cooking experiments compared to PM_1 when using the default RIE_{Org} = 1.4. To determine RIE_{COA} for the individual experiments (or, more specifically, the product of RIE_{COA} and CE; we assume CE = 1), the $PM_{1,AMS+BC}$ time series was correlated with the one of PM_1 for each experiment separately and the RIE_{COA} was adjusted to obtain a slope of 1 for the correlation. For the grilling experiments, the RIE values were determined separately for the experimental phases "grilling" and "grill warm-up" with the latter ones not considered as RIE_{COA}. A typical example correlation for each cooking method is shown in Figure S4. The resulting RIE_{COA} values for the cooking experiments were in the range of 1.53 – 2.52 and thus frequently significantly above the default value of 1.4 (Fig. ~~5~~6 and Table S5). The uncertainty for the determined RIE_{COA} value was estimated to be 38%, based on the method of Katz et al. (2021) with uncertainty propagation (see Sect. S3).

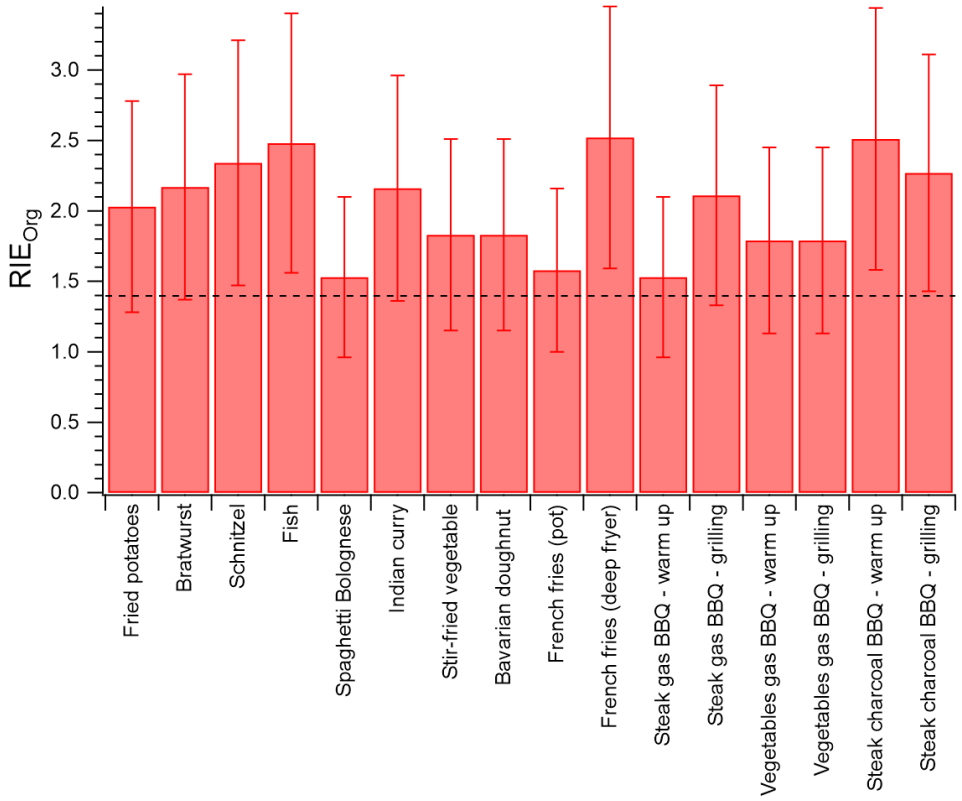

Figure ~~5~~6: RIE_{COA} obtained for the different cooking experiments. The default RIE_{Org} of 1.4 is shown as dashed line.

In previous AMS studies of cooking-related emissions, the determined RIE_{COA} was also above 1.4. Reyes-Villegas et al. (2018) determined RIE values of 1.56 – 3.06 for cooking emissions from different types of dishes through comparison of the measured concentrations (CE = 1) with SMPS (scanning mobility particle sizer) size distribution measurements (d_p = 18 – 514 nm), comparable to our results. In contrast, from indoor aerosol measurements during cooking events, Katz et al. (2021) determined considerably higher RIE_{COA} values of 4.26 – 6.50 with CE = 1, also through comparison with SMPS data (d_p = 4 – 532 nm). A possible explanation for the larger values from Katz et al. (2021) could be that the RIE_{COA} depends on the fatty acid composition of the oil or fat containing droplets. For oleic acid, the main fatty acid of rapeseed oil which was used in the present study and the one of Reyes-Villegas et al. (2018), Katz et al. (2021) obtained an RIE value of 3.18 ± 0.95, similar to the value of 3.0 measured

by Xu et al. (2018), while for linoleic acid, the main component of soy oil, which Katz et al. (2021) used for their cooking experiments, an RIE value of 5.77 ± 1.73 was found.

Summarizing the results from the current and previous studies, we recommend for measurements close to cooking emission sources an RIE_{COA} larger than 1.4 for the COA fraction of the measured organic aerosol. Depending on the cooking oil, which presumably has a strong influence on the RIE_{COA} value, we suggest for soy oil-based cooking an average RIE_{COA} of 5.16 ± 0.77 (average of all measurements with standard deviation), based on the measurements by Katz et al. (2021), while for rapeseed oil-based cooking we recommend an average RIE_{COA} of 2.17 ± 0.48 (average of averages from both studies and standard error) based on the presented measurements of this study and the ones by Reyes-Villegas et al. (2018). The individual values used for this estimate are listed in Table S5.

3.2 Emission dynamics related to temperature and cooking activities

To study the emission dynamics during cooking as a consequence of different activities, the concentration time series determined for all dishes and for all measured variables were inspected in combination with the webcam recordings. For six emission variables increases and changes over the preparation time were identified: particle number concentration of smaller and larger particles measured by the CPC (PNC, d_p > 5 nm) and OPC ($PNC_{d>250\ nm}$), PM concentration (PM_1, $PM_{2.5}$, PM_{10}), BC, PAH, and organics mass concentrations (shown exemplarily for the experiment "frying bratwurst" in Fig. S~~4~~5). From these six, $PNC_{d>250nm}$, organics and PM mass concentrations are all associated with the total emitted particle mass and therefore show similar emission dynamics. No increase above the detection limit was observed for the measured trace gas concentrations, except for NO_x during the grilling experiments and SO_2 during the charcoal grilling experiment.

For the six variables, two kinds of systematic changes were observed. Firstly, the measured concentrations for these variables increased over the preparation period, along with a~~n~~ general increase of the food and cookware temperature, as deduced from repeated manual temperature measurements with the IR camera. The emission concentrations usually started to increase only after a certain heating or cooking period, probably when the used oil and food reached a certain temperature. Also, during inactivity of sufficiently long times, i.e. more than approximately 30 – 60 s, the $PNC_{d>250\ nm}$ and organics mass concentration increased as probably certain locations of the food reached sufficiently high temperatures. Such increased particle mass and number emissions with higher temperature were also observed in previous studies, e.g. by Buonanno et al. (2009), Amouei Torkmahalleh et al. (2012), and Zhang et al. (2010).

Reason for this progressive increase of concentrations is presumably the increasing vaporization of substances with rising temperatures. After emission, the vaporized substances cool down again, finally resulting in increased particle number and mass concentration due to nucleation and re-condensation. Accordingly, the emission concentrations decreased when the power of the stove was turned down.

An increase of BC and PAH mass concentrations was observed only for cooking methods operating at high temperatures like grilling or in the final phase of preparing stir-fried dishes. PAHs are formed at high temperature, especially above 400 °C, and due to incomplete combustion like during grilling, where BC is formed as well (Jägerstad and Skog, 2005; Lijinsky, 1991; Omidvarborna et al., 2015). The described dependence of the measured concentrations on temperature is ~~shown~~ schematically illustrated in Fig. ~~6~~7. Due to the substantial heterogeneity of the temperature distribution throughout the food and cookware and the unknown location of the generation of emissions, this relationship can only be presented qualitatively.

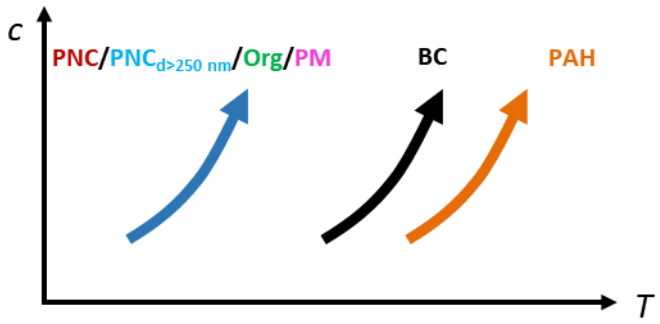

Figure ~~7~~6: Schematic diagram of the temperature (*T*) dependence of the emission concentrations (*c*) of six relevant species.

The second systematic observation are short-time concentration changes associated with different activities during cooking, e.g. tilting the pan or flipping the food, which have not been studied in such detail so far. The activities leading to these short-time changes are schematically shown in Fig. ~~7~~ 8 ~~(symbols explained in Fig. S5)~~, grouped by emission variables, with the increase factors by which the concentrations change from right before the increase up to the corresponding maximum concentration. The factors are color-coded, in green for relative increases below one order of magnitude, in yellow for increases above one order of magnitude and in red for increases above two orders of magnitude.

~~T~~Presumably the emission concentrations rise briefly when hot material of the cooked food is brought to the surface by stirring or similar activities, facilitating vaporization. This leads to increased particle formation and growth through condensation of these substances. Furthermore, contact of cold, water-containing food with strongly heated surfaces, such as the pan, grill or hot oil, leads to rapid vaporization of oil, various other substances, and, above all, water, which can cause bubbling of oil. The associated enhancement of the oil surface presumably leads to increased vaporization of oil and mechanical formation of larger particles due to bursting of oil bubbles. These processes rapidly decrease as the hot surface cools down. Similarly, short-term increases in concentration occur when droplets or components of the grilled food, as well as residues from cleaning the grate, fall onto hot surfaces, such as the charcoal, and quickly vaporize or burn. Due to the high temperatures at these locations, also transient concentration increases of BC and PAH are generated. The strongest increases in the emission concentrations for almost all variables were observed when the oven was opened during baking, presumably due to the low concentrations before the oven was opened and the sudden release of emissions which had accumulated within the oven.

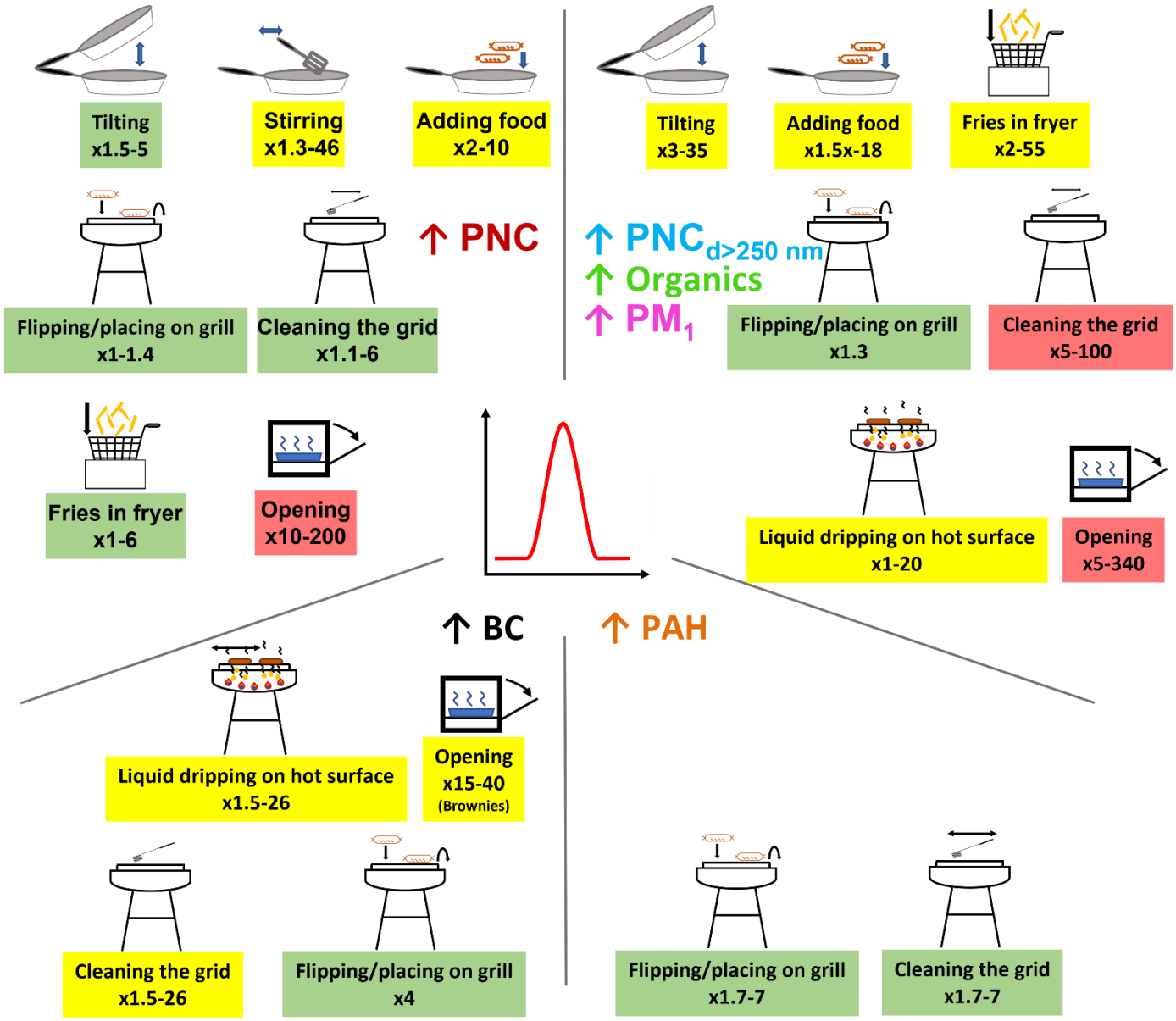

Figure ~~8~~7: Schematic diagram of short-time concentration increases for the different variables due to various activities during preparation of the dishes ~~(see Fig. S45 for the meaning of the symbols)~~. PM_1 is shown representatively for PM. The range of factors by which the concentrations typically increase are shown as numbers and color-coded, in green for small, in yellow for medium and in red for high concentration increases.

3.3 Influence of preparation method and cooking activities on the particle size distribution

The averaged particle number and volume size distributions of the emitted aerosols were similar for dishes with the same preparation method in terms of position and intensity of the particle mode. An overview of the mode diameters for the aerosols emitted during preparation of different dishes, grouped by the preparation method or dish type, is shown in Table 5~~Table 4~~. The average standard deviation of the mode diameters from the three repetitions was 5 nm for the particle number size distribution and 25 nm for the particle volume size distribution. Therefore, the observed differences between the distributions for the different preparation methods were partially statistically significant.

The particle number distribution for most dishes was dominated by Aitken mode particles. The mode diameters ($d_{p,N}$) varied, depending on the preparation method, between 20 – 50 nm (Fig. S6). During the warm up phase of the grilling experiments, the size distribution was broader and plateau-like, presumably due to a combination of different particle generation processes like

combustion of leftovers from the grid and incomplete combustion of the charcoal, but also dominated by Aitken mode particles (10 – 30 nm).

The average volume size distributions showed more variability for different preparation methods (Fig. S7). The distributions were mostly bimodal with an Aitken or accumulation mode and a coarse mode. During baking and grilling with gas the mode diameter of the fine particles was in the Aitken mode range ($d_{p,V}$ = 50 – 70 nm) while during frying and grilling with charcoal the distribution was dominated by accumulation mode particles (200 – 300 nm). The coarse mode diameter was in the range of 2 – 3 µm.

Table 54: Range of mode diameters from the averaged particle number and volume size distributions for particles emitted from the cooking of different dishes, sorted by mode diameter (dN/dlogd_p).

Preparation method/ dish type	Dishes	Mode diameter dN/dlogd_p ($d_{p,N}$)	Mode diameter dV/dlogd_p ($d_{p,V}$)
Grill warm up (gas, charcoal)		20 ─ 30 nm	Gas: 50 ─ 60 nm, 2.5 ─ 3 µm Charcoal: 300 nm, 720 nm, 2.2 µm
Deep-frying in pot	French fries, Bavarian doughnut	20 ─ 30 nm	275 ─ 280 nm, 2 µm
Stir-frying with sauce	Spaghetti Bolognese, stir-fried vegetables, Indian curry	20 ─ 35 nm	205 ─ 220 nm, 2 ─ 3 µm
Grilling with gas	Vegetable skewers, steak	30 ─ 35 nm	60 ─ 70 nm, 2 ─ 5 µm
Baking	Baked potatoes, pizza, brownies	30 ─ 35 nm	45 ─ 70 nm, 2 ─ 3 µm
Stir-frying	Fried potatoes, bratwurst, schnitzel, fish	40 ─ 50 nm	205 ─ 220 nm, 2 ─ 3 µm
Deep-frying in deep fryer	French fries	50 nm	205 nm, 2 ─ 3 µm
Grilling with charcoal	Steak	50 nm	205 nm, 600 nm, 2.2 µm
Boiling	Boiled potatoes, rice, noodles	No clear result due to small concentrations	300 ─ 465 nm

Presumably, the observed mode diameter of the emitted fine (i.e. submicron) aerosol is mostly influenced by the temperature of the prepared food and cookware. With higher temperature more oil and other substances can vaporize, leading to stronger particle growth and consequently larger particles. For example, particles from stir-fried dishes were larger ($d_{p,N}$ = 40 – 50 nm) than from stir-fried dishes with sauce (20 – 35 nm) as the addition of the sauce cooled down the food and pan and the sauce effectively covered the hottest part of the system, the base of the pan. Furthermore, the available amount of material which can vaporize influences the particle growth. For example, during frying, compared to baking, more oil is available which can vaporize, leading to larger particles. During grilling with charcoal, compared to gas, the particles were larger as the incomplete combustion of charcoal generates smoke and, due to the higher temperature, additional substances can vaporize, also from the charcoal itself.

The coarse mode particles are generated by mechanical processes, presumably from oil bubble bursting. During grilling with charcoal, the combustion of the charcoal also leads to the emission of coarse particles. The particles emitted from the boiled dishes are presumably initially coarse particles from water bubble bursting with droplets containing dissolved salt and other food components which shrink due to the low relative humidity to accumulation mode particles.

In accordance with our measurements, similar dependencies for the mode diameter of the temperature and available amount of material which can vaporize were observed in previous studies. With increasing cooking temperatures Amouei Torkmahalleh et al. (2012), Buonanno et al. (2009), and Zhang et al. (2010) measured particle size distributions with larger mode diameters.

Furthermore, Buonanno et al. (2009) observed for emissions from grilling (without oil on electric or gas grill) of fatty foods, like cheese, bacon, and sausage larger number mode diameters ($d_{p,N}$ = 40 – 50 nm) compared to those from cooking vegetables ($d_{p,N}$ = 30 nm) showing that the availability of easily vaporizable substances, here fat or its decomposition products, leads to larger particles.

Apart from the preparation method, which is mainly characterized by the cooking temperature and availability of water, oil, or fat, individual activities during the cooking also influence the particle size distribution of the emitted aerosol. Such influences are shown in Fig. ~~8~~ 9 using the example of deep-frying French fries in the deep fryer, showing the number size distributions (15 - 30 s time periods, averaged over all repetitions) of emissions during different activities or preparation phases. Included are the corresponding PM_1 mass concentrations for the same periods; colored arrows illustrate the temporal changes.

In the beginning, the particle number concentration, size and mass concentration increase as the frozen fries are placed in the basket above the oil and then submerged into the oil (pink arrow). When the fries are put into the basket, the oil starts to bubble as small parts of the fries and ice crystals drop into the hot oil and the water vaporizes immediately. The bubbling increases when the fries are submerged into the oil as more water rapidly vaporizes. The bubbles lead to a larger oil surface, enhancing the vaporization of oil and therefore the particle formation and growth. As a consequence of the frozen fries in the oil, the oil cools down and less oil vaporizes and consequently the particle number concentration, size and mass concentration decrease (green arrow). As the oil slowly heats up again towards the end of the cooking process all variables increase again due to increased oil vaporization (yellow arrow).

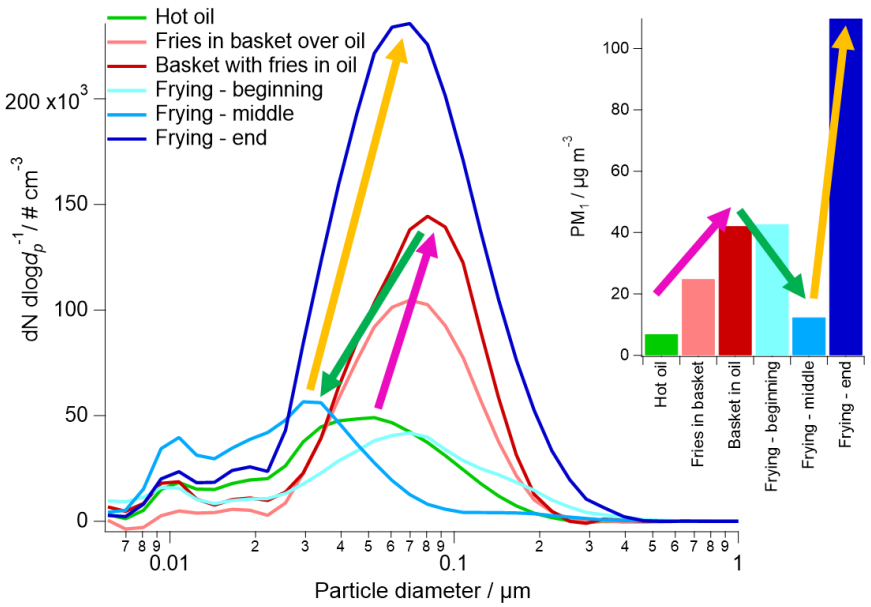

Figure ~~9~~8: Average number size distribution and PM_1 mass concentration for six different cooking activities / periods during the preparation of French fries in the deep fryer. The arrows illustrate the temporal trends.

The presented example illustrates the main parameters which influence the particle emissions: 1. the temperature of the prepared food and cookware, 2. the oil surface, and 3. the available amount of vaporable material, as also observed for the particle number concentration and mass concentration for various variables (see Sect. 3.2). Similar dependencies were also observed during the preparation of other dishes (Table ~~5~~6). Usually the mode diameter increased over the preparation period, as observed e.g. during the heating of the oven and grilling with charcoal. Presumably, the temperature increase of the food and the cookware led to stronger vaporization of oil and other substances. Also, various activities during the preparation of the food resulted in transient changes of the size of the emitted particles analogous to the changes of the emission intensity, as presented in Sect. 3.2. In addition,

when the grid of the grill was cleaned with a brush, the particle size increased, presumably because leftovers fell off grid onto the charcoal and burned or vaporized. A similar process was observed when steaks were cut on the grill and the meat juice drops vaporized off the hot grid or charcoal, leading to larger particles as well.

Table ~~5~~6: Overview of the particle mode diameter changes due to individual activities.

Process/activity	Mode diameter dN/dlogd_p	Reason
Grilling on charcoal	35 nm → 170 nm	Increase of temperature over time
Stir-frying	30 nm → 60 nm	Increase of temperature over time
Heating of oven	17 nm → 40 nm	Increase of temperature over time
Cleaning the grid of the grill	Increase by 5 – 10 nm	Food leftovers from the grid vaporized on hot surface
Cutting steaks on grill	Increase by 5 – 10 nm	Meat juice vaporized from hot surface

3.4 Quantification of cooking emissions: Emission factors

To be able to quantitatively estimate emissions from cooking activities and their impact on air quality based on the mass of prepared food, emission factors (amount of emitted substance per kg of prepared food) were calculated for all dishes from this study and for all relevant variables (Table S6). The PN (particle number, as measured by the CPC) and PM_1 emission factors are shown exemplarily in Fig. ~~9~~ 10 for all dishes, grouped by the respective preparation method. For other mass-based variables, e.g. organics, the general trends are similar to those of PM_1, which are described in the following.

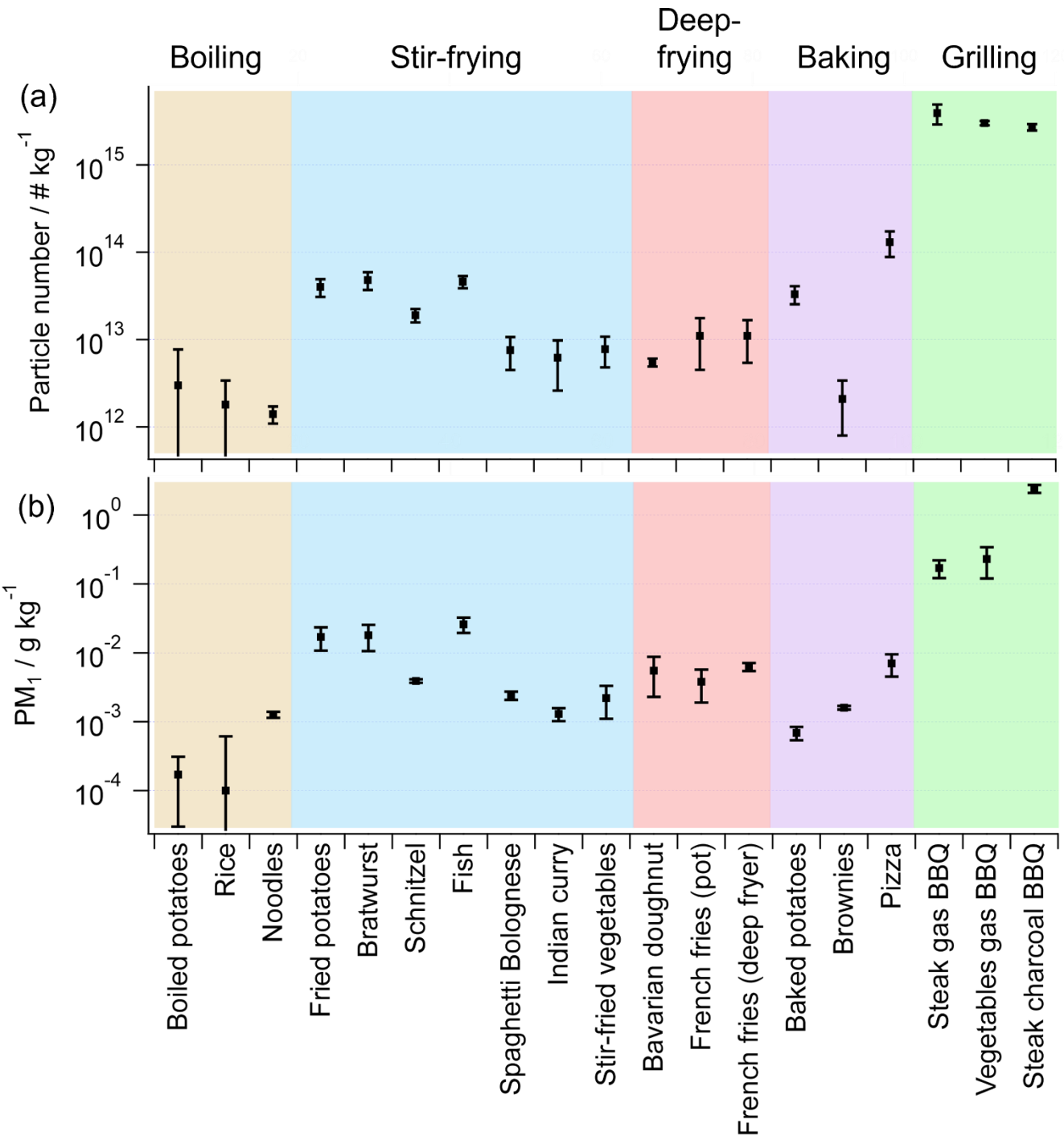

Figure 10: Emission factors for (a) PN and (b) PM_1 for all dishes, with standard deviation from the three repetitions as error bars. The values are grouped by the preparation methods, highlighted with different colors.

For dishes with the same preparation method the emission factors are similar and at most one order of magnitude apart from each other. The highest PN emission factors were observed for the grilling experiments with up to $4 \cdot 10^{15}$ kg^{-1} while the emission factors for the oil-based or fat-containing dishes, including the preparation methods stir-frying, deep-frying, and baking, are substantially smaller, ranging from $2.1 \cdot 10^{12}$ – $1.3 \cdot 10^{14}$ kg^{-1}. The smallest emission factors were observed for boiled dishes with values up to $3 \cdot 10^{12}$ kg^{-1}.

A similar trend was observed for PM_1 with highest emission factors for the grilling experiments (0.2 – 2.4 g kg^{-1}) and one to two orders of magnitude smaller emission factors for stir-fried, deep-fried and baked dishes ($7 \cdot 10^{-4}$ – 0.026 g kg^{-1}). Again, the smallest emission factors were found for boiled dishes ($1 \cdot 10^{-4}$ – $1.3 \cdot 10^{-3}$ g kg^{-1}).

The $PN_{d>250\ nm}$ (number of particles measured by the OPC, i.e. with d_p >250 nm) emission factors range from $5 \cdot 10^{7}$ – $2 \cdot 10^{10}$ kg^{-1} for boiled and baked dishes, from more than $2 \cdot 10^{10}$ – $9 \cdot 10^{11}$ kg^{-1} for stir-fried, deep-fried, and gas-grilled dishes, and up to $2 \cdot 10^{13}$ kg^{-1} for the charcoal-grilled dish. BC and PAH emissions were only observed for dishes where cooking temperatures were sufficiently high for their formation, e.g. the grilling and stir-frying experiments (18 – 28,000 µg kg^{-1} and 3 – 208 µg kg^{-1}, respectively). Sulfate was only observed for dishes containing onions and grilled dishes (6 – 354 µg kg^{-1}). The emission factors for all variables are listed in Table S6.

Generally, the trends in the observed emission factors for the different preparation methods were similar for the different measured variables. For mass-based or -related variables (PM_1, organics, PAH, BC, and $PN_{d>250\ nm}$) the emission factors from the charcoal grilling experiment are usually one order of magnitude higher compared to those of the gas grilling experiments. The incomplete combustion of the charcoal leads to the additional emission of smoke which includes larger particles and in total higher emitted mass. The combustion of charcoal during the warm up of the grill contributes already 34 – 52% of the total emissions for the whole cooking experiment, depending on the variable (PN, NO_x, organics: 34 – 40 %; PAH, $PM_{1/2.5/10}$, $PN_{d>250\ nm}$: 40 – 50 %; BC: 52 %). The emissions from grilling, compared to other preparation methods, are one to two orders of magnitude higher presumably due to burning of food leftovers from the grid and due to the higher temperatures leading to more vaporization of substances and hence increased particle formation and growth due to re-condensation.

The emission factors for the stir-fried, deep-fried, and baked dishes were similar to each other as in these cases the emissions are mostly due to vaporization and re-condensation of oil and other substances as well as mechanical processes like vaporization of water leading to oil bubbling and splashing. The lowest emissions were observed for boiled dishes which was the only applied preparation method without any oil or fatty food involved. For this preparation method, the only source for particles is bubble bursting leading to droplets which contain dissolved salt or other components.

Oil based cooking (e.g. deep-frying and stir-frying) leading to higher particle number concentrations compared to water-based cooking (boiling and steaming) was also observed by See and Balasubramanian (2006), Wu et al. (2012), and Zhang et al. (2010). Similar observations were made for the emitted particle mass (Alves et al., 2014; See and Balasubramanian, 2006) and PAH emissions (Chen et al., 2007; Zhao et al., 2019).

For comparison with the results from previous studies, PN and $PM_{2.5}$ emission rates (Table ~~Table 6~~7) were calculated for 1 kg of cooked food and 60 min preparation time (assuming that the food preparation takes one hour) for different preparation methods. The emission rates determined from our experiments were mostly comparable to those obtained from previous studies (He et al., 2004; Liao et al., 2006) or agreed with them within an order of magnitude (Lee et al., 2001; Nasir and Colbeck, 2013). In contrast, up to two orders of magnitude higher emission rates were reported by Buonanno et al. (2009) for PN and by Olson and Burke (2006) for $PM_{2.5}$ emissions.

Table ~~6~~7: PN and $PM_{2.5}$ emission rates for 1 kg of cooked food per hour preparation time, for different preparation methods. Comparison of our results with those of previous studies.

	PN / kg^{-1} h^{-1}	$PM_{2.5}$ / mg kg^{-1} h^{-1}
Stir-frying		
This work	$5.2 \cdot 10^{13}$	23
Buonanno et al. (2011)	$4.5 \cdot 10^{15} – 5.4 \cdot 10^{15}$	
Nasir and Colbeck (2013)	$8 \cdot 10^{12}$	78
He et al. (2004)	$1.5 \cdot 10^{13}$	
Baking		
This work	$8.6 \cdot 10^{13}$	5
Nasir and Colbeck (2013)	$2.6 \cdot 10^{13}$	45
He et al. (2004)	$1.2 \cdot 10^{13}$	
Olson and Burke (2006)		600
Grilling		
This work		280 – 2700
Olson and Burke (2006)		10380
Deep-frying		
This work		10
Liao et al. (2006)		3.2 – 8
Lee et al. (2001)		70
Olson and Burke (2006)		3600

In the case of the study by Buonanno et al. (2011), these differences may be caused by different measurement conditions, as the emissions in that study were measured in a closed kitchen with mechanical ventilation, at a distance of 2 m from the stove and not by capturing all emissions as in our study. In the case of the study by Olson and Burke (2006), who performed measurements with body-worn instruments to assess personal exposure, the massively ~~larger~~ higher emission rates they found compared to our and previous studies were presumably due to a combination of reasons such as the influence of the high relative humidity on the measured particle mass, their assumptions about dilution of the emissions, and the use of peak concentrations for their calculation rather than averages over the entire experiment. ~~Firstly, the high relative humidity during cooking led to larger particles and consequently an overdetermination of particle concentrations due to increased light scattering in the nephelometers, which were used in their study to infer $PM_{2.5}$. In addition, the authors assumed that the emissions would be diluted equally in the whole apartment volume; however, as stated in their manuscript, inhomogeneous distribution of the emissions caused differences in the inferred emission rates depending on the measurement location (i.e. kitchen vs. living room). Finally, for their calculations of the emission rates they considered only the peak concentrations during cooking, while in the present study the whole cooking period was considered.~~

Overall, the comparison of emission rate measurements shows that the obtained emission rates are dependent not only on the cooking conditions themselves, but also on the measurement (dilution) conditions and the method to calculate the emission factors or rates. This complicates the comparison of different studies.

To obtain an idea about the relevance of the emissions from cooking activities in relation to those from other emission sources, emissions from the various preparation methods were compared with emissions from traffic, biomass burning, burning of candles, and smoking. To this end, we calculated the emissions from these sources for activities over a period of one hour each, i.e. for the

one-time preparation of a dish ("cooking"), for driving a car over a distance of 100 km ("~~traffic~~driving a car"), for smoking two cigarettes ("smoking"), and for ~~biomass~~ wood burning-based heating a room of 50 m^2 ("~~biomass burning~~wood home heating") or burning a candle ("candle burning") for one hour. The emission factors for the various activities were taken from the literature, as summarized in Table S7. As these activities are chosen partially arbitrary, this comparison only serves as a rough classification of cooking emissions compared to those of other emission sources.

The calculated emissions for the dishes with the same preparation method were averaged for four variables: ~~PN,~~ PM_1, PN, BC, and PAH (Fig. 1~~0~~1 ~~and Fig. S8~~76), and their standard deviation is used as uncertainty. For the emissions from other sources, the ranges of emissions calculated from the emission factors found in the literature are presented as bars to reflect the variability of emission levels.

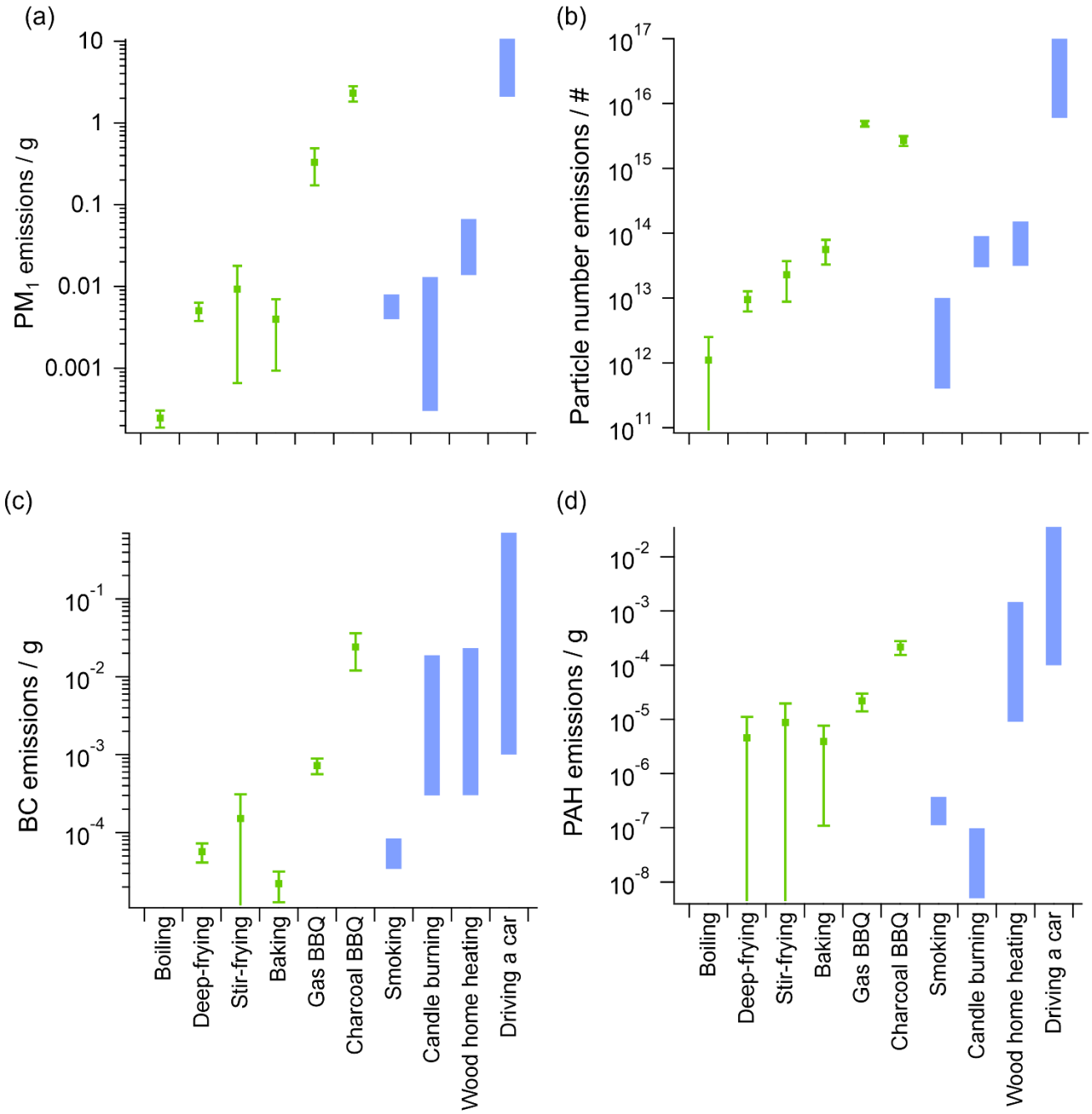

Figure 1110: Total emissions per unit activity of (a) PM_1 mass, and (b) particle number, (c) black carbon mass, and (d) PAH mass for cooking one dish, averaged for the different preparation types with the standard deviation as error bars, and comparison with emissions from various other activities during one hour, shown as bars indicating the variability found in the literature.

For the mass-based variables (PM_1, BC, PAH) the highest cooking emissions which were from charcoal grilling are in the same range as those observed from traffic car driving, indicating the potential for a significant local impact of grilling on air quality. This assumption is supported by a study of Kaltsonoudis et al. (2017), which shows that during a Greek holiday when traditionally meat is grilled everywhere in the city the contribution of COA reached up to 85% of the measured organic aerosol.

Stir-frying, deep-frying and baking, all oil-based preparation methods, show emissions of similar order of magnitude to each other, typically on the lower end of emissions from biomass wood burning-based room heating, and on the upper end of emissions from candle burning and cigarette smoking. This finding is consistent with observations from ambient measurements, which show that COA can easily make up similar proportions of total organics as traffic- and biomass wood burning-related organic aerosols, especially in urban environments (e.g., Mohr et al., 2012; Struckmeier et al., 2016). In indoor environments, cooking is one of the major emission sources leading to high emissions of fine particulate matter, number and mass wise, even exceeding the emissions due to light smoking (Abdullahi et al., 2013; Zhou et al., 2016; He et al., 2004).

Boiling, on the other hand, causes much smaller emissions, which are at the lower end or even below those of smoking and candle burning. Unlike oil-based preparation methods, boiling therefore will usually have no strong contribution to the total ambient aerosol load, which is in line with the conclusion that ambient COA consists mainly of externally mixed (Freutel et al., 2013) oil droplets (Allan et al., 2010).

3.5 Ambient measurements at two Christmas markets

At both Christmas markets, substantial aerosol concentration increases were measured during the opening hours compared to the background (i.e., the hours when the markets were closed) for the same six species which were also relevant during the laboratory measurements: PNC and $PNC_{d>250\ nm}$, PM, BC, PAH, and organics mass concentrations (Fig. S98 and Fig. S109). Additionally, CO_2 and particulate chloride (probably from burning of wood) concentrations increased, especially at the market in Ingelheim, presumably due to burning of wood at the market (Fachinger et al., 2018; Levin et al., 2010; Williams et al., 2012). A summary of measured concentrations (represented in box plots) for time periods inside and outside the opening hours is shown in Fig. 121, which illustrates the increase of concentrations due to the Christmas market emissions.

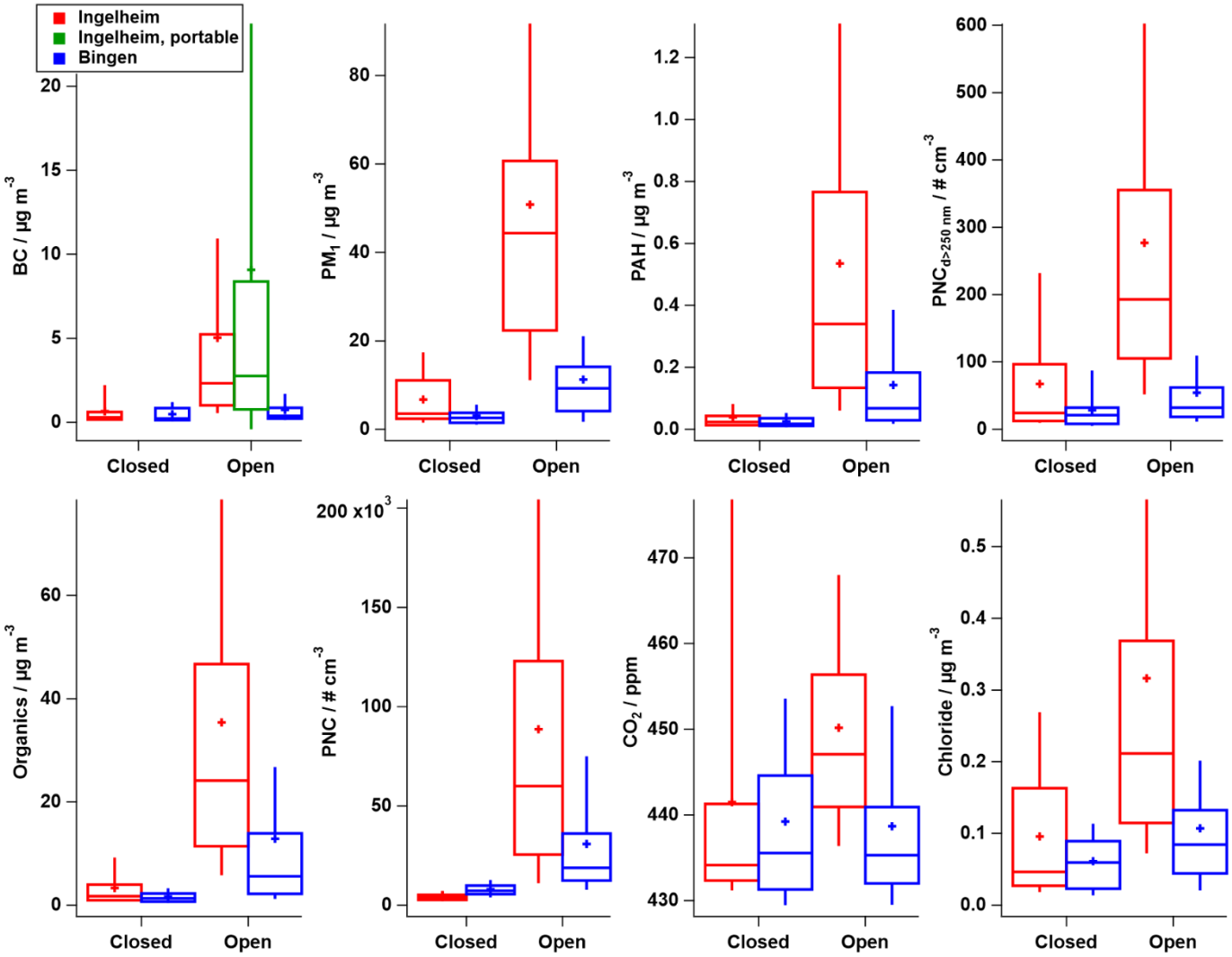

Figure ~~12~~11: Pollutant concentrations measured during (open) and outside (closed) the opening hours for the Christmas markets in Ingelheim (red and green) and Bingen (blue). For each variable, the average concentration is shown as cross, the 25th and 75th percentiles as box, with the median as horizontal bar, and the 10th and 90th percentiles as whiskers.

In Ingelheim, the median PNC and the organics, PM_1 and PAH mass concentrations were larger during the opening hours by more than one order of magnitude compared to the background period. The median $PNC_{d>250\ nm}$, BC, and particulate chloride mass concentrations were enhanced by a factor of 4 – 8. The median CO_2 volume mixing ratio was larger by 13 ppm. In Bingen, the median concentration enhancements due to the Christmas market emissions were smaller: for organics, PM_1, and PAH mass concentrations by a factor of 3.5 – 4.5, for the other variables by a factor of 1.5 – 2.5, except for CO_2, which did not show an increase during the opening hours.

The different concentration levels between both locations during the opening hours are presumably due to two reasons. First, in Ingelheim the measurement location was very close (few meters) to the food stands, while in Bingen the distance to the next food stand was about 25 m. Second, the Christmas market in Ingelheim was larger with more visitors and food stands which stood more densely. Generally, the measurements show that emissions from a Christmas market might lead to substantial pollutant concentration enhancements at a local level.

In Ingelheim, the BC mass concentrations were additionally measured with a portable aethalometer (Fig. 1~~1~~2, green box plot for BC) while repeatedly walking across the Christmas market during the opening hours to estimate the personal exposure of market visitors. The median value measured during these mobile measurements across the market was similar to the median value from

the stationary measurements directly downwind the market. This indicates that the measured concentrations at a single location at the downwind edge are representative for the overall market. At the same time, the average concentration measured with the portable instrument (9.1 µg m^{-3}) was almost twice as high as the average of the stationary measurements (5.0 µg m^{-3}). Thus, visitors of the market can be exposed to much higher transient BC concentrations, presumably when they walk close by fire places or other strong sources, increasing their personal exposure.

3.5.1 PMF analysis of the AMS organics data

For detailed information about the contribution of different aerosol types, the AMS organics mass spectra were analyzed using positive matrix factorization (PMF), separately for both Christmas markets. For both markets, BBOA, COA, and OOA (which is usually associated with aged background aerosol), were identified as aerosol types from the most reasonable PMF solution (Figs. S10~~11~~ and S11~~12~~). The challenge during this analysis was that two emission sources, cooking and biomass burning, were close to each other with similar activity times, while a requirement for the PMF algorithm to separate different types of aerosols is a characteristic temporal variation, different for each aerosol type. This resulted in an incomplete separation of the OOA factor for the measurements in Ingelheim with considerable OOA concentration increases during the opening hours of the market, while for this background-related aerosol type rather constant concentrations independent of the opening times are expected (as seen in Bingen).

The mass spectra of COA, BBOA, and OOA are similar for both locations and exhibit the typical markers for the respective aerosol types. In the mass spectra of OOA the most intense signal is at *m/z* 44 (CO_2^+), originating from thermal decomposition of oxidized organic compounds (Ng et al., 2010). BBOA could be identified by the elevated signal intensities at *m/z* 60 and 73, whose ratio of 2.6 at both markets points to levoglucosan (see Sect. 3.1.2), which is a result of the pyrolysis of cellulose (Schneider et al., 2006). In the COA mass spectra, the highest signal intensities are at *m/z* 41 and 55 and the signal ratio of *m/z* 55 and 57 is 2.6, which is consistent with results from previous studies (Mohr et al., 2012; Sun et al., 2011; Xu et al., 2020) and our laboratory studies (Sect. 3.1.2). The correlation with corresponding reference mass spectra (averaged from the available mass spectra from the AMS database, see Table S3) supported the assignment of the identified factors, with correlation coefficients of 0.93 and 0.97 for COA, 0.98 and 0.95 for OOA, and 0.83 and 0.77 for BBOA, for Ingelheim and Bingen, respectively.

The COA and BBOA concentrations were significantly enhanced during the opening hours while the OOA concentrations remained almost constant (OOA for Ingelheim not regarded here due to incomplete separation). The average concentrations of COA (CE = 1; RIE = 2.27; see Sect. 3.5.2) were 3.5/0.14 µg m^{-3} and 2.5/0.05 µg m^{-3} and of BBOA (CE = 0.5; RIE = 1.4) 17.1/0.54 µg m^{-3} and 2.4/0.21 µg m^{-3} during/outside the opening hours for Ingelheim and Bingen, respectively. In Bingen the OOA concentration (CE = 0.5; RIE = 1.4) were mostly below 2 µg m^{-3} over the whole measurement period suggesting that this PMF factor can be attributed to the background aerosol. The observed stepwise changes of the OOA concentration (Fig. S10~~11~~) were due to wind direction changes. The fraction of OOA at both Christmas markets during the opening hours was similar with 15 % and 17 %, while BBOA amounts to 71 % and 40 % and COA to 14 % and 43 % for Ingelheim and Bingen, respectively. The higher BBOA fraction in Ingelheim might be due to a second wood fire barrel at 25 m distance to MoLa on two afternoons and a flame-grilled salmon stand with an open wood fire within the food stands circle where MoLa was located.

3.5.2 Validation of laboratory measurements using the Christmas market data

To assess whether the results from the laboratory experiments are also applicable to ambient measurements, we used the Christmas market data to verify different aspects of our results. Due to the higher fraction of COA measured during the Christmas market

opening hours in Bingen (43 %) compared to Ingelheim (14 %) the analysis was only performed with the data set collected in Bingen.

The dishes prepared at the Christmas market which were also studied in the laboratory are bratwurst frying, deep-frying French fries (in a deep fryer), and steaks grilled on a gas grill. A linear correlation of the average COA mass spectrum from the PMF analysis of the Christmas market data with the mass spectra of the above mentioned three dishes showed very high similarity between the spectra (Pearson's r = 0.99), as did the correlation with the one of rapeseed oil (r = 0.98) and oleic acid (r = 0.93). The ratio of f_{67}/f_{69} for this COA mass spectrum was 1.4, similar to the ratios of previously measured ambient COA (1.2 ± 0.1) and the laboratory measurements (1.1 – 1.6), supporting our suggestion of f_{67}/f_{69} as additional COA marker (see Sect. 3.1.2).

To verify whether the densities for the organic fraction derived from the cooking emission experiments can be applied to ambient measurements, the densities for the three Christmas market-related dishes as well as for the COA PMF factor from the measurements at the market were calculated based on the formula of Kuwata et al. (2012). The density of COA with 0.94 g cm^{-3} is in agreement with the densities for the three dishes (0.94 – 0.98 g cm^{-3}, Table S5). This finding along with the high mass spectral similarity discussed above suggests that the observed ambient COA is composed to a substantial amount~~mostly consisted~~ of vaporized and re-condensed oil or decomposed fats.

In order to validate whether the RIE_{COA} values determined from laboratory measurements are applicable to ambient measurements of cooking-related aerosols, PM_1 (from FMPS and OPC measurements, Sect. S1) was compared to PM_1 calculated from BC and AMS species ($PM_{1,AMS+BC}$) for two different value sets of RIE_{COA} and CE_{COA}: i) the default AMS values, i.e. RIE_{COA} = 1.4 and CE_{COA} = 0.5 (Fig. 13~~2~~a); and ii) average values derived from the laboratory measurements of the three Christmas market-related dishes (RIE_{COA} = 2.27 and CE_{COA} = 1; Fig. 13~~2~~b). Additionally, the fractions of the different aerosol species of the Christmas market PM_1 emissions (after background subtraction) are shown in Fig. 1~~2~~3 as pie charts which were calculated by applying for COA the respective RIE and CE values. In both cases, default RIE and CE values were used for the other AMS species including BBOA and OOA (i.e., assuming externally mixed COA; Freutel et al., 2013). As illustrated in Fig. 13, the correlations between the two types of PM_1 values are characterized by a considerable amount of scatter, particularly in the lower PM_1 concentration range. This is likely due to the fact that several sources for cooking-related PM_1 as well as for other types of organic aerosol are in close proximity to the measurement location, resulting in significant variability in the data from the instruments used to determine PM_1. This is also reflected in the poor correlation coefficients for both approaches to calculate PM_1 from AMS and BC data (r^2 = 0.56 and 0.58 with the default and laboratory values for RIE_{COA} and CE_{COA}, respectively). ~~According to~~ Figure~~.~~ 13~~2~~a~~,~~ illustrates that $PM_{1,AMS+BC}$ ~~seems~~ appears to be overestimated for higher PM_1 concentrations when~~ using~~ the default values are employed.~~,~~ In contrast, when~~ while with~~ RIE_{COA} and CE_{COA} ~~taken~~ are derived from the laboratory results, the PM_1 values scatter more around ~~align reasonably well with~~ the one-to-one line (Figure~~.~~ 13~~2~~b), suggesting ~~a better~~improved mass closure. ODR fitting of the two pairs of PM_1 data with the intercept forced through the origin yields $PM_{1,AMS+BC}$ = 1.71 * PM_1 and $PM_{1,AMS+BC}$ = 0.68 * PM_1, respectively, for the default and the laboratory values. These results indicate a slight improvement in the agreement between the two sets of data when the laboratory RIE_{COA} and CE_{COA} values were employed.~~, though~~~~However, no definitive answer can be given due to the low correlation coefficient in both cases (r = 0.56 and 0.58 with the default and laboratory values, respectively) as a result of the strong scatter in the correlations, probably due to the proximity of the sources to the measurement site~~. The pie charts highlight the effect of the different RIE and CE values on the calculated fraction of COA of the emitted Christmas market PM_1. Using the default values, the COA fraction would be 26% larger compared to that when using the laboratory values, showing the importance of choosing correct RIE and CE values for COA.

Generally, the result of this comparison is in agreement with those of previous ambient measurements of cooking emissions which also suggest a higher RIE_{COA} value than the default RIE_{Org} of 1.4 (Katz et al., 2021; Reyes-Villegas et al., 2018).

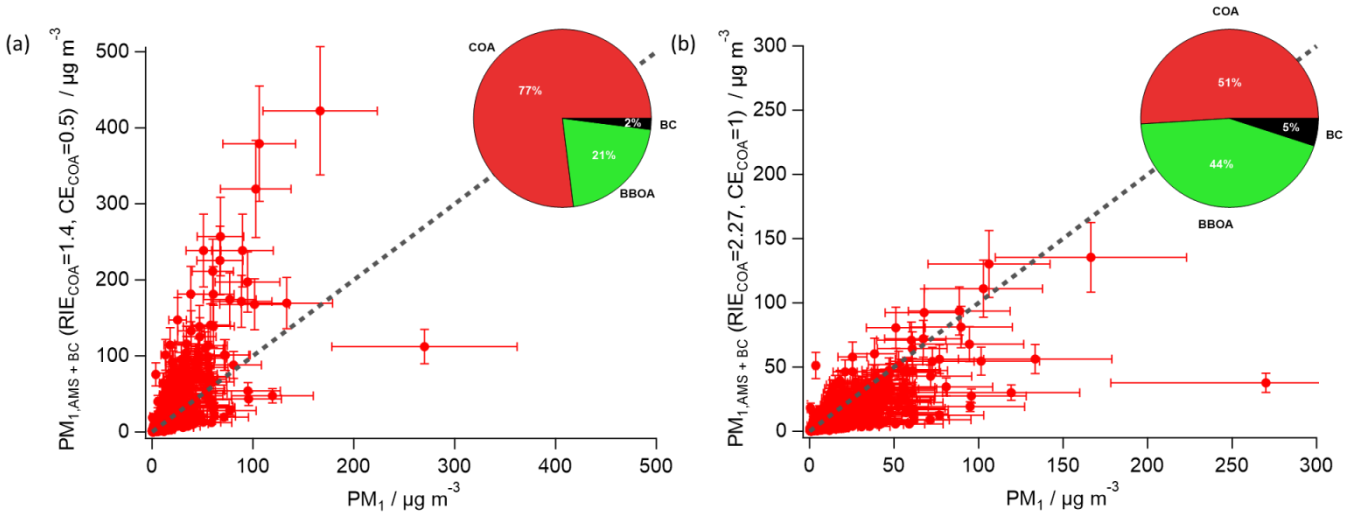

Figure 13: Comparison of measured $PM_{1,AMS+BC}$ with PM_1 with (a) RIE_{COA} = 1.4, CE_{COA} = 0.5 and (b) RIE_{COA} = 2.27, CE_{COA} = 1 for the COA fraction. The 1:1 line serves as guidance. The pie charts show the calculated PM_1 composition of the Christmas market emissions (i.e., only for opening times, after background subtraction).

Based on the results of the laboratory experiments as well as those of previous studies, no strong contribution of BC was expected from cooking emissions (Zhang et al., 2010; Zhao et al., 2007), and the observed BC was assumed to originate mainly from biomass burning. Indeed, the ratio of BBOA (RIE = 1.4 and CE = 0.5) to BC mass concentrations on average was 3.3 during the Christmas market opening times, which is well within the range of 1.7 – 33 observed for open biomass burning (Reid et al., 2005) and close to the ratios of 4.0 and 3.16 measured for mainly domestic heating in urban environments by Crippa et al. (2013) and Elser et al. (2016).

The applicability of the laboratory emission factors (see Sect. 3.4) to ambient measurements was verified by testing whether they can reproduce the concentrations measured during the Christmas market in a simple model. For this purpose, the emission factors for dishes which were prepared at the Christmas market were used (bratwurst frying, deep-frying French fries in the deep fryer and steaks from the gas grill) for the variables PN, PM_1, and organics. Here, we assume that the emission factors obtained in the laboratory for the marinated steak are not strongly different from those for the non-marinated steak, which was used for cooking on the Christmas market. Gas grilling rather than charcoal grilling emission factors were used here since PMF likely apportions part of the charcoal grilling to the biomass burning factor, causing an underestimate of the respective COA emissions.

The emissions per hour (EM) needed to generate the measured concentrations were calculated using the average concentration during the opening hours ($\overline{c_{CM}}$) minus the average background concentration ($\overline{c_{BG}}$) and the volumetric flow rate Q_{CM} with which the emissions were diluted (Eq. (3)). The volumetric flow rate Q_{CM} was estimated based on the average wind speed (1.15 m s^{-1}, mostly from the west), the height of the houses (8 m) surrounding the square up to which we assumed the emissions would be diluted, and the width of the street that runs from west to east transporting most of the air mass, resulting in $Q_{CM} = 5 \cdot 10^5$ m^3 h^{-1} (138 m^3 s^{-1}). ~~Finally, u~~Using the emission factors EF from the laboratory experiments, we calculated which amount of food (m) would be needed to be cooked per hour in order to generate the calculated emissions per hour (Eq. (4)).

$$EM = (\overline{c_{CM}} - \overline{c_{BG}}) \cdot Q_{CM} \quad (3)$$

$$m = \frac{EM}{EF} \quad (4)$$

Finally, assuming that a bratwurst has a mass of 150 g, a schnitzel has a mass of 180 g, and a unit of French fries has a mass of 250 g, the calculated masses were converted into food units to make the results more tangible. As the emission factors were determined from cooking activities, we considered only the COA-related fraction of the measured Christmas market emissions for the mass-based variables PM_1 and organic mass concentration. The COA concentration was calculated using RIE_{COA} = 2.27 and CE_{COA} = 1 and considering only the emissions of the Christmas market (background subtracted). For PM_1 the fraction that is related to COA amounts to 51% (Fig. 132b), and for the total measured AMS organics to 54%. As it is not possible to determine the COA-related fraction for PN based on the results for PM_1, we ~~estimated~~ assumed that the COA fraction for PN would be somewhere between 20% and 80% and performed the calculations for these two extreme scenarios.

Figure14~~Figure 143~~ shows, for the three selected ~~chosen~~ variables, the ~~amount~~ number of ~~of~~ food units ~~which~~ that would ~~be~~ need~~ed~~ to be cooked ~~of the respective single dishes~~ per hour of each dish ~~in order~~ to account for the observed emissions. For the mass-based variables, the calculated ~~masses for~~numbers of steaks were ~~12~~67 – ~~17~~94 ~~kg h^{-1}~~per hour, and for bratwurst and French fries, the numbers were at least ~~one~~ an order of magnitude ~~higher~~ higher with ~~115~~ 770 – ~~538~~ 2150 ~~kg h^{-1}~~units per hour. For PN, the calculated numbers of food units ~~amount~~ for the chosen COA fraction range of 20% to 80% ~~was~~ were ~~similar~~ smaller ~~as~~than those for the mass-based variables for ~~with 0.6 – 2.4 kg h^{-1} of~~ steaks with 3 – 13 units per hour and similar to those for the mass-based variables with ~~47 – 803 kg h^{-1} of~~ 310 - 1250 units of bratwurst and 800 – 3200 units of French fries. These calculated ~~masses~~ units of food prepared per hour are ~~all~~ in a realistic order of magnitude assuming a reasonable mix of different types of food being prepared and the overall emissions being dominated by those from grilling steaks ~~(especially for the steak dish)~~, suggesting that the laboratory-derived emission factors for PN, PM_1, and organics are applicable to ambient measurements within an acceptable range of uncertainty.

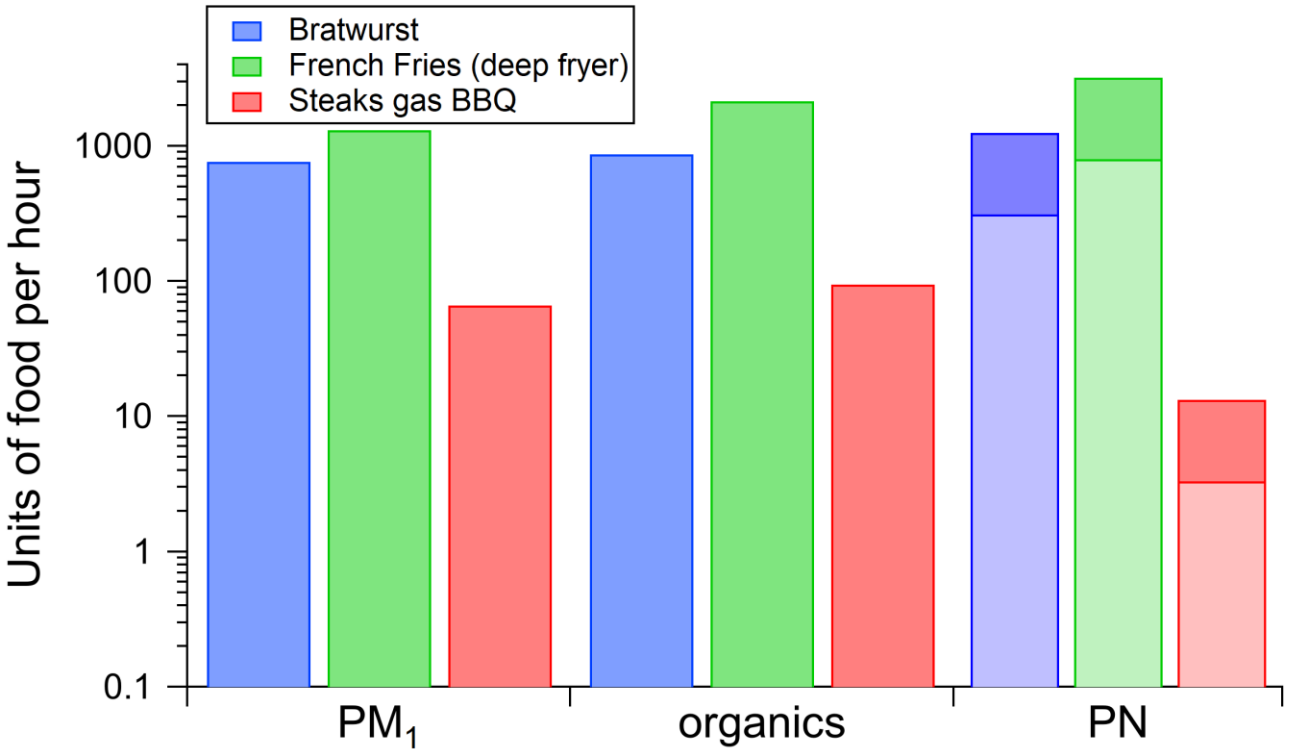

Figure ~~1413~~: ~~Amount~~ Units of food which need~~s~~ to be prepared per hour to generate the same concentrations (after background subtraction) as measured at the Christmas market in Bingen, calculated based on the emissions factors for three different dishes and on the local aerosol transport conditions. For each variable, the respective COA fraction was calculated with RIE_{COA} = 2.27 and CE_{COA} = 1 and for PN a COA fraction range of 20% (light bar) to 80% (dark bar) was assumed.

4 Conclusion

In a comprehensive laboratory study, various aspects of cooking-related emissions were studied in real time with multiple instruments, including the chemical composition of PM_1 and particle size distributions as well as emission dynamics and the quantification of emissions through calculation of emission factors. In addition, the influence of cooking activities on the ambient aerosol was investigated at two German Christmas markets.

From the laboratory experiments, it was found that measured particle number concentrations as well as several mass-based variables (PM, BC, PAH, organics) were strongly affected by the cooking activities. Measurements with the AMS ~~indicate~~ suggest that the PM_1 fraction of the measured emissions ~~was mostly~~contains a substantial fraction ~~composed~~ of vaporized and recondensed oil or fatty acids as shown through comparison of the mass spectra of the measured emissions with the one of rapeseed oil, the used cooking oil. Therefore, we assume that particle formation and growth is ~~mainly~~ to a large degree the result of oil vaporization or fat decomposition and re-condensation of the emitted vapors.

Through comparison of the AMS-measured organics mass concentrations with the mass concentration derived from size distributions, we found that higher values for the RIE_{COA} (1.53 – 2.52) compared to the default value of 1.4 are required for correct determination of mass concentrations of cooking-related organic aerosols. These results confirm and extend the findings of previous studies. As a conclusion, we recommend using different RIE_{COA} values depending on the cooking oil since it has an influence on the RIE_{COA}: for cooking with rapeseed oil an RIE_{COA} of 2.17 ± 0.48 based on this study and the one by Reyes-Villegas et al. (2018), and for soy oil-based cooking an RIE_{COA} of 5.16 ± 0.77 based on the measurements by Katz et al. (2021).

Furthermore, to support the AMS data analysis of organic aerosol types, a new diagram type is presented that enables a simple and quick way to check whether PMF succeeded in separating different aerosol types using known markers and also to identify and validate new markers, e.g. for real-time identification of aerosol types. Using the data of multiple measurement campaigns, the variability of the mass spectra for individual aerosol types is accounted for and this provides the opportunity to evaluate how well the separation of aerosol types works, based on the selected markers. Here, we identified and evaluated the ratio $f_{67}/f_{69} > 1$ as additional COA marker. The presented examples show the importance of combining markers or indicators to achieve a robust separation from other aerosol types, like for COA f_{55} (> 0.06) and f_{55}/f_{57} (> 2) for separation especially from HOA.

The relevant parameters influencing the amount of cooking emissions are the cooking temperature, use of oil, ingredients, and activities during the cooking process. These are mostly dependent on the preparation method; hence we observed similar results for dishes with similar preparation methods. A change of concentrations of the relevant variables (PM, BC, PAH, organics) as well as of the particle size could be attributed to changes of the temperature of the food and cookware as well as different activities during the preparation. Due to rising temperature, more substances vaporize and condense leading to higher emissions as well as larger particles. The emission of BC and PAH was observed only at higher temperature, e.g. towards the end of preparation. Different activities lead to transient concentration and particle size changes as they 1. facilitate the vaporization of substances, e.g. through stirring or tilting the pan, 2. increase the amount of vaporizable material, e.g. by cleaning the grill grid, or 3. suddenly release accumulated emissions, e.g. by opening the oven.

The used ingredients themselves also have a strong influence on the aerosol composition. The emissions from boiled dishes differ from the emissions of other dishes mostly due to the broad absence of oil and fatty ingredients. Another example is the occurrence of sulfur-containing species in the emitted aerosol for dishes with fried onions.

For quantification of the emissions, emission factors were determined for all relevant variables individually for all dishes. The highest emissions were released from preparing dishes on a gas and a charcoal grill due to the highest cooking temperatures, burning of food leftovers from the grid, and, in the case of charcoal grilling, due to additional emissions from the charcoal burning itself. The emission levels from cooking stir-fried, deep-fried, and baked dishes were similar to each other as oil or fatty ingredients

were used for all dishes. The preparation of boiled dishes resulted in the release of the lowest emissions as no oil was used and no or only little amounts of fatty ingredients were available, limiting the amount of vaporizable substances. Furthermore, a comparison to other relevant indoor and ambient emission sources showed that grilling one dish emits similar amounts of particles as driving 100 km by car and emissions from oil-based cooking, like frying, are of similar order of magnitude as such from domestic biomass burning over a comparable time interval.

The average PM_1 concentrations during the opening hours at a Christmas market were found to be as high as 51 µg m^{-3}. Locally, visitors could be exposed to even higher concentrations as shown for BC concentrations measured with a portable aethalometer across the market, which were on average twice as high as those of the stationary measurements immediately downwind the market. Though this is not a 24 h average value, these elevated concentrations show that events like Christmas markets have a strong influence on local air quality.

This result together with those from the laboratory measurements show that cooking activities contribute substantially to indoor and ambient aerosol. The amount of emissions is mainly determined by the preparation method, with barbecues as especially strong emission source.

Author contribution. JP and FD conceptualized the measurements. JP carried out the experiments, analyzed the MoLa data with support from FF and prepared the paper with contributions from FD, FF und SB.

Competing interests. The authors declare that they have no conflict of interest.

Acknowledgements. We thank Thomas Böttger and the mechanical workshop for technical support. The authors thank David Troglauer, Lasse Moormann, and Philipp Schuhmann for support during the laboratory measurements. We also thank the organizers of the Christmas markets for the possibility to perform our measurements. Furthermore, we acknowledge the Max Planck Institute for Chemistry for funding of this work.

References

Abbatt, J. P. D. and Wang, C.: The atmospheric chemistry of indoor environments, Environ. Sci.: Processes Impacts, 22, 25–48, https://doi.org/10.1039/c9em00386j, 2020.

Abdullahi, K. L., Delgado-Saborit, J. M., and Harrison, R. M.: Emissions and indoor concentrations of particulate matter and its specific chemical components from cooking: A review, Atmos. Environ., 71, 260–294, https://doi.org/10.1016/j.atmosenv.2013.01.061, 2013.

Alfarra, M. R., Coe, H., Allan, J. D., Bower, K. N., Boudries, H., Canagaratna, M. R., Jimenez, J. L., Jayne, J. T., Garforth, A. A., Li, S.-M., and Worsnop, D. R.: Characterization of urban and rural organic particulate in the Lower Fraser Valley using two Aerodyne Aerosol Mass Spectrometers, Atmos. Environ., 38, 5745–5758, https://doi.org/10.1016/j.atmosenv.2004.01.054, 2004.

Allan, J. D., Williams, P. I., Morgan, W. T., Martin, C. L., Flynn, M. J., Lee, J., Nemitz, E., Phillips, G. J., Gallagher, M. W., and Coe, H.: Contributions from transport, solid fuel burning and cooking to primary organic aerosols in two UK cities, Atmos. Chem. Phys., 10, 647–668, https://doi.org/10.5194/acp-10-647-2010, 2010.

Alves, C. A., Duarte, M., Nunes, T., Moreira, R., and Rocha, S.: Carbonaceous particles emitted from cooking activities in Portugal, Glob. Nest J., 16, 411–419, https://doi.org/10.30955/gnj.001313, 2014.

Alves, C. A., Evtyugina, M., Cerqueira, M., Nunes, T., Duarte, M., and Vicente, E.: Volatile organic compounds emitted by the stacks of restaurants, Air Qual. Atmos. Health., 8, 401–412, https://doi.org/10.1007/s11869-014-0310-7, 2015.

Amouei Torkmahalleh, M., Goldasteh, I., Zhao, Y., Udochu, N. M., Rossner, A., Hopke, P. K., and Ferro, A. R.: PM2.5 and ultrafine particles emitted during heating of commercial cooking oils, Indoor Air, 22, 483–491, https://doi.org/10.1111/j.1600-0668.2012.00783.x, 2012.

Baron, P. A., Kulkarni, P., and Willeke, K. (Eds.): Aerosol measurement: Principles, techniques, and applications, 3rd ed., Engineering professional collection, John Wiley & Sons, Inc., New York, 883 pp., 2011.

Boelens, M., Valois, P. J. de, Wobben, H. J., and van der Gen, A.: Volatile flavor compounds from onion, J. Agric. Food Chem., 19, 984–991, https://doi.org/10.1021/jf60177a031, 1971.

Buonanno, G., Johnson, G., Morawska, L., and Stabile, L.: Volatility characterization of cooking-generated aerosol particles, Aerosol Sci. Technol., 45, 1069–1077, https://doi.org/10.1080/02786826.2011.580797, 2011.

Buonanno, G., Morawska, L., and Stabile, L.: Particle emission factors during cooking activities, Atmos. Environ., 43, 3235–3242, https://doi.org/10.1016/j.atmosenv.2009.03.044, 2009.

Canagaratna, M. R., Jayne, J. T., Jimenez, J. L., Allan, J. D., Alfarra, M. R., Zhang, Q., Onasch, T. B., Drewnick, F., Coe, H., Middlebrook, A., Delia, A., Williams, L. R., Trimborn, A. M., Northway, M. J., DeCarlo, P. F., Kolb, C. E., Davidovits, P., and Worsnop, D. R.: Chemical and microphysical characterization of ambient aerosols with the aerodyne aerosol mass spectrometer, Mass Spectrom. Rev., 26, 185–222, https://doi.org/10.1002/mas.20115, 2007.

Chafe, Z. A., Brauer, M., Klimont, Z., van Dingenen, R., Mehta, S., Rao, S., Riahi, K., Dentener, F., and Smith, K. R.: Household cooking with solid fuels contributes to ambient PM2.5 air pollution and the burden of disease, Environ. Health Perspect., 122, 1314–1320, https://doi.org/10.1289/ehp.1206340, 2014.

Chen, Y., Ho, K. F., Ho, S. S. H., Ho, W. K., Lee, S. C., Yu, J. Z., and Sit, E. H. L.: Gaseous and particulate polycyclic aromatic hydrocarbons (PAHs) emissions from commercial restaurants in Hong Kong, J. Environ. Monit., 9, 1402–1409, https://doi.org/10.1039/b710259c, 2007.

Cheng, S., Wang, G., Lang, J., Wen, W., Wang, X., and Yao, S.: Characterization of volatile organic compounds from different cooking emissions, Atmos. Environ., 145, 299–307, https://doi.org/10.1016/j.atmosenv.2016.09.037, 2016.

Christie, W. W.: The Lipid Web, https://www.lipidmaps.org/resources/lipidweb/lipidweb_html/index.html, last access: 18 September 2023.

Crippa, M., DeCarlo, P. F., Slowik, J. G., Mohr, C., Heringa, M. F., Chirico, R., Poulain, L., Freutel, F., Sciare, J., Cozic, J., Di Marco, C. F., Elsasser, M., Nicolas, J. B., Marchand, N., Abidi, E., Wiedensohler, A., Drewnick, F., Schneider, J., Borrmann, S., Nemitz, E., Zimmermann, R., Jaffrezo, J.-L., Prévôt, A. S. H., and Baltensperger, U.: Wintertime aerosol chemical composition and source apportionment of the organic fraction in the metropolitan area of Paris, Atmos. Chem. Phys., 13, 961–981, https://doi.org/10.5194/acp-13-961-2013, 2013.

Diffey, B. L.: An overview analysis of the time people spend outdoors, Br. J. Dermatol., 164, 848–854, https://doi.org/10.1111/j.1365-2133.2010.10165.x, 2011.

Drewnick, F., Böttger, T., Weiden-Reinmüller, S.-L. v. d., Zorn, S. R., Klimach, T., Schneider, J., and Borrmann, S.: Design of a mobile aerosol research laboratory and data processing tools for effective stationary and mobile field measurements, Atmos. Meas. Tech., 5, 1443–1457, https://doi.org/10.5194/amt-5-1443-2012, 2012.

Elser, M., Huang, R.-J., Wolf, R., Slowik, J. G., Wang, Q., Canonaco, F., Li, G., Bozzetti, C., Daellenbach, K. R., Huang, Y., Zhang, R., Li, Z., Cao, J., Baltensperger, U., El-Haddad, I., and Prévôt, A. S. H.: New insights into $PM_{2.5}$ chemical composition and sources in two major cities in China during extreme haze events using aerosol mass spectrometry, Atmos. Chem. Phys., 16, 3207–3225, https://doi.org/10.5194/acp-16-3207-2016, 2016.

Faber, P., Drewnick, F., Veres, P. R., Williams, J., and Borrmann, S.: Anthropogenic sources of aerosol particles in a football stadium: Real-time characterization of emissions from cigarette smoking, cooking, hand flares, and color smoke bombs by high-resolution aerosol mass spectrometry, Atmos. Environ., 77, 1043–1051, https://doi.org/10.1016/j.atmosenv.2013.05.072, 2013.

Fachinger, F., Drewnick, F., Gieré, R., and Borrmann, S.: Communal biofuel burning for district heating: Emissions and immissions from medium-sized (0.4 and 1.5 MW) facilities, Atmos. Environ., 181, 177–185, https://doi.org/10.1016/j.atmosenv.2018.03.014, 2018.

Fachinger, J. R. W., Gallavardin, S. J., Helleis, F., Fachinger, F., Drewnick, F., and Borrmann, S.: The ion trap aerosol mass spectrometer: field intercomparison with the ToF-AMS and the capability of differentiating organic compound classes via MS-MS, Atmos. Meas. Tech., 10, 1623–1637, https://doi.org/10.5194/amt-10-1623-2017, 2017.

Freutel, F., Schneider, J., Drewnick, F., Weiden-Reinmüller, S.-L. v. d., Crippa, M., Prévôt, A. S. H., Baltensperger, U., Poulain, L., Wiedensohler, A., Sciare, J., Sarda-Estève, R., Burkhart, J. F., Eckhardt, S., Stohl, A., Gros, V., Colomb, A., Michoud, V., Doussin, J. F., Borbon, A., Haeffelin, M., Morille, Y., Beekmann, M., and Borrmann, S.: Aerosol particle measurements at three stationary sites in the megacity of Paris during summer 2009: meteorology and air mass origin dominate aerosol particle composition and size distribution, Atmos. Chem. Phys., 13, 933–959, https://doi.org/10.5194/acp-13-933-2013, 2013.

Gao, J., Cao, C., Wang, L., Song, T., Zhou, X., Yang, J., and Zhang, X.: Determination of size-dependent source emission rate of cooking-generated aerosol particles at the oil-heating stage in an experimental kitchen, Aerosol Air Qual. Res., 13, 488–496, https://doi.org/10.4209/aaqr.2012.09.0238, 2013.

Goldstein, A. H., Nazaroff, W. W., Weschler, C. J., and Williams, J.: How do indoor environments affect air pollution exposure?, Environ. Sci. Technol., 55, 100–108, https://doi.org/10.1021/acs.est.0c05727, 2021.

Hallgren, B., Ryhage, R., Stenhagen, E., Sömme, R., and Palmstierna, H.: The mass spectra of methyl oleate, methyl linoleate, and methyl linolenate, Acta Chem. Scand., 13, 845–847, https://doi.org/10.3891/acta.chem.scand.13-0845, 1959.

He, C., Morawska, L., Hitchins, J., and Gilbert, D.: Contribution from indoor sources to particle number and mass concentrations in residential houses, Atmos. Environ., 38, 3405–3415, https://doi.org/10.1016/j.atmosenv.2004.03.027, 2004.

He, L.-Y., Lin, Y., Huang, X.-F., Guo, S., Xue, L., Su, Q., Hu, M., Luan, S.-J., and Zhang, Y.-H.: Characterization of high-resolution aerosol mass spectra of primary organic aerosol emissions from Chinese cooking and biomass burning, Atmos. Chem. Phys., 10, 11535–11543, https://doi.org/10.5194/acp-10-11535-2010, 2010.

IPCC: Climate Change 2021: The Physical Science Basis, Cambridge University Press, Cambridge, New York, 2021.

Jägerstad, M. and Skog, K.: Genotoxicity of heat-processed foods, Mutat. Res., 574, 156–172, https://doi.org/10.1016/j.mrfmmm.2005.01.030, 2005.

Kaltsonoudis, C., Kostenidou, E., Louvaris, E., Psichoudaki, M., Tsiligiannis, E., Florou, K., Liangou, A., and Pandis, S. N.: Characterization of fresh and aged organic aerosol emissions from meat charbroiling, Atmos. Chem. Phys., 17, 7143–7155, https://doi.org/10.5194/acp-17-7143-2017, 2017.

Katragadda, H. R., Fullana, A., Sidhu, S., and Carbonell-Barrachina, Á. A.: Emissions of volatile aldehydes from heated cooking oils, Food Chemistry, 120, 59–65, https://doi.org/10.1016/j.foodchem.2009.09.070, 2010.

Katz, E. F., Guo, H., Campuzano-Jost, P., Day, D. A., Brown, W. L., Boedicker, E., Pothier, M., Lunderberg, D. M., Patel, S., Patel, K., Hayes, P. L., Avery, A., Hildebrandt Ruiz, L., Goldstein, A. H., Vance, M. E., Farmer, D. K., Jimenez, J. L., and DeCarlo, P. F.: Quantification of cooking organic aerosol in the indoor environment using aerodyne aerosol mass spectrometers, Aerosol Sci. Technol., 55, 1099–1114, https://doi.org/10.1080/02786826.2021.1931013, 2021.

Klein, F., Platt, S. M., Farren, N. J., Detournay, A., Bruns, E. A., Bozzetti, C., Daellenbach, K. R., Kilic, D., Kumar, N. K., Pieber, S. M., Slowik, J. G., Temime-Roussel, B., Marchand, N., Hamilton, J. F., Baltensperger, U., Prévôt, A. S. H., and El Haddad, I.: Characterization of Gas-Phase Organics Using Proton Transfer Reaction Time-of-Flight Mass Spectrometry: Cooking Emissions, Environ. Sci. Technol., 50, 1243–1250, https://doi.org/10.1021/acs.est.5b04618, 2016.

Kreyling, W. G., Semmler-Behnke, M., and Möller, W.: Health implications of nanoparticles, J. Nanopart. Res. (Journal of Nanoparticle Research), 8, 543–562, https://doi.org/10.1007/s11051-005-9068-z, 2006.

Kuwata, M., Zorn, S. R., and Martin, S. T.: Using elemental ratios to predict the density of organic material composed of carbon, hydrogen, and oxygen, Environ. Sci. Technol., 46, 787–794, https://doi.org/10.1021/es202525q, 2012.

Lee, S. C., Li, W.-M., and Lo Yin Chan: Indoor air quality at restaurants with different styles of cooking in metropolitan Hong Kong, Sci. Total Environ., 279, 181–193, https://doi.org/10.1016/S0048-9697(01)00765-3, 2001.

Levin, E. J. T., McMeeking, G. R., Carrico, C. M., Mack, L. E., Kreidenweis, S. M., Wold, C. E., Moosmüller, H., Arnott, W. P., Hao, W. M., Collett, J. L., and Malm, W. C.: Biomass burning smoke aerosol properties measured during Fire Laboratory at Missoula Experiments (FLAME), J. Geophys. Res., 115, https://doi.org/10.1029/2009jd013601, 2010.

Liao, C.-M., Chen, S.-C., Chen, J.-W., and Liang, H.-M.: Contributions of Chinese-style cooking and incense burning to personal exposure and residential PM concentrations in Taiwan region, Sci. Total Environ., 358, 72–84, https://doi.org/10.1016/j.scitotenv.2005.03.026, 2006.

Lijinsky, W.: The formation and occurrence of polynuclear aromatic hydrocarbons associated with food, Mutat. Res. - Genet. Toxicol., 259, 251–261, https://doi.org/10.1016/0165-1218(91)90121-2, 1991.

Liu, T., Wang, Z., Huang, D. D., Wang, X., and Chan, C. K.: Significant production of secondary organic aerosol from emissions of heated cooking oils, Environ. Sci. Technol. Lett., 5, 32–37, https://doi.org/10.1021/acs.estlett.7b00530, 2018.

Liu, T., Li, Z., Chan, M., and Chan, C. K.: Formation of secondary organic aerosols from gas-phase emissions of heated cooking oils, Atmos. Chem. Phys., 17, 7333–7344, https://doi.org/10.5194/acp-17-7333-2017, 2017a.

Liu, T., Liu, Q., Li, Z., Huo, L., Chan, M., Li, X., Zhou, Z., and Chan, C. K.: Emission of volatile organic compounds and production of secondary organic aerosol from stir-frying spices, Sci. Total Environ., 599-600, 1614–1621, https://doi.org/10.1016/j.scitotenv.2017.05.147, 2017b.

Liu, Y., Ma, H., Zhang, N., and Li, Q.: A systematic literature review on indoor PM2.5 concentrations and personal exposure in urban residential buildings, Heliyon, 8, e10174, https://doi.org/10.1016/j.heliyon.2022.e10174, 2022.

Marć, M., Śmiełowska, M., Namieśnik, J., and Zabiegała, B.: Indoor air quality of everyday use spaces dedicated to specific purposes-a review, Environ. Sci. Pollut. Res., 25, 2065–2082, https://doi.org/10.1007/s11356-017-0839-8, 2018.

Martin, W. J., Ramanathan, T., and Ramanathan, V.: Household air pollution from cookstoves: Impacts on health and climate, in: Climate Change and Global Public Health. Respiratory Medicine, Humana,Cham, 369–390, https://doi.org/10.1007/978-3-030-54746-2_17.

Marval, J. and Tronville, P.: Ultrafine particles: A review about their health effects, presence, generation, and measurement in indoor environments, Build. Environ., 216, 108992, https://doi.org/10.1016/j.buildenv.2022.108992, 2022.

Matthew, B. M., Middlebrook, A. M., and Onasch, T. B.: Collection Efficiencies in an Aerodyne Aerosol Mass Spectrometer as a Function of Particle Phase for Laboratory Generated Aerosols, Aerosol Science and Technology, 42, 884–898, https://doi.org/10.1080/02786820802356797, 2008.

McLafferty, F. W. and Turecek, F.: Interpretation of Mass Spectra, 4th ed., University Science Books, Melville, 371 pp., 1993.

Mohr, C., DeCarlo, P. F., Heringa, M. F., Chirico, R., Slowik, J. G., Richter, R., Reche, C., Alastuey, A., Querol, X., Seco, R., Peñuelas, J., Jiménez, J. L., Crippa, M., Zimmermann, R., Baltensperger, U., and Prévôt, A. S. H.: Identification and quantification of organic aerosol from cooking and other sources in Barcelona using aerosol mass spectrometer data, Atmos. Chem. Phys., 12, 1649–1665, https://doi.org/10.5194/acp-12-1649-2012, 2012.

Mohr, C., Huffman, A., Cubison, M. J., Aiken, A. C., Docherty, K. S., Kimmel, J. R., Ulbrich, I. M., Hannigan, M., and Jimenez, J. L.: Characterization of primary organic aerosol emissions from meat cooking, trash burning, and motor vehicles with high-resolution aerosol mass spectrometry and comparison with ambient and chamber observations, Environ. Sci. Technol., 43, 2443–2449, https://doi.org/10.1021/es8011518, 2009.

Nasir, Z. A. and Colbeck, I.: Particulate pollution in different housing types in a UK suburban location, Sci. Total Environ., 445-446, 165–176, https://doi.org/10.1016/j.scitotenv.2012.12.042, 2013.

Ng, N. L., Canagaratna, M. R., Zhang, Q., Jimenez, J. L., Tian, J., Ulbrich, I. M., Kroll, J. H., Docherty, K. S., Chhabra, P. S., Bahreini, R., Murphy, S. M., Seinfeld, J. H., Hildebrandt, L., Donahue, N. M., DeCarlo, P. F., Lanz, V. A., Prévôt, A. S. H., Dinar, E., Rudich, Y., and Worsnop, D. R.: Organic aerosol components observed in Northern Hemispheric datasets from Aerosol Mass Spectrometry, Atmos. Chem. Phys., 10, 4625–4641, https://doi.org/10.5194/acp-10-4625-2010, 2010.

Olson, D. A. and Burke, J. M.: Distributions of PM2.5 source strengths for cooking from the Research Triangle Park particulate matter panel study, Environ. Sci. Technol., 40, 163–169, https://doi.org/10.1021/es050359t, 2006.

Omidvarborna, H., Kumar, A., and Kim, D.-S.: Recent studies on soot modeling for diesel combustion, Renew. Sust. Energ. Rev., 48, 635–647, https://doi.org/10.1016/j.rser.2015.04.019, 2015.

Paatero, P. and Tapper, U.: Positive matrix factorization: A non-negative factor model with optimal utilization of error estimates of data values, Environmetrics, 5, 111–126, https://doi.org/10.1002/env.3170050203, 1994.

Pope, C. A. and Dockery, D. W.: Health effects of fine particulate air pollution: lines that connect, J. Air Waste Manag. Assoc., 56, 709–742, https://doi.org/10.1080/10473289.2006.10464485, 2006.

Pope, C. A., Burnett, R. T., Thurston, G. D., Thun, M. J., Calle, E. E., Krewski, D., and Godleski, J. J.: Cardiovascular mortality and long-term exposure to particulate air pollution: epidemiological evidence of general pathophysiological pathways of disease, Circulation, 109, 71–77, https://doi.org/10.1161/01.CIR.0000108927.80044.7F, 2004.

Reid, J. S., Koppmann, R., Eck, T. F., and Eleuterio, D. P.: A review of biomass burning emissions part II: intensive physical properties of biomass burning particles, Atmos. Chem. Phys., 5, 799–825, https://doi.org/10.5194/acp-5-799-2005, 2005.

Reyes-Villegas, E., Bannan, T., Le Breton, M., Mehra, A., Priestley, M., Percival, C., Coe, H., and Allan, J. D.: Online chemical characterization of food-cooking organic aerosols: Implications for source apportionment, Environ. Sci. Technol., 52, 5308–5318, https://doi.org/10.1021/acs.est.7b06278, 2018.

Robinson, E. S., Gu, P., Ye, Q., Li, H. Z., Shah, R. U., Apte, J. S., Robinson, A. L., and Presto, A. A.: Restaurant impacts on outdoor air quality: Elevated organic aerosol mass from restaurant cooking with neighborhood-scale plume extents, Environ. Sci. Technol., 52, 9285–9294, https://doi.org/10.1021/acs.est.8b02654, 2018.

Rogge, W. F., Hildemann, L. M., Mazurek, M. A., Cass, G. R., and Simoneit, B. R. T.: Sources of fine organic aerosol. 1. Charbroilers and meat cooking operations, Environ. Sci. Technol., 25, 1112–1125, https://doi.org/10.1021/es00018a015, 1991.

Schneider, J., Weimer, S., Drewnick, F., Borrmann, S., Helas, G., Gwaze, P., Schmid, O., Andreae, M. O., and Kirchner, U.: Mass spectrometric analysis and aerodynamic properties of various types of combustion-related aerosol particles, Int. J. Mass Spectrom., 258, 37–49, https://doi.org/10.1016/j.ijms.2006.07.008, 2006.

See, S. W. and Balasubramanian, R.: Physical Characteristics of Ultrafine Particles Emitted from Different Gas Cooking Methods, Aerosol Air Qual. Res., 6, 82–92, https://doi.org/10.4209/aaqr.2006.03.0007, 2006.

Shiraiwa, M., Ueda, K., Pozzer, A., Lammel, G., Kampf, C. J., Fushimi, A., Enami, S., Arangio, A. M., Fröhlich-Nowoisky, J., Fujitani, Y., Furuyama, A., Lakey, P. S. J., Lelieveld, J., Lucas, K., Morino, Y., Pöschl, U., Takahama, S., Takami, A., Tong, H., Weber, B., Yoshino, A., and Sato, K.: Aerosol health effects from molecular to global scales, Environ. Sci. Technol., 51, 13545–13567, https://doi.org/10.1021/acs.est.7b04417, 2017.

Struckmeier, C., Drewnick, F., Fachinger, F., Gobbi, G. P., and Borrmann, S.: Atmospheric aerosols in Rome, Italy: sources, dynamics and spatial variations during two seasons, Atmos. Chem. Phys., 16, 15277–15299, https://doi.org/10.5194/acp-16-15277-2016, 2016.

Sun, Y.-L., Zhang, Q., Schwab, J. J., Demerjian, K. L., Chen, W.-N., Bae, M.-S., Hung, H.-M., Hogrefe, O., Frank, B., Rattigan, O. V., and Lin, Y.-C.: Characterization of the sources and processes of organic and inorganic aerosols in New York city with a high-resolution time-of-flight aerosol mass apectrometer, Atmos. Chem. Phys., 11, 1581–1602, https://doi.org/10.5194/acp-11-1581-2011, 2011.

Takhar, M., Li, Y., and Chan, A. W. H.: Characterization of secondary organic aerosol from heated-cooking-oil emissions: evolution in composition and volatility, Atmos. Chem. Phys., 21, 5137–5149, https://doi.org/10.5194/acp-21-5137-2021, 2021.

Thomas, R. J.: Particle size and pathogenicity in the respiratory tract, Virulence, 4, 847–858, https://doi.org/10.4161/viru.27172, 2013.

Ulbrich, I. M., Canagaratna, M. R., Zhang, Q., Worsnop, D. R., and Jimenez, J. L.: Interpretation of organic components from Positive Matrix Factorization of aerosol mass spectrometric data, Atmos. Chem. Phys., 9, 2891–2918, https://doi.org/10.5194/acp-9-2891-2009, 2009.

Ulbrich, I. M., Handschy, A., Lechner, M., and Jimenez, J.L.: High-Resolution AMS Spectral Database, http://cires.colorado.edu/jimenez-group/HRAMSsd/, last access: 18 September 2023.

von der Weiden, S.-L., Drewnick, F., and Borrmann, S.: Particle Loss Calculator – a new software tool for the assessment of the performance of aerosol inlet systems, Atmos. Meas. Tech., 2, 479–494, https://doi.org/10.5194/amt-2-479-2009, 2009.

Wallace, L. and Ott, W.: Personal exposure to ultrafine particles, J. Expo. Sci. Environ. Epidemiol., 21, 20–30, https://doi.org/10.1038/jes.2009.59, 2011.

Wallace, L. A., Emmerich, S. J., and Howard-Reed, C.: Source strengths of ultrafine and fine particles due to cooking with a gas stove, Environ. Sci. Technol., 38, 2304–2311, https://doi.org/10.1021/es0306260, 2004.

Wang, Q., He, X., Zhou, M., Huang, D. D., Qiao, L., Zhu, S., Ma, Y.-g., Wang, H.-l., Li, L., Huang, C., Huang, X. H. H., Xu, W., Worsnop, D., Goldstein, A. H., Guo, H., and Yu, J. Z.: Hourly measurements of organic molecular markers in urban Shanghai, China: Primary organic aerosol source identification and observation of cooking aerosol aging, ACS Earth Space Chem., 4, 1670–1685, https://doi.org/10.1021/acsearthspacechem.0c00205, 2020.

WHO: WHO global air quality guidelines: Particulate matter (PM2.5 and PM10), ozone, nitrogen dioxide, sulfur dioxide and carbon monoxide, WHO European Centre for Environment and Health, Bonn, 285 pp., 2021.

WHO: Household air pollution, https://www.who.int/news-room/fact-sheets/detail/household-air-pollution-and-health, last access: 27 July 2023.

Williams, A., Jones, J. M., Ma, L., and Pourkashanian, M.: Pollutants from the combustion of solid biomass fuels, Prog. Energy Combust. Sci., 38, 113–137, https://doi.org/10.1016/j.pecs.2011.10.001, 2012.

Wu, C. L., Chao, C. Y. H., Sze-To, G. N., Wan, M. P., and Chan, T. C.: Ultrafine particle emissions from cigarette smouldering, incense burning, vacuum cleaner motor operation and cooking, Indoor Built Environ., 21, 782–796, https://doi.org/10.1177/1420326X11421356, 2012.

Xu, J., Wang, P., Li, T., Shi, G., Wang, M., Huang, L., Kong, S., Gong, J., Yang, W., Wang, X., Geng, C., Han, B., and Bai, Z.: Exposure to source-specific particulate matter and health effects: a review of epidemiological studies, Curr. Pollution Rep. (Current Pollution Reports), 381, 705, https://doi.org/10.1007/s40726-022-00235-6, 2022.

Xu, W., He, Y., Qiu, Y., Chen, C., Xie, C., Lei, L., Li, Z., Sun, J., Li, J., Fu, P., Wang, Z., Worsnop, D. R., and Sun, Y.: Mass spectral characterization of primary emissions and implications in source apportionment of organic aerosol, Atmos. Meas. Tech., 13, 3205–3219, https://doi.org/10.5194/amt-13-3205-2020, 2020.

Xu, W., Lambe, A., Silva, P., Hu, W., Onasch, T., Williams, L., Croteau, P., Zhang, X., Renbaum-Wolff, L., Fortner, E., Jimenez, J. L., Jayne, J., Worsnop, D., and Canagaratna, M.: Laboratory evaluation of species-dependent relative ionization efficiencies in the Aerodyne Aerosol Mass Spectrometer, Aerosol Sci. Technol., 52, 626–641, https://doi.org/10.1080/02786826.2018.1439570, 2018.

Yeung, L. L. and To, W. M.: Size distributions of the aerosols emitted from commercial cooking processes, Indoor Built Environ., 17, 220–229, https://doi.org/10.1177/1420326X08092043, 2008.

Yin, J., Cumberland, S. A., Harrison, R. M., Allan, J., Young, D. E., Williams, P. I., and Coe, H.: Receptor modelling of fine particles in southern England using CMB including comparison with AMS-PMF factors, Atmos. Chem. Phys., 15, 2139–2158, https://doi.org/10.5194/acp-15-2139-2015, 2015.

Yu, Y., Guo, S., Wang, H., Shen, R., Zhu, W., Tan, R., Song, K., Zhang, Z., Li, S., Chen, Y., and Hu, M.: Importance of Semivolatile/Intermediate-Volatility Organic Compounds to Secondary Organic Aerosol Formation from Chinese Domestic Cooking Emissions, Environ. Sci. Technol. Lett., 9, 507–512, https://doi.org/10.1021/acs.estlett.2c00207, 2022.

Zhang, Q., Gangupomu, R. H., Ramirez, D., and Zhu, Y.: Measurement of ultrafine particles and other air pollutants emitted by cooking activities, Int. J. Environ. Res. Public Health., 7, 1744–1759, https://doi.org/10.3390/ijerph7041744, 2010.

Zhang, Z., Zhu, W., Hu, M., Wang, H., Chen, Z., Shen, R., Yu, Y., Tan, R., and Guo, S.: Secondary organic aerosol from typical chinese domestic cooking emissions, Environ. Sci. Technol. Lett., 8, 24–31, https://doi.org/10.1021/acs.estlett.0c00754, 2021.

Zhao, W., Hopke, P. K., Norris, G., Williams, R., and Paatero, P.: Source apportionment and analysis on ambient and personal exposure samples with a combined receptor model and an adaptive blank estimation strategy, Atmos. Environ., 40, 3788–3801, https://doi.org/10.1016/j.atmosenv.2006.02.027, 2006.

Zhao, Y., Liu, L., Tao, P., Zhang, B., Huan, C., Zhang, X., and Wang, M.: Review of effluents and health effects of cooking and the performance of kitchen ventilation, Aerosol Air Qual. Res., 19, 1937–1959, https://doi.org/10.4209/aaqr.2019.04.0198, 2019.

Zhao, Y., Hu, M., Slanina, S., and Zhang, Y.: Chemical compositions of fine particulate organic matter emitted from Chinese cooking, Environ. Sci. Technol., 41, 99–105, https://doi.org/10.1021/es0614518, 2007.

Zhou, L., Liu, T., Yao, D., Guo, H., Cheng, C., and Chan, C. K.: Primary emissions and secondary production of organic aerosols from heated animal fats, Science of The Total Environment, 794, 148638, https://doi.org/10.1016/j.scitotenv.2021.148638, 2021.

Zhou, Z., Liu, Y., Yuan, J., Zuo, J., Chen, G., Xu, L., and Rameezdeen, R.: Indoor PM2.5 concentrations in residential buildings during a severely polluted winter: A case study in Tianjin, China, Renew. Sust. Energ. Rev., 64, 372–381, https://doi.org/10.1016/j.rser.2016.06.018, 2016.

Zhu, W., Guo, S., Zhang, Z., Wang, H., Yu, Y., Chen, Z., Shen, R., Tan, R., Song, K., Liu, K., Tang, R., Liu, Y., Lou, S., Li, Y., Zhang, W., Zhang, Z., Shuai, S., Xu, H., Li, S., Chen, Y., Hu, M., Canonaco, F., and Prévôt, A. S. H.: Mass spectral characterization of secondary organic aerosol from urban cooking and vehicular sources, Atmos. Chem. Phys., 21, 15065–15079, https://doi.org/10.5194/acp-21-15065-2021, 2021.